RESEARCH REPORT

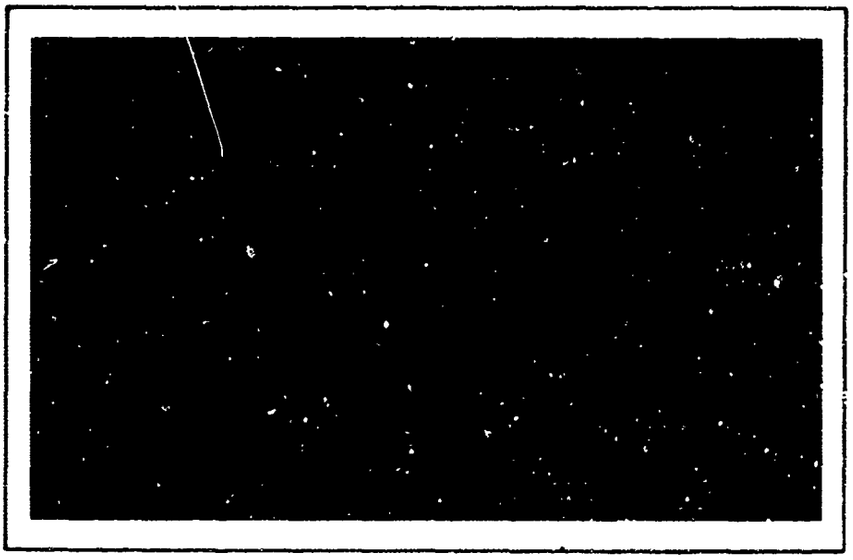

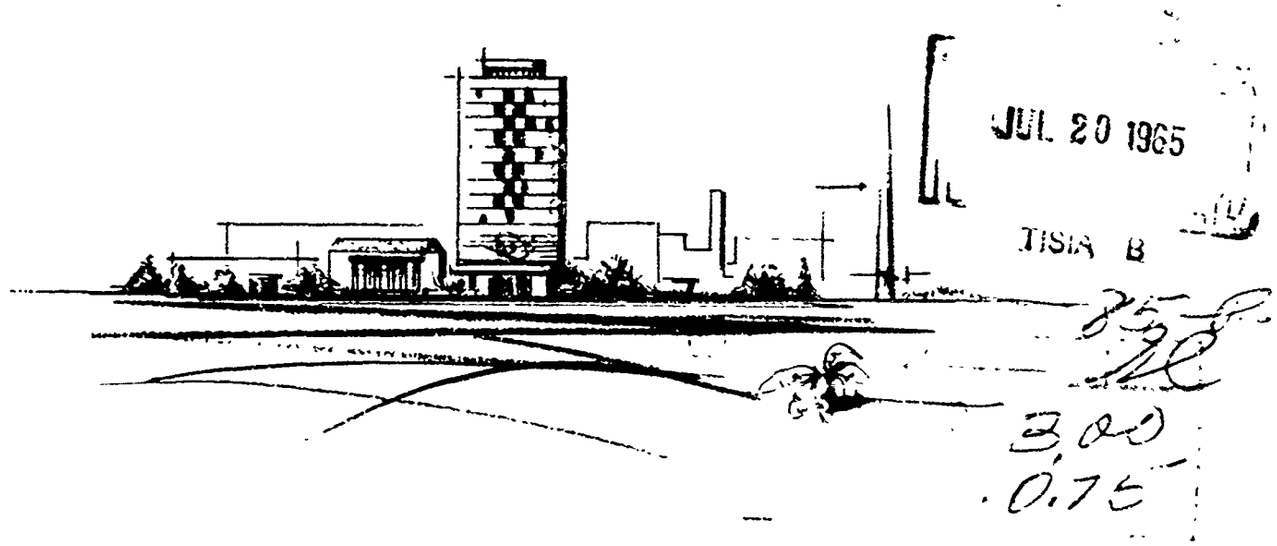

BATTELLE MEMORIAL INSTITUTE

COLUMBUS LABORATORIES

BATTELLE MEMORIAL INSTITUTE

COLUMBUS LABORATORIES • 505 KING AVENUE • COLUMBUS, OHIO 43201

DEDICATED TO THE ADVANCEMENT OF SCIENCE

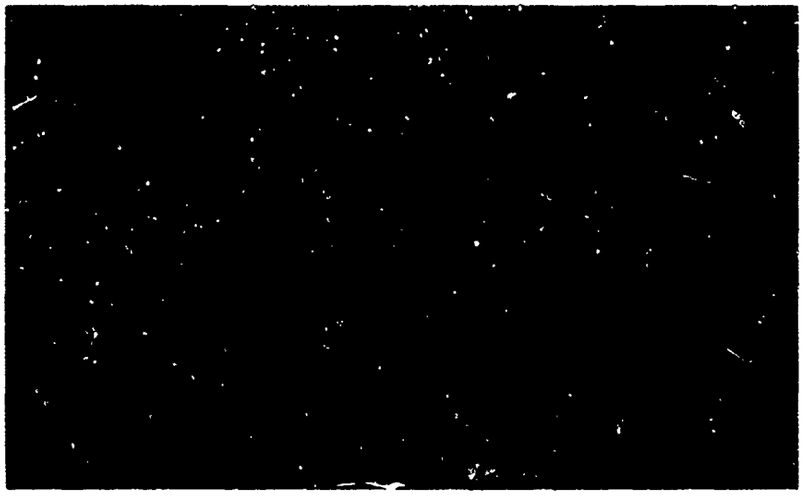

FIELDS OF RESEARCH

Aeronautics — Astronautics
Agricultural Chemistry
Agricultural Economics
Alloy Development
Applied Mathematics
Area Economics
Biochemistry
Biophysics — Bionics
Catalysis — Surface Chemistry
Ceramics
Chemical Engineering
Chemical Processes
Communications Science
Computer Technology
Corrosion Technology
Earth — Atmospheric Sciences
Electrochemistry
Electronics
Energy Conversion
Engineering — Structural Materials
Environmental Systems
Extractive Metallurgy
Extreme-Temperature Technology
Ferrous Metallurgy
Food Technology
Foundry Practice
Fuels — Combustion
Glass Technology
Graphic Arts Technology
Immunology — Cancer Studie
Industrial Economics
Industrial Physics
Information Research
Inorganic Chemistry
Instrumentation
Light Alloys — Rare Metals
Lubricant Technology
Materials Separation — Concentration
Mechanical Engineering
Metal Fabrication Engineering
Metal Finishing
Metallurgical Processes
Microbiology
Microscopy — Mineralogy
Nondestructive Evaluation Technology
Nonferrous Metallurgy
Nucleonics
Ocean Engineering
Organic Chemistry
Organic Coatings
Packaging Research
Particle Dynamics
Petrochemicals
Petroleum Engineering
Pharmaceutical Chemistry
Physical Chemistry
Production Engineering
Psychological Sciences
Pulp — Paper Technology
Radioisotopes — Radiation
Reactor Technology
Refractories
Reliability Engineering
Rubber — Plastics
Semiconductors — Solid-State Devices
Sound — Vibration
Systems Engineering
Textiles — Fibers
Theoretical — Applied Mechanics
Thermodynamics
Transportation
Welding — Metals-Joining Technology
Wood — Forest Products

FINAL REPORT

on

ANALYTICAL STUDY OF AIRCRAFT ARRESTING GEAR CABLE DESIGN

to

UNITED STATES NAVY
BUREAU OF NAVAL WEAPONS

May 28, 1965

by

P. T. Gibson and H. A. Cress

Contract No. NOw 64-0461-f

BATTELLE MEMORIAL INSTITUTE
505 King Avenue
Columbus, Ohio 43201

Battelle Memorial Institute · COLUMBUS LABORATORIES

505 KING AVENUE COLUMBUS, OHIO 43201 · AREA CODE 614, TELEPHONE 299-3151 · CABLE ADDRESS: BATMIN

June 8, 1965

Mr. George Yoder
RRMA 223
Materials Section
Bureau of Weapons
United States Navy
Washington 25, D. C.

Dear Mr. Yoder:

Enclosed is the Final Report on the first year of our arresting gear cable study entitled "Analytical Study of Aircraft Arresting Gear Cable Design". We have enjoyed working on this program and are looking forward to turning our theories into practice during the next year. The accomplishments of the past year would not have been possible without your co-operation and the assistance from the various Navy personnel that we have contacted and obtained information and samples from during the past year.

Sincerely,

Hobart A. Cress

Hobart A. Cress
Project Leader
Machine Dynamics Division

HAC:pjf
Enc.

BLANK PAGE

LIST OF SYMBOLS

A	Area of cable cross section, in.^{2}
B'	Damper force/velocity factor
c	Longitudinal-wave velocity in cable, ft/sec
c'	Length of strand center line in one lay, in.
$\Delta c'$	Change in length of strand due to tension, in.
$\bar{c}$	Transverse-wave velocity relative to cable, ft/sec
d	Wire diameter, inch
e	Base of natural logarithms, 2.71828
E	Modulus of elasticity, lb/in.^{2}
f	Coefficient of friction between cable and hook
F	Force, lb
F_B	Increase in interstrand contact force due to bending cable around hook, lb/in.
F_H	Contact force between hook and cable, lb/in.
F_r	Radial force supporting strand, lb/in.
F_T	Interstrand contact force due to tension, lb/in.
F_{TB}	Interstrand contact force due to tension and bending, lb/in.
$\bar{F}$	Slope of arresting engine slope/time curve, lb/sec
g	Acceleration of gravity, ft/sec^2
I	Moment of inertia, ft^4
ℓ	Length of wire in one lay, in.
$\Delta\ell$	Change in length of wire due to tension, in.
m	Mass of a body, lb
n	Number of wires in one layer
P_T	Force per contact point due to tension, lb
P_{TB}	Force per contact point due to tension and bending, lb
P_T'	Force per region of contact between two strands due to tension, lb
P_{TB}'	Force per region of contact between two strands due to tension and bending, lb
r	Distance from strand center line to wire center line, in.
r'	Average distance from strand center line to center line of wires in one layer, inch
$\bar{r}$	Distance from rope center line to strand center line, in.

R	Minor principal radius of curvature of a body, in.
R'	Major principal radius of curvature of a body, in.
R_H	Radius of hook, in.
$\overline{R}$	$= (r + R)/\overline{r}$
S	$= 2\pi r$
t	Elapsed time after hook impact, sec
t^*	Slack pickup time, sec
T	Tension in cable, lb
T_s	Tension in one strand, lb
u	Cable velocity, ft/sec
u_p	Cable velocity on port side of hook, ft/sec
u_s	Cable velocity on starboard side of hook, ft/sec
V	Impact velocity, ft/sec
w	Kink velocity relative to deck, ft/sec
α	Lay angle of wire in strand
α_c	Deformation due to compression, in.
α'	Average lay angle of all wires in one layer
$\overline{\alpha}$	Cable wrap angle around sheave
β	Lay angle of strand in rope
$\overline{\beta}$	Cable impact angle
γ	Cable wrap angle around hook
ϵ	Strain in cable
$\Delta\epsilon$	Change in strain across a longitudinal wave
θ	Crossing angle of two contacting bodies
λ	Distance between fixed and moving crosshead sheaves, battery position, ft
μ	Poisson's ratio
ρ_o	Density of unstrained cable, lb/ft
σ	Tensile or compressive stress, lb/in.^{2}
σ_{yp}	Yield-point stress in tension or compression, lb/in.^{2}
τ	Shear stress, lb/in.^{2}
τ_G	Octahedral stress, lb/in.^{2}
τ_{yp}	Yield-point shear stress, lb/in.^{2}
ϕ	Cable kink angle
ϕ_o	Reference angle used for computing radius of curvature

TABLE OF CONTENTS

TABLE OF CONTENTS
(Continued)

LIST OF FIGURES

LIST OF FIGURES
(Continued)

LIST OF FIGURES
(Continued)

ANALYTICAL STUDY OF AIRCRAFT ARRESTING GEAR CABLE DESIGN

by

P. T. Gibson and H. A. Cress

INTRODUCTION AND SUMMARY

The objective of this investigation is to develop a comprehensive cable design theory which will provide a basis for improved design and construction of wire rope. In order to accomplish this objective, the following items are included in a detailed analysis of the problem:

(1) Definition of the patterns and magnitudes of dynamic loads generated in wire rope by the action of sustained tensile loads and transverse impact loads, similar to the conditions found in aircraft arresting cables

(2) Effect of cable slippage around the arresting hook on the magnitude of the peak tensile load on the cable

(3) Effect of longitudinal-wave loading rate on the peak cable tension

(4) Influence of constructional variations on the peak tensile stress developed in the cable during aircraft arrestment

(5) Calculation of tensile loads and stresses on the wires of a rope under pure tension

(6) Calculation of interstrand forces and stresses for a rope under pure tension

(7) Effects of bending the cable around a hook or sheave on the internal loads and stresses

(8) Contact force and stress between the hook and the cable for the static condition

(9) Comparison of flattened strand, Lang-lay and round strand, regular-lay cables

(10) Mode of failure of deck pendants

(11) Contact force produced by impact of hook on deck pendant

(12) Wire rope abrasion resistance

(13) Wire rope flexibility.

The results discussed in the section on Cable Dynamics provide a time history of tension in an aircraft arresting cable at the point of hook impact. This tension is calculated neglecting internal cable damping and assuming perfect reflection of longitudinal waves from the hook. Also, all longitudinal waves are treated as having an infinite rate of loading, thus providing an "ideal" time-tension curve.

The effects of these idealized assumptions are discussed, and it is shown that a reduced value for the peak cable tension is more realistic. By considering slippage of the cable around the hook during impact of a longitudinal wave, plus the effects of wave attenuation and a noninfinite loading rate, a value of 85,000 pounds is obtained for the peak cable tension under the conditions assumed.

An analysis of the effects of the wire-rope constructional variations on the peak tensile stress in the cable is also presented. The peak tensile stress developed during an aircraft arrestment is shown graphically as a function of cable elastic modulus and the ratio of cable density to metallic cross-sectional area. It is found that the peak stress is reduced by a reduction of either of these variables.

Calculations are presented to show the maximum internal stresses experienced by a flattened strand, Lang-lay cable. These calculations include the tensile stresses on the wires, the interstrand crossed-wire contact stresses, and the contact stresses between the cable and the hook for the condition of peak cable tension plus bending. The results are then compared with those reported previously[31]* for a round-strand, regular-lay cable.

This analysis of the internal stresses developed in a flattened-strand, Lang-lay cable reveals that for a tension of 85,000 pounds, the interstrand crossed-wire contact stresses are approximately 25 percent lower than those for a round-strand, regular-lay rope. The contact stresses between the hook and the cable are 30 percent less. The decrease in interstrand contact stresses is due primarily to the reduction in the lay angles for the Lang-lay rope and the use of slightly larger-diameter wires. The lower contact stresses between the hook and the cable can be attributed to the increase in length of wire contact provided by the flattening of the strands and the use of Lang lay.

Inspection of used deck pendants revealed that failure is caused by the combined effects of abrasion and impact of the arresting hook. This hook-cable impact situation is defined analytically and the problem of abrasion resistance is investigated qualitatively. It is found that the effects of these two conditions can be reduced by a change in the wire cross-sectional shape and a change in the geometry of the individual strands.

As a result of these investigations, comprehensive criteria for the evaluation of arresting cable are presented, and a number of recommendations are made for an improved wire-rope design. On the basis of these recommendations, new rope designs are proposed and discussed, and their performance for use in aircraft arrestment is predicted. A discussion of the applicability of the new designs to purchase cable and a strong recommendation for the use of plated wire in purchase cable are also included.

An analysis of one suggested new design shows that its adoption should virtually eliminate the problems of interstrand notching and wire breakage due to impact by the

*References are given in the Bibliography, page 74.

hook. However, it is pointed out that experimental work is necessary before concrete conclusions can be reached.

CABLE DYNAMICS

The phenomena of wave propagation along an elastic fiber have long been established in the literature of physics and solid mechanics.[14,35] In these early treatments of the problem, the nonlinear partial differential equations are linearized by several assumptions, one of which is the premise that deflections of the fiber are to be small. In this way a qualitative description of wave propagation is presented.

Two distinct wave types can travel along an elastic fiber (string, wire, cable, or what-have-you) that is subjected to a tensile load and a disturbance. One, the longitudinal wave, can be described as a discontinuity in stress level (or axial cable velocity) traveling at the acoustic velocity in the fiber material. The other, the transverse wave, is essentially a traveling "kink" with a velocity of propagation much lower than that of the longitudinal wave. In a material satisfying Hooke's Law (a linear stress-strain relationship), these waves can propagate virtually undistorted in the absence of one another. Two longitudinal waves traveling in opposite directions can pass undistorted; two transverse waves, however, will interact to produce longitudinal waves as well as distortion. A longitudinal wave meeting or overtaking a transverse wave will interact, distorting both waves.

For some problems, the aircraft arresting cable being a prime example, the elementary linearized theory is inadequate owing to the large deflections incurred in the generation of transverse waves. The equations of motion as applied to the arresting-cable problem are presented by Ringleb[37,38,39] as nonlinear partial differential equations. These are solved for the case of motion that is purely that of a longitudinal or transverse wave, and the resulting solution is a function of geometry, cable strain, and cable parameters. A meeting of two singularities can then be analyzed by means of a geometric approach using the properties of singular wave propagation thus established.

These wave- and cable-velocity formulas are summarized below in terms of fiber (or cable) strain, ϵ:

$c_o = \sqrt{AE/\rho_o}$ = Longitudinal-wave velocity relative to cable at zero strain, ft/sec,

where

A = Cable metallic cross section, in.^{2}

E = Elastic modulus of the cable, lb/in.^{2}

ρ_o = Cable mass per unit length at zero strain, lb/ft.

$c = (1 + \epsilon)c_o$ = Longitudinal-wave velocity relative to cable at strain ϵ, ft/sec,

where

ϵ = Strain (change in length per unit length), in./in.

$\bar{c} = \sqrt{\epsilon(1+\epsilon)}c_o$ = Transverse-wave velocity relative to cable, ft/sec

$\Delta u = (\epsilon_2 - \epsilon_1)c_o$ = Change in cable velocity across a longitudinal wave, ft/sec

ϕ_1 = arc sin $[(V/\bar{c}) \sin \bar{\beta}]$ = Initial kink angle in cable, degrees,

where

V = Initial velocity of aircraft, ft/sec

$\bar{\beta}$ = (90° – misalignment angle of aircraft), degrees.

With these relationships Ringleb[37] has developed mathematical models describing the interactions of singularities and the effects of various cable end conditions. These are presented by Neidhardt, Eslinger, and Sasaki[28] in terms of cable strain.

Since the original derivations of the mathematical models are geometric in nature (based on the states of the cable before and after the various dynamic events), solutions by graphical methods are only natural. The technique involves velocity diagrams drawn to scale, with the known quantities drawn first and the unknown quantities (functions of the unknown strain, ϵ, following interaction) determined by trial. To eliminate the trial-and-error facet of the solutions, nomograms are drawn that facilitate the construction of the unknown strain functions. Those of interest to this program are repeated in summarized form below. The dynamic events considered include:

(1) Impact of the hook on the cable

(2) Meeting of a kink and a longitudinal wave

(3) Kink being overtaken by a longitudinal wave

(4) Impact of kink on deck sheave

(5) Impact of kink against a fixed point.

Impact of Hook on Cable

Initially the cable is at rest with some small tensile load producing a strain ϵ_o. The aircraft engages the cable at Point P, as shown in Figure 1, with a velocity V and at an angle $\bar{\beta}$. It is assumed that the cable does not slip across the arresting hook, and the initial point of engagement moves along PR with the aircraft. The behavior of the cable to the left of Point R will be studied.

After impact, a longitudinal wave propagates along the cable away from Point P with a velocity $(1 + \epsilon_o)c_o$. In Figure 1, Point S is the position of this singularity. To the left of this point, the cable is as yet undisturbed, while to the right of Point S, the cable has an unknown strain ϵ_1 and is moving toward Point P with a velocity $u_1 = (\epsilon_1 - \epsilon_o)c_o$. The transverse wave or kink moves away from Point P with a velocity $\bar{c}_1 = \sqrt{\epsilon_1(1+\epsilon_1)}c_o$ relative to this part of the cable. The velocity of the kink relative

to Point P is $(\bar{c}_1 - u_1)$. Since Q and R are formed simultaneously at Point P, their velocities correspond to the sides of Triangle PQR and are shown on Figure 1 in dimensionless forms. The law of cosines and the law of sines may be used to solve for ϵ_1 and ϕ_1 respectively.

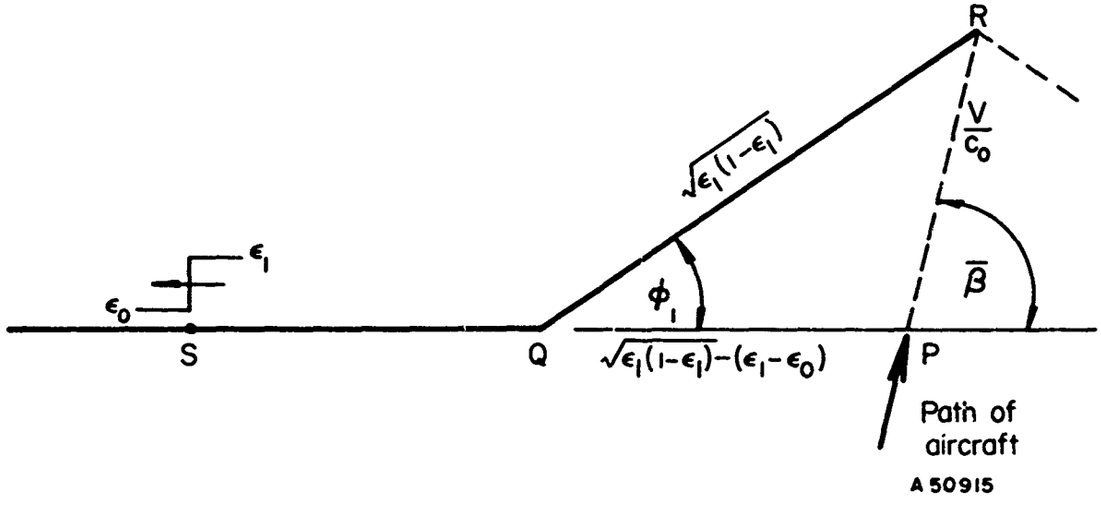

FIGURE 1. IMPACT OF AIRCRAFT AGAINST CABLE

This solution is greatly simplified, however, by the use of Nomogram Number One shown in Figure 2. Triangle PQR is redrawn as shown in Figure 3 with the known dimensions shown by solid lines. Point O of Figure 3 corresponds to the origin of the nomogram. The portion OPR is drawn on the nomogram to the scale indicated thereon, with OP along the horizontal axis. Point R then falls on the circle of the nomogram that is labeled with the value of ϵ_1 sought (interpolation may be necessary). Point Q then corresponds to the center of the circle on which R has fallen. The kink angle ϕ_1 can then be scaled.

Impact of Kink on Deck Sheave

When a traveling kink reaches a deck sheave, a longitudinal wave and a new kink are generated. The following analysis is used to find the magnitudes of the new strain and kink angle. For the case of a well-lubricated cable and a small cable wrap angle, it may be assumed that the system is frictionless (the same effect is achieved with a massless sheave).

With reference to Figure 4, suppose a kink K of angle ϕ_1 is traveling toward a sheave at Point P and that the strain in the cable is ϵ_1 while the cable velocity is u_1 clockwise around the sheave. Then the kink K must be approaching P with velocity $\bar{c}_1 - u_1$. When the kink reaches the sheave, a new strain ϵ is produced and extends from P to the newly formed longitudinal singularity S, which propagates away from the sheave. This new strain also propagates around the sheave toward the energy absorber.

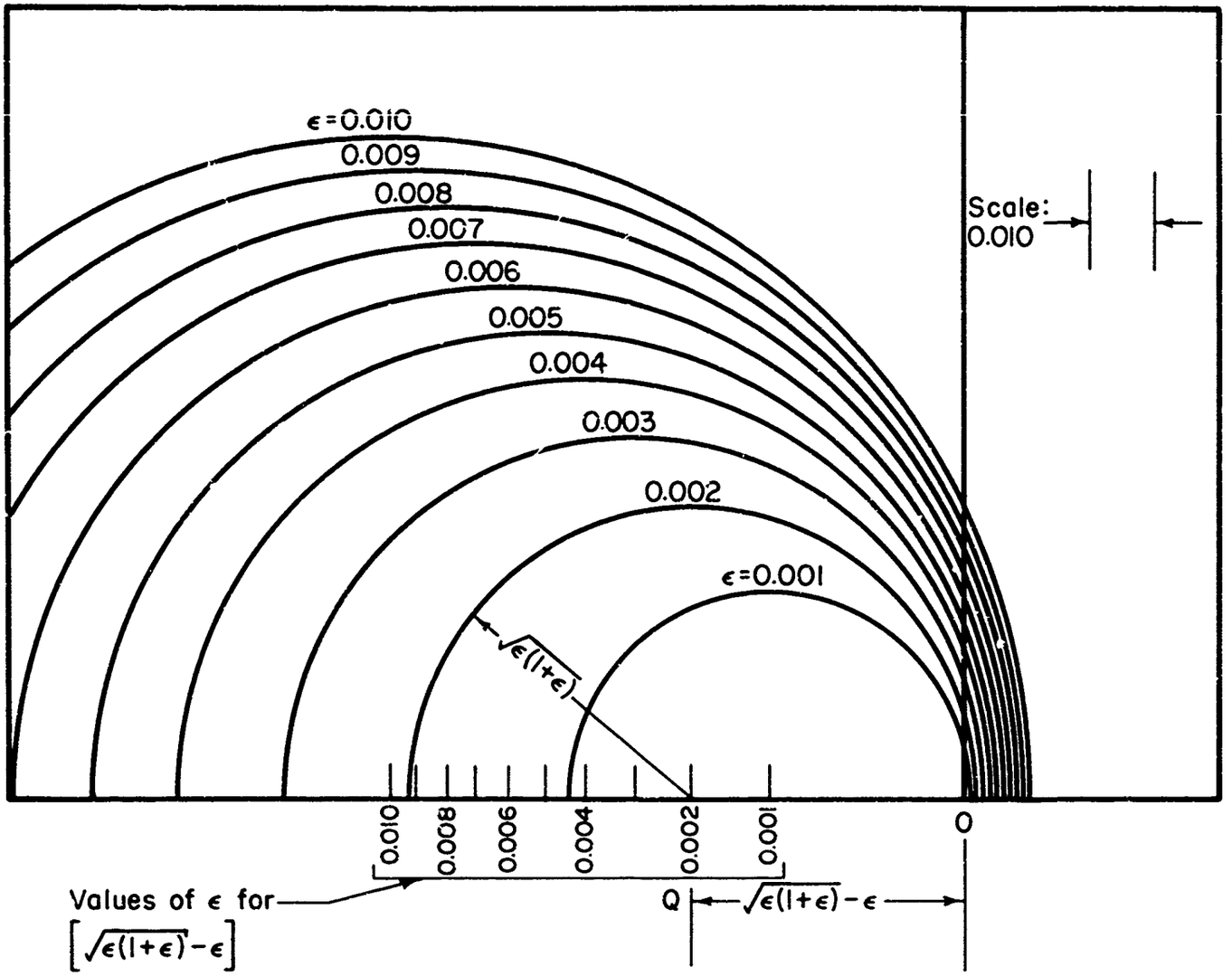

FIGURE 2. NOMOGRAM NUMBER ONE

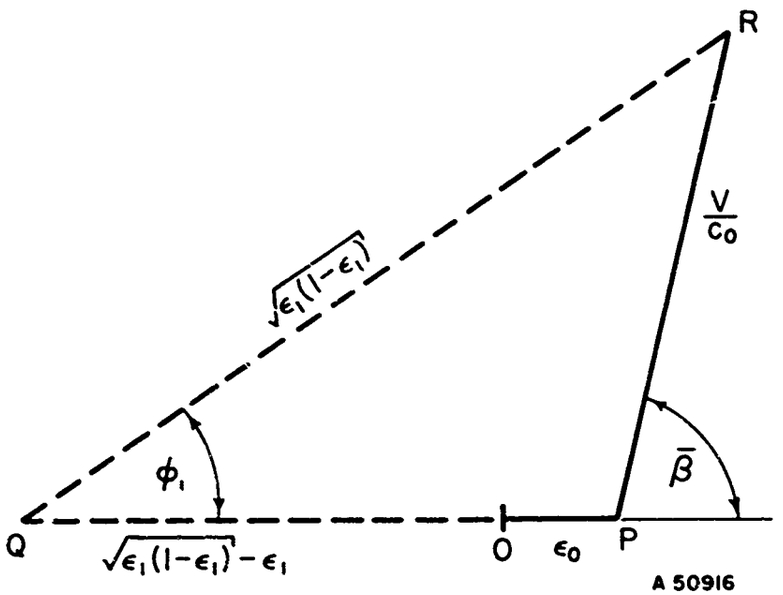

FIGURE 3. NOMOGRAM SOLUTION FOR IMPACT OF AIRCRAFT AGAINST CABLE

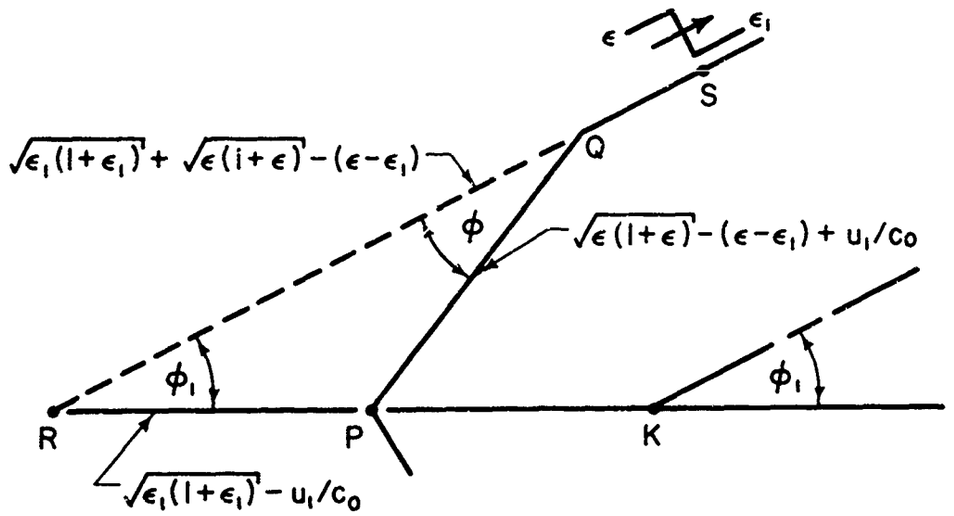

FIGURE 4. IMPACT OF KINK ON DECK SHEAVE

Beyond S the cable is not yet affected by the impact at the sheave. The projection R of the unaffected cable is thus a continuation of the motion of K; hence, R moves away from P with velocity $\bar{c}_1 - u_1$ and away from the unaffected cable with velocity $\bar{c}_1$. The cable in the wake of S moves back from the unaffected cable with a velocity u given by $u = (\epsilon - \epsilon_1)c_o$ so that the reflected kink Q moves toward the unaffected cable with a velocity $\bar{c} - u$. Thus, Q and R separate with a velocity $\bar{c}_1 + \bar{c} - u$.

Since the new strain ϵ propagated around the sheave (assuming no friction), the cable is now fed over the sheave with a velocity $u_1 + (\epsilon - \epsilon_1)c_o$. Thus, kink Q propagates away from P with a velocity $\bar{c} + u_1 + (\epsilon - \epsilon_1)c_o$.

These velocities correspond to the sides of triangle PQR and are shown in dimensionless form in Figure 4. Using the law of cosines the value of ϵ may be found by trial. The new kink angle ϕ may be found using the law of sines.

A much easier solution is obtained if triangle PQR is redrawn as shown in Figure 5. Here the known quantities are shown as solid lines. Nomogram Number Two, shown in Figure 6, provides the solution.

The known portion ORP of triangle PQR is drawn on the nomogram to the proper scale and with Point O at the origin. An arc of radius $u_1/c_o - \epsilon_1$ is then drawn with Point P as the center. This arc will be tangent to the circle of the nomogram which is labeled with the value of ϵ sought, and A is the point of tangency. Interpolation may be necessary.

Note that the portion OQA is now completed by the nomogram, with Q corresponding to the center of the circle on which A now lies. If desired, the kink angle ϕ may now be scaled.

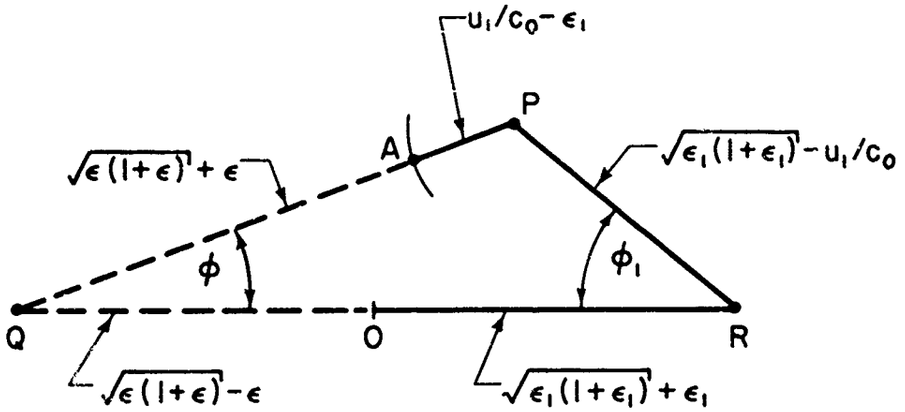

FIGURE 5. NOMOGRAM SOLUTION FOR IMPACT OF KINK ON DECK SHEAVE

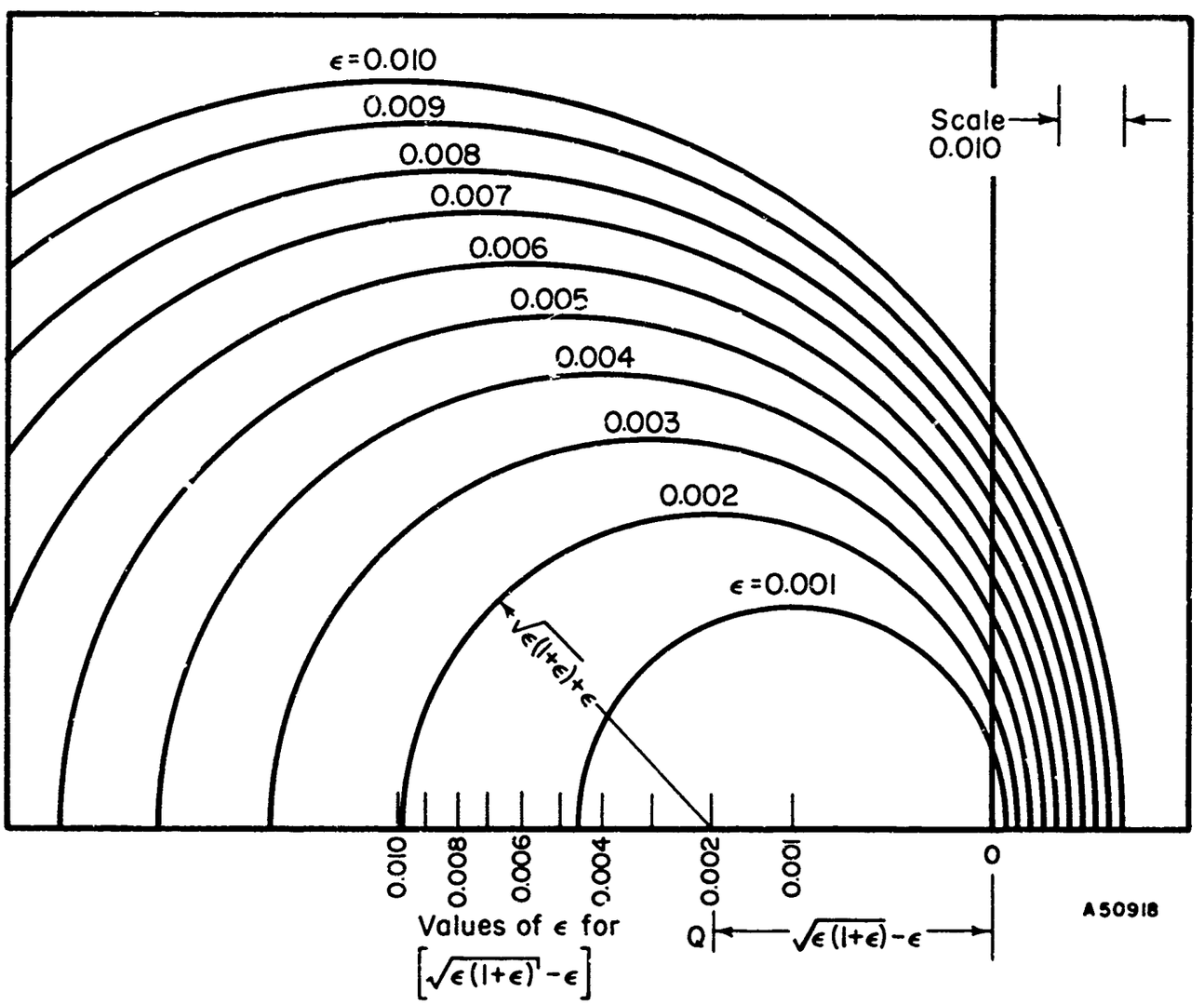

FIGURE 6. NOMOGRAM NUMBER TWO

Meeting of Kink and Longitudinal Wave

During an aircraft arrestment, many longitudinal waves are generated within the system. Since these strain discontinuities travel at the acoustic velocity, they overtake and meet the slower moving kinks many times. Each of these interactions produces two new longitudinal waves, traveling in opposite directions, and also two new kinks.

The following discussion of the meeting of a kink and a longitudinal wave is presented by Neidhardt, et al.[28]:

Consider a cable under strain ϵ_1 on which a kink K of angle ϕ_1 is propagating to the left. Figure 7 shows the cable as viewed from a frame of reference that is moving with K. Hence, the cable appears to move to the right and up the diagonal from K with a velocity $u_1 = \bar{c}_1$. Suppose now that a longitudinal wave S approaches K from the left, and that the strain behind it is ϵ_2. Then the cable in the wake of S moves toward K with a velocity $u_2 = u_1 - (\epsilon_2 - \epsilon_1)c_o$.

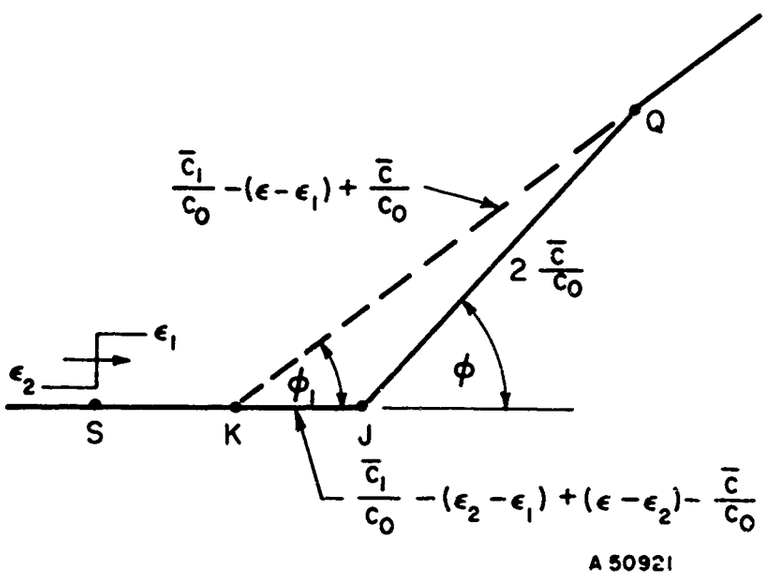

FIGURE 7. MEETING OF KINK AND LONGITUDINAL WAVE

When S reaches K a new strain ϵ will propagate out in both directions, and instead of K there will be two kinks J and Q, Q being the reflection. The diagram depicts J moving slower than K, which would be the case if $\epsilon_2 < \epsilon_1$; however, this detail has no bearing on the final results. Now the cable moves toward K with velocity $u = u_2 + (\epsilon - \epsilon_2)c_o$. Kink J moves to the left relative to the cable with velocity $\bar{c}$ so that it moves to the right relative to K with a velocity $u - \bar{c}$. The cable just ahead of Q moves away from K with a velocity $\bar{c}_1 - (\epsilon - \epsilon_1)c_o$ so that Q must be moving away from K with a velocity $\bar{c}_1 - (\epsilon - \epsilon_1)c_o + \bar{c}$. The two kinks J and Q separate with a velocity $2\bar{c}$.

These velocities are shown in Figure 7 in dimensionless form. The law of cosines may be used with triangle JKQ to determine the unknown strain ϵ by trial, and the law of sines may be used to find the new kink angle ϕ.

This solution is greatly simplified if triangle JKQ is redrawn as shown in Figure 8, where the known quantities are shown as solid lines. Nomogram Number Three, shown in Figure 9, then provides the solution. The known portion OKA of triangle JKQ is drawn on the nomogram to the scale indicated thereon and with Point O at the origin. The solution is found by selecting the Point J so that AJ = OQ and also so that Point J falls on the nomogram circle whose center corresponds to Q. This circle then gives the value of ϵ. Again, interpolation may be necessary. In case $\epsilon_2 > \epsilon_1$, J will be below K instead of above it as shown in Figure 8. The new kink angle ϕ may now be scaled.

Kink Overtaken by Longitudinal Wave

Consider a cable under strain ϵ_1 on which a kink K of angle ϕ_1 is propagating to the left. Figure 10 shows the cable as viewed from a frame of reference that is moving with K. Hence, the cable appears to move to the right and up the diagonal from K with a velocity $u_1 = \bar{c}_1$. Suppose now that a longitudinal wave S approaches K from the right and that the strain behind it is ϵ_2. For this condition the kink is being overtaken by the strain discontinuity.

When S reaches K, a new strain ϵ will propagate out in both directions, and instead of kink K there will be two kinks J and Q, Q being the reflection. The diagram depicts J moving slower than K which would be the case for $\epsilon_2 < \epsilon_1$; however, this detail has no bearing on the final results.

In this case, the velocity of the cable moving away from K beyond Q is changed once by $(\epsilon_1 - \epsilon_2)c_o$ and again by $(\epsilon - \epsilon_2)c_o$. The velocity of the cable coming in from the left is changed only once by $(\epsilon_1 - \epsilon)c_o$.

After these interactions, the cable to the left of K moves towards K with a velocity $u = u_1 - (\epsilon_1 - \epsilon)c_o = \bar{c}_1 - (\epsilon_1 - \epsilon)c_o$. Kink J moves to the left relative to the cable with a velocity $\bar{c}$ so that it moves to the right relative to K with a velocity $u - \bar{c}$. The cable just ahead of Q moves away from K with a velocity $\bar{c}_1 - (\epsilon_1 - \epsilon_2)c_o - (\epsilon - \epsilon_2)c_o$ so that Q must be moving away from K with a velocity $\bar{c}_1 - (\epsilon_1 - \epsilon_2)c_o - (\epsilon - \epsilon_2)c_o + \bar{c}$. The two kinks J and Q separate with a velocity $2\bar{c}$.

These velocities are shown in dimensionless form in Figure 10. The unknown strain ϵ may be found by trial using triangle JKQ and the law of cosines. The new kink angle ϕ may then be found using the law of sines.

This solution is simplified if triangle JKQ is redrawn as shown in Figure 11 where the known quantities are shown by solid lines. Nomogram Number Three, shown in Figure 9, provides the solution. The known portion OKA of triangle JKQ is drawn on the nomogram to the scale indicated thereon with Point O at the origin. Point J is selected so that AJ = OQ and also so that J falls on the nomogram circle for which Q is the center. This circle gives the value of ϵ, and the new kink angle ϕ may be scaled. In case $\epsilon_2 > \epsilon_1$, then J will be below K instead of above it as shown in Figure 11.

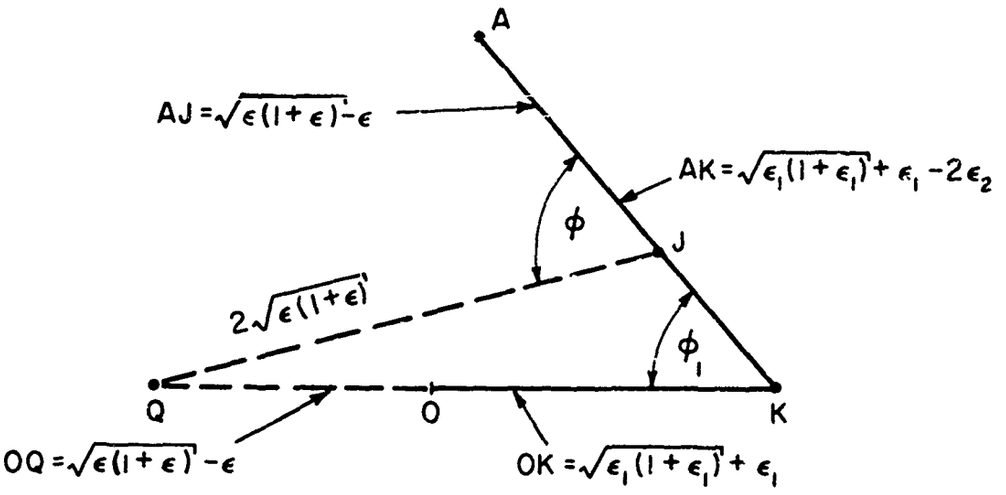

FIGURE 8. NOMOGRAM SOLUTION FOR MEETING OF KINK AND LONGITUDINAL WAVE

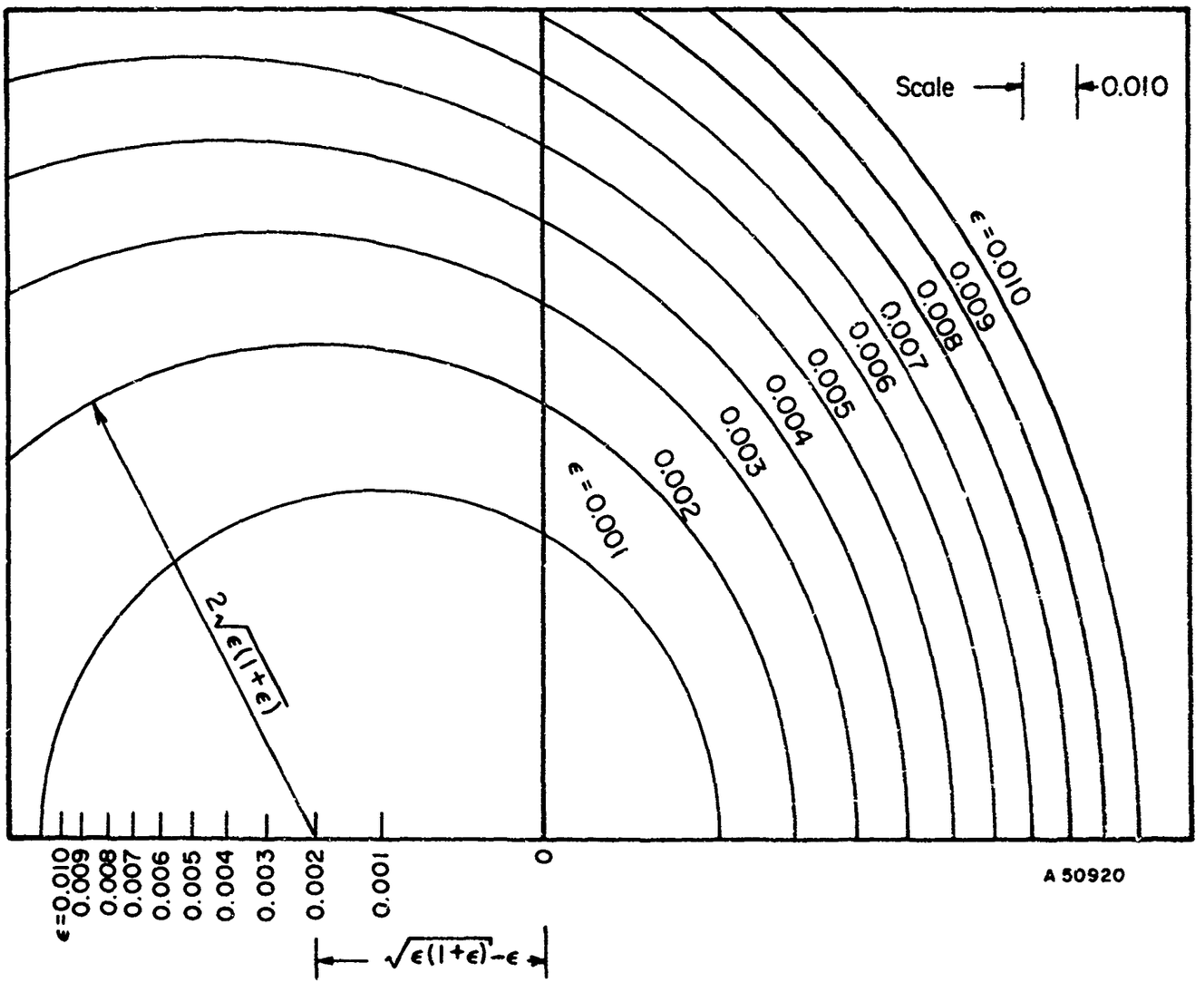

FIGURE 9. NOMOGRAM NUMBER THREE

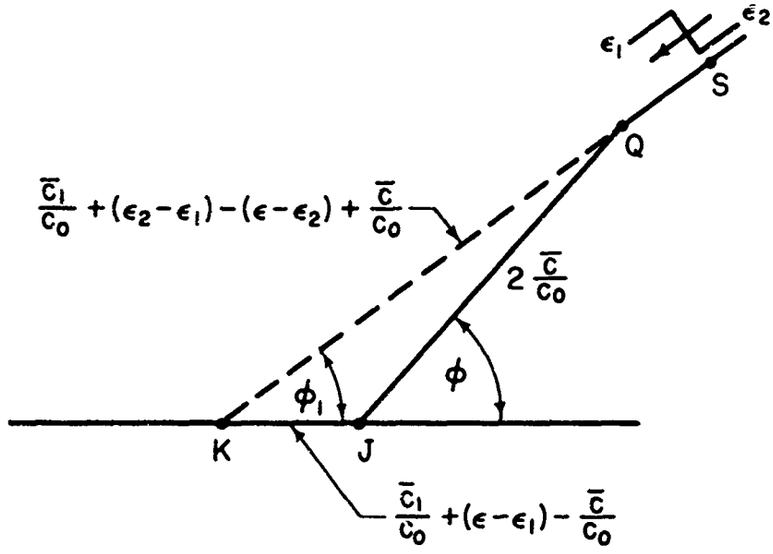

FIGURE 10. KINK OVERTAKEN BY LONGITUDINAL WAVE

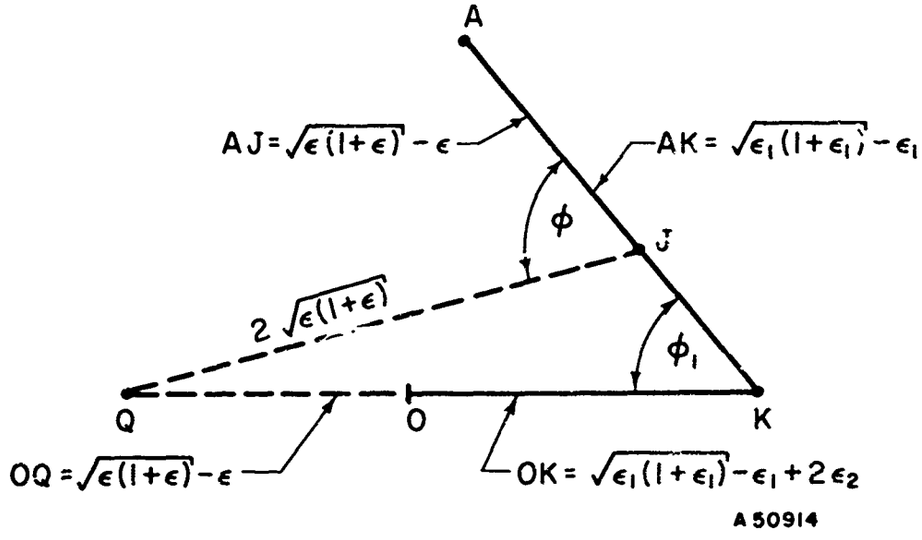

FIGURE 11. NOMOGRAM SOLUTION FOR KINK OVERTAKEN BY LONGITUDINAL WAVE

Nomogram Number Three, Figure 9, is used.

Impact of Kink Against a Fixed Point

When a kink is reflected after impacting on a deck sheave, it propagates along the cable toward the aircraft arresting hook. When it impacts on the hook, a new kink and a longitudinal wave are formed. It is assumed here that the cable is fixed to the hook.

Consider a cable under strain ϵ_1 with a fixed end P toward which a kink K with angle ϕ_1 is propagating, as shown in Figure 12. The velocity of K is $\bar{c}_1$. When the kink reaches the fixed end it is reflected, and a longitudinal wave S propagates away from P. A new increased strain ϵ extends from P to S. The cable in the wake of S moves back relative to the cable with a velocity $u = (\epsilon - \epsilon_1)c_o$. The reflected kink Q moves away from P with a velocity $\bar{c}$. The velocity of Q relative to the unaffected cable to the right of S is $\bar{c} - u$. Since the projection R of the unaffected cable can be regarded as a continuation of the motion of K, it moves away from P and from the unaffected cable with velocity $\bar{c}_1$. Hence, Q and R separate with a velocity $\bar{c}_1 + \bar{c} - u$.

These velocities are shown on Figure 12 in dimensionless form. The new strain ϵ may be found by trial using triangle PQR and the law of cosines. The new kink angle ϕ may be found using the law of sines.

By redrawing triangle PQR as shown in Figure 13 with known quantities represented by solid lines, a solution is made possible using Nomogram Number One. The known portion ORP of triangle PQR is drawn on the nomogram to the scale indicated thereon with Point O at the origin. Point P then falls on the circle of the nomogram that is labeled with the value of ϵ sought.

Note that the portion PQR is now completed by the nomogram, with Q corresponding to the center of the circle on which R has fallen. The new kink angle ϕ may now be scaled.

DETERMINATION OF CABLE TENSION VERSUS TIME

To investigate the internal dynamics of the wire rope, stress versus time at a point in the cable (considered here a homogeneous fiber) must first be calculated. Considering the dynamic action of the cable as a series of singular events gives an idealized picture of average stress versus time; it is felt, however, that this method of analysis results in a usable and reasonably definite stress picture.

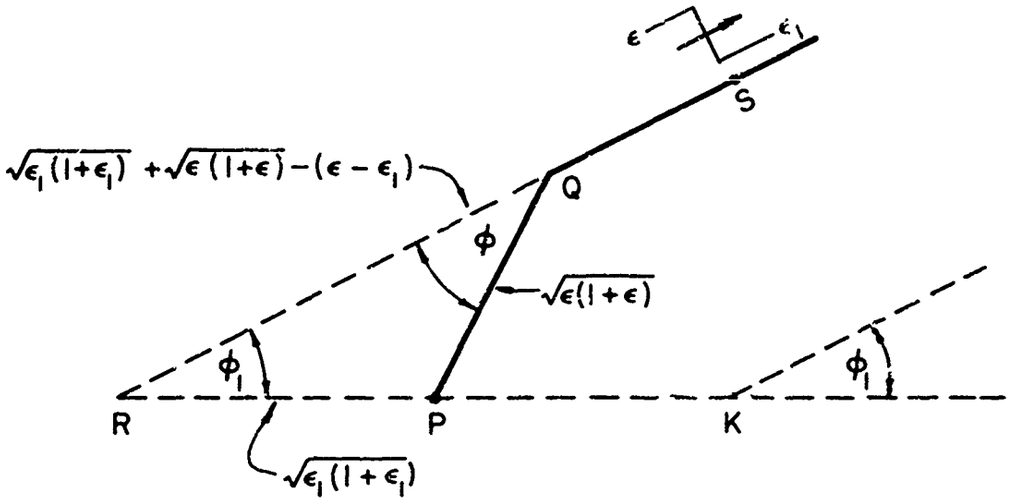

FIGURE 12. IMPACT OF KINK AGAINST A FIXED POINT

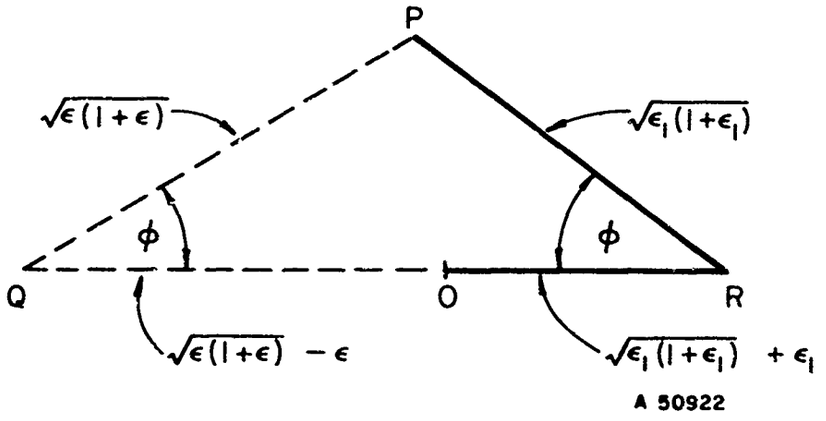

FIGURE 13. NOMOGRAM SOLUTION FOR IMPACT OF KINK AGAINST A FIXED POINT

Nomogram Number One, Figure 2, is used.

The following parameters have been selected for these calculations:

Parameter	Units	Nominal	Maximum
Arrestment velocity, V	Knots	120	150
Aircraft weight	Lb	50,000	60,000
Off-center distance (port)	Ft	0	20
Landing angle, $\bar{\beta}$	Deg	90	84
Longitudinal-wave velocity, c_o	Ft/sec	10,000	10,000
Normalized initial velocity, V/c_o		.0203	.0253
Deck-pendant length (to sheave ℄)	Ft	120	--
Purchase-cable length, deck sheave to first engine sheave	Ft	150	--
Sheave separation, λ, battery position	Ft	43	--
Cable elastic modulus, E	Lb/in.^{2}	12.7×10^6	12.7×10^6
Cable metallic cross section, A	In.^{2}	.87	.87(a)
Slope of engine force/time curve, $\bar{F}$	Lb/sec	4.53×10^6	5.44×10^6(b)
Engine reeving ratio, 2n'		18	(Mark 7 A. G.)
Initial strain in battery position		0	(See below)
Damper force/velocity factor, B'	Lb-sec/ft	5,000	

(a) Approximately for 6 x 30 rope.
(b) Approximately Mark 7 A.G.

The initial strain in Navy gear is approximately 0.0002, which has a subsequent effect of about 0.0001 on strain level [see Reference (39)]; therefore it is assumed zero to simplify the calculations. A cable modulus of elasticity of 12.7×10^6 lb/in.^{2} is chosen on the basis of previous work in cable dynamics.

Effect of Sheave Damper

To simplify the cable dynamic analysis with a deck sheave damper present, a linear force/velocity relationship and negligible damper and sheave mass are assumed. As the longitudinal wave passes the damper sheave, the sheave is quickly accelerated and the initial impact strain is reduced and propagated in both directions (see Figure 14). The assumptions made will affect the shape and duration of the strain transient,

which will in the limit approach the ideal step change in strain. Under these simple criteria, the damper relationships become:

$$v_2 = \frac{c_o}{1 + \frac{B'c_o}{2\sin\bar{\alpha}AE}} \epsilon_1, \text{ damper velocity}$$

$$\epsilon_2 = \frac{Bc_o}{2\sin\bar{\alpha}AE + B'c_o} \epsilon_1, \text{ reduced strain in cable}$$

where

B' = damper force/damper velocity

c_o = longitudinal (acoustic) wave velocity

$\bar{\alpha}$ = cable wrap half-angle

A = cable metallic cross section

E = cable modulus of elasticity.

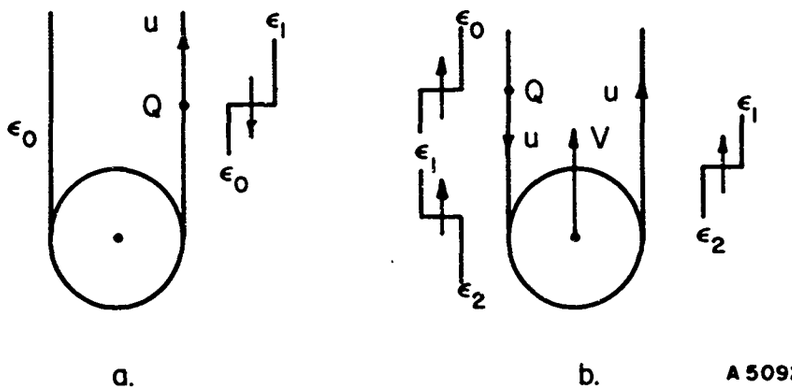

FIGURE 14. SHEAVE DAMPER REACTION TO PASSING LONGITUDINAL WAVE

The deck sheave damper relationships thus established are quite reasonable for the first 3/10 second after impact; beyond this point the sheave damper decelerates to the end of its stroke and can, for all practical purposes, be disregarded. Test results from arresting gear experiments conducted at the Naval Air Testing Facility, Lakehurst, New Jersey, support the above conclusions.

Using the test results of Shot 1023 (a Mark 7, Mod. 2-3 A.G.) conducted with a 50,195-pound dead load, on-center at 121 knots, a value of force versus velocity can be estimated. To determine this, an average sheave velocity and an average cable tension are calculated from areas under the respective curves. This provides the following simple relations for damper sheave velocity and reduced strain:

$v_2 \doteq 3000\epsilon_1$ ft/sec, damper sheave velocity

$\epsilon_2 \doteq 0.7\epsilon_1$, reduced cable strain.

This checks reasonably well with selected peak values of cable tension and sheave velocity.

Effect of Arresting Engine

The effects of the arresting engine are analyzed in Chapter V of Reference (37). Owing to crosshead motion, slack is formed in the cable, and until this slack is picked up, the original longitudinal stress wave will not reach the cable anchor. Upon complete pickup of slack, the stress wave is reflected back toward the deck pendant at the acoustic velocity, c. An approximation of this slack pickup time is given for the case where the force F on the crosshead increases linearly with time:

$$F = \overline{F}\, t$$

$$t^* = \frac{2n'}{c}\left(\frac{AEu}{\overline{F}} + \frac{\lambda}{2}\right) \text{ sec},$$

where

t^* = slack pickup time, sec

$2n'$ = reeving ratio

u = cable velocity

λ = distance between fixed and moving crosshead sheaves, battery position

$\overline{F}$ = slope of force versus time, F = force on crosshead

A = metallic cross section of cable

E = effective modulus of elasticity.

Sequence of Dynamic Events

Using the nomograms and graphical constructions of the previous sections, a sequence of dynamic events may be calculated to determine cable strain versus time. In these calculations no attempt is made to account for nonsymmetry of the arresting gear, effects of the vertical component of hook force, or slipping of the cable over the hook.

Upon impact of the aircraft arresting hook, a longitudinal wave and a transverse wave (kink K_1) are generated, the magnitudes of which are determined by the graphical construction in Figure 3 with the aid of Nomogram Number One (Figure 2). The longitudinal wave, traveling at the much higher acoustic velocity, interacts with the sheave damper: the resulting longitudinal wave, reduced in strain level, propagates in both directions, down the purchase cable to the arresting engine, and back along the deck pendant toward the more slowly moving kink. The wave passing into the engine (and subsequent longitudinal waves) is "lost" in the process of slack pickup and can be disregarded for several tenths of a second. The "mirror image" of this wave meets

kink K_1, and this interaction generates two new longitudinal waves traveling, again, in both directions. One wave reflects from the hook and quickly overtakes the kink. The other reacts with the sheave damper, and a wave of reduced strain is reflected toward the kink to interact.

It is seen that an infinite number of interactions take place as the kink travels from point of impact to deck sheave. Some liberties must be taken to assure a finite problem. It is assumed, therefore, that secondary kinks can be ignored (these are generally 1 or 2 degrees in angle and of no consequence) and that changes in the primary kink angle of orientation are small. Interactions after the first several are disregarded except in that they tend to reduce the cable strain level to a "stabilized" value. This value is estimated more by test data than calculation. The many interactions and changes in kink velocity make the times between events estimations at best. Here an "average" velocity is used.

Impact of the kink on the deck sheave produces a reflected kink, K_2, at a new angle ϕ_{10} relative to the initial angle ϕ_1. The orientation of the kink relative to the cross-deck axis, which we can call angle θ, is $\varphi_1 + \phi_{10}$. A new family of longitudinal waves is immediately initiated, and again engineering license demands a "stabilized" strain to manage the infinite interactions.

Attention is now turned to the arresting engine. An estimated time is calculated for slack pickup and travel of the longitudinal wave reflected from the purchase cable anchor. This wave reacts with the sheave damper and passes out into the deck pendant. From this time on, the sheave damper is assumed to have no further action, being close to its maximum stroke.

Experimental results indicate that the most extreme stresses occur within the first 3/10 second after impact. The problem of the on-center landing (nominal) is terminated, therefore, following the impact of the kink K_2 on the arresting hook. A negligible decrease in aircraft velocity is assumed. The off-center landing (maximum) is calculated through two round-trips of the primary kink, due to the shorter travel and generally higher kink velocity.

The following results are obtained for the sequence of dynamic events:

	Units	Nominal	Maximum
(1) Impact of arresting hook			
V/c_o		.0203	.0253
ϵ_1		.0035	.0067
ϕ_1	Degrees	20.0	18.3
L (impact point to deck sheave)	Ft	60	40
w_1 (kink velocity, cross-deck)	Ft/sec	558	754

	Units	Nominal	Maximum
(2) ϵ_1 to sheave damper (longitudinal wave)			
Δt_{1-2}	Sec	.0060 (.0060)*	.0040 (.0040)*
$\epsilon_2 \doteq 0.7\epsilon_1$		.0025	.0047
(3) ϵ_2 meets kink K_1 (secondary kinks disregarded)			
Δt_{2-3}	Sec	.0054 (.0114)	.0034 (.0074)
x_{K_1} (cross-deck travel of K_1)	Ft	6.3	5.6
ϵ_3		.0028	.0051
ϕ_3	Degrees	21.6	19.6
w_3	ft/sec	481	626
(4) Reflection of ϵ_3 from hook			
Δt_{3-4}	Sec	.0007 (.0121)	.0006 (.0080)
$\epsilon_4 = \epsilon_3 - (\epsilon_1 - \epsilon_3)$		.0021	.0035
(5) Kink K_1 overtaken by ϵ_4 (disregarding secondary kinks)			
Δt_{4-5}	Sec	.0007 (.0128)	.0006 (.0086)
x_{K_1} (cumulative cross-deck travel)	Ft	7.0	6.4
ϵ_5		.0023	.0040
ϕ_5	Degrees	22.5	20.6
(6) Reflection of ϵ_5 from hook			
Δt_{5-6}	Sec	.0007 (.0135)	.0006 (.0092)
$\epsilon_6 = \epsilon_5 - (\epsilon_4 - \epsilon_5)$		.0025	.0045

*Elapsed time from impact in parenthesis.

	Units	Nominal	Maximum
(7) Kink K_1 overtaken by ϵ_6 (disregarding secondary kinks and change in ϕ)			
Δt_{6-7}	Sec	.0008 (.0143)	.0007 (.0099)
x_{K_1} (cumulative cross-deck travel)	Ft	7.7	7.2
ϵ_7		.0023	.0043
(8) Reflection of ϵ_7 from hook			
Δt_{7-8}	Sec	.0008 (.0151)	.0007 (.0106)
ϵ_8		.0021	.0041
(9) Continued interactions of kink K_1 and longitudinal waves reflected from the hook and the damper sheave tend to stabilize the strain and kink angle at approximately . . .			
ϵ_9		.0020	.0032
ϕ_9	Degrees	26.0	25.0
(10) Impact of kink K_1 on deck sheave			
t_{10}	Sec	.1440 (0.1440)	.0742 (.0742)
ϵ_{10} (kink K_2)		.0050	.0068
ϕ_{10} (kink K_2)	Degrees	13.1	13.8
w_{10} (kink K_2)	Ft/sec	786	922
(11) ϵ_{10} to sheave damper			
Δt_{10-11}	Sec	.0005 (0.1445)	.0005 (.0747)
$\epsilon_{11} \doteq 0.7\epsilon_{10}$		.0035	.0048
(12) ϵ_{11} overtakes kink K_2 (disregarding secondary kinks)			
Δt_{11-12}	Sec	.0005 (0.1450)	.0005 (.0752)
ϵ_{12}		.0035	.0049

	Units	Nominal	Maximum
ϕ_{12}	Degrees	14.3	15.0
w_{12}	Ft/sec	683	812
(13) ϵ_{12} to sheave damper			
Δt_{12-13}	Sec	.0005 (0.1455)	.0005 (.0757)
$\epsilon_{13} \doteq 0.7\epsilon_{12}$		.0025	.0034
(14) ϵ_{13} overtakes kink K_2 (disregarding secondary kinks and change in ϕ)			
Δt_{13-14}	Sec	.0005 (0.1460)	.0005 (.0762)
ϵ_{14}		.0025	.0035
(15) Reflection of ϵ_{10} from hook			
Δt_{10-15}	Sec	.0067 (0.1507)	.0046 (.0788)
$\epsilon_{15} = \epsilon_{10} - (\epsilon_9 - \epsilon_{10})$		.0080	.0104
(16) Reflection of ϵ_{12} from hook (after interaction with ϵ_{15})			
Δt_{12-16}	Sec	.0067 (0.1517)	.0046 (.0798)
$\epsilon_{16} = \epsilon_{15} - 2(\epsilon_{10} - \epsilon_{12})$		.0050	.0066
(17) Reflection of ϵ_{14} from hook (after interaction with ϵ_{15} and ϵ_{16})			
Δt_{14-17}	Sec	.0068 (0.1528)	.0047 (.0809)
$\epsilon_{17} = \epsilon_{16} - 2(\epsilon_{12} - \epsilon_{14})$		.0030	.0038
(18) Continued interactions of kink K_2 and longitudinal waves reflected from the hook and the damper sheave tend to stabilize the strain and kink angle at approximately...			
ϵ_{18}		.0022	.0030
ϕ_{18}	Degrees	18.0	17.0

	Units	Nominal	Maximum
(19) Slack pickup Purchase cable length, deck sheave to first engine sheave	Ft	150	150
Δt_{2-19}	Sec	.0150 (.0210)	.0150 (.0190)
Δt^* (slack pickup time)	Sec	0.1486 (0.1696)	0.2105 (0.2295)
(20) Reflection of ϵ_2 from anchor, assume $\epsilon_{20} = 2\epsilon_2$ (probably high)		.0050	.0094
(21) ϵ_{20} to sheave damper (assume no damper effect after this time) Approximate purchase cable length to deck sheave, $L = 2n'\lambda + 150$	Ft	925	925
Δt_{20-21}	Sec	.0925 (0.2621)	.0925 (0.3220)
$\epsilon_{21} = 0.7\epsilon_{20}$		.0035	.0066
(22) Reflection of ϵ_{21} from hook (assume negligible interaction with kink K_2) Δt_{21-22}	Sec	.0080 (0.2701)	*
$\epsilon_{22} = \epsilon_{21} - (\epsilon_{18} - \epsilon_{21})$		.0048	
(23) Impact of kink K_2 on hook (assume negligible decrease in aircraft velocity) Δt_{10-23}	Sec	0.1415 (0.2855)	.0836 (0.1578)
ϵ_{23}		.0105	.0067
ϕ_{23} kink K_3	Degrees	12.0	11.3
w_{23}	Ft/sec	540	651
(24) ϵ_{23} to sheave damper		**	
Δt_{23-24}	Sec		.0061 (0.1639)
$\epsilon_{24} \doteq 0.7\epsilon_{23}$			.0047

*Arrives after impact of kink K_2 on hook.

**Calculation discontinued at impact of kink on hook.

	Units	Nominal	Maximum
(25) ϵ_{24} meets kink K_3			
Δt_{24-25}	Sec		.0051 (0.1690)
ϵ_{25}			.0048
ϕ_{25}	Degrees		12.6
(26) Reflection of ϵ_{25} from hook			
Δt_{25-26}	Sec		.0007 (0.1697)
$\epsilon_{26} = \epsilon_{25} - (\epsilon_{23} - \epsilon_{25})$			.0029
(27) Assume continued interactions stabilize the strain and kink angle at approximately ...			
ϵ_{27}			.0041
ϕ_{27}	Degrees		14.0
(28) Impact of kink K_3 at deck sheave			
Δt_{23-28}	Sec		0.1207 (0.2785)
ϵ_{28}			.0051
ϕ_{28} kink K_4	Degrees		7.6
w_{28}	Ft/sec		889
(29) Reflection of ϵ_{28} from hook			
Δ_{28-29}	Sec		.0084 (0.2869)
$\epsilon_{29} = \epsilon_{28} - (\epsilon_{27} - \epsilon_{28})$			.0061
(30) ϵ_{29} meets kink K_4			
Δt_{29-30}	Sec		.0073 (0.2942)
ϵ_{30}			.0059

	Units	Nominal	Maximum
(31) Continued interactions of kink K_4 and longitudinal waves reflected from hook tend to stabilize strain and kink angle at approximately ...			
ϵ_{31}			.0060
ϕ_{31}	Degrees		7.0
(32) Reflection of ϵ_{21} from hook		*	
Δt_{21-32}	Sec		.0095 (0.3315)
$\epsilon_{32} = \epsilon_{21} - (\epsilon_{31} - \epsilon_{21})$			.0072
(33) Impact of kink K_4 on hook (assume negligible interaction between ϵ_{32} and K_4 prior to impact)			
Δt_{28-32}	Sec		0.1100 (0.3885)
ϵ_{33}			.0085

*Calculation discontinued at impact of kink on hook.

Comparison of the calculated tension (strain) versus time sequence with the results of tests (in particular, Shot No. 1023) performed at the Naval Air Testing Facility, Lakehurst, New Jersey, shows a qualitative (if not strictly quantitative) coincidence. Figures 15 and 16 show the idealized, calculated tension/time curves. Figure 17 is the cable tension/time curve for Shot No. 1023, 50,195-pound dead-load, 121 knots on-center, reproduced from Navy data. The elapsed time between events is longer by calculation, possibly owing to the estimated "average" kink velocity, to a higher actual acoustic velocity, or to different deck-pendant or purchase-cable lengths at Track 4 of the test site. The additional "hash" in Figure 17 is due to the many wave interactions ignored in the calculations.

These results appear to be quite realistic up to the time when the strain wave due to slack pickup is produced in the arresting engine. The resulting high stress as found in the calculations is not confirmed by experimental data. This computed stress is probably unrealistic due to an incorrect assumption as to the magnitude of the slack-pickup strain wave.

From Figure 16, then, the worst case for both peak stress and maximum change in stress can be estimated and these values used to examine the internal dynamics of the cable.

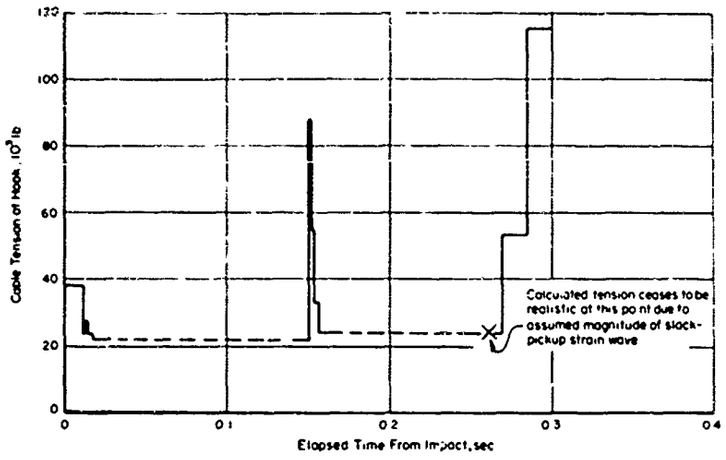

FIGURE 15. CALCULATED CABLE TENSION AT HOOK VERSUS TIME FOR NOMINAL (ON-CENTER) LANDING

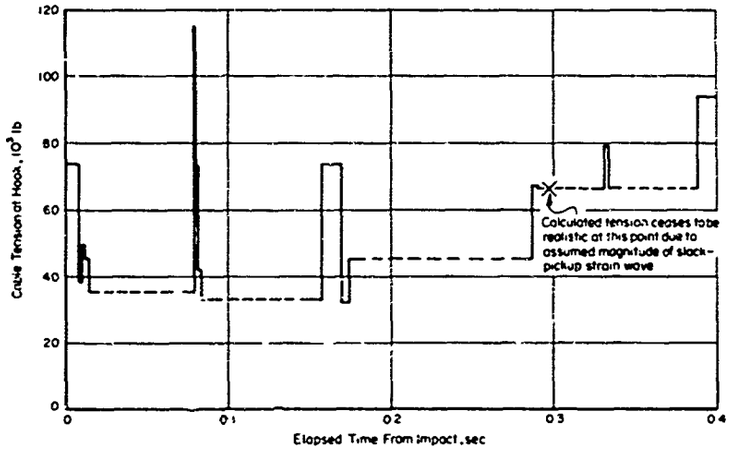

FIGURE 16. CALCULATED CABLE TENSION AT HOOK VERSUS TIME FOR MAXIMUM (OFF-CENTER, MISALIGNED) LANDING

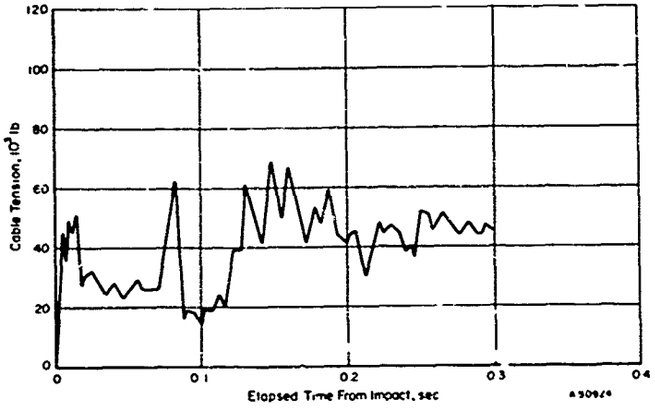

FIGURE 17. CABLE TENSION APPROXIMATED FROM NAVY DATA, SHOT NO. 1023 (ON-CENTER)

MAXIMUM CABLE TENSION

Idealized Peak Cable Tension

Using the idealized assumptions of negligible internal cable damping, perfect reflection of longitudinal waves from the hook, and an infinite rate of loading for the longitudinal waves, it has been found that the peak cable tension occurs at 0.0788 second after hook impact. This peak tension develops when longitudinal wave $\epsilon_{10} = 0.0068$ is reflected from the hook. Prior to this time the cable is under a stabilized strain of $\epsilon_9 = 0.0032$.

Longitudinal wave ϵ_{10} is produced when kink K_1 impacts on the deck sheave. The change in strain which then propagates toward the hook has a value of

$$\Delta\epsilon = \epsilon_{10} - \epsilon_9 = 0.0036 \quad .$$

If it is assumed that this wave is perfectly reflected from the hook, the final cable strain becomes

$$\epsilon_{15} = \epsilon_9 + 2\Delta\epsilon = 0.0104 \quad .$$

A Realistic Value of Peak Cable Tension

In the actual case, the cable is not fixed to the hook, and some portion of an impinging longitudinal wave will propagate around the hook while the remainder is reflected back. In this case, the maximum value of cable tension will be less than in the case of perfect reflection. The interaction of the hook and longitudinal waves has been investigated further in order to obtain a more realistic value of maximum cable tension.[33]

Effect of Cable Slippage Around Hook

The following analysis takes into account slippage of the cable around the hook during the impact of a longitudinal wave.

Assume that immediately prior to the impact of wave ϵ_{10} the cable is not moving with respect to the hook. The initial strain in the cable is ϵ_9 (see Figure 18).

After impact of the wave on the hook, two waves propagate away on opposite sides of the hook (see Figure 19). ϵ_p and ϵ_s are the valves of strain behind these waves on the port and starboard sides, respectively, and u_p and u_s are the corresponding cable velocities.

$$u_p - u_{10} = (\epsilon_{10} - \epsilon_p)\, c_o$$

and

$$u_{10} = c_o\Delta\epsilon = c_o(\epsilon_{10} - \epsilon_9) \quad ;$$

thus

$$u_p / c_o = \epsilon_9 + 2\Delta\epsilon - \epsilon_p \qquad (1)$$

also

$$u_s / c_o = \epsilon_s - \epsilon_9 \quad . \qquad (2)$$

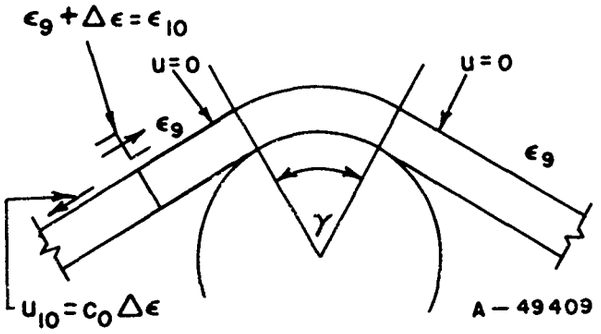

FIGURE 18. IMPACT OF LONGITUDINAL WAVE ON HOOK

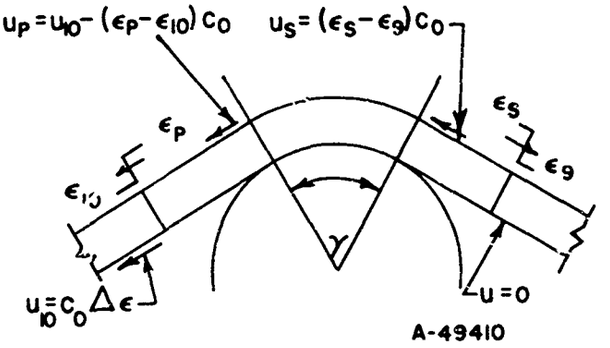

FIGURE 19. REFLECTION OF LONGITUDINAL WAVE FROM HOOK

Considering continuity of mass:

$$\rho_p A_p u_p = \rho_s A_s u_s$$

But

$$\rho_p = \frac{\rho_o}{1 + \epsilon_p}, \quad \rho_s = \frac{\rho_o}{1 + \epsilon_s}, \quad \text{and } A_p \sim A_s \quad ;$$

thus

$$\frac{u_p}{1 + \epsilon_p} = \frac{u_s}{1 + \epsilon_s} \quad . \tag{3}$$

Consideration of force equilibrium leads to

$$\frac{\epsilon_p}{\epsilon_s} = e^{f\gamma} \quad . \tag{4}$$

Combining Equations (1) through (4) results in

$$\epsilon_p^2 + 1/2 \left[1 - \epsilon_9 - 2\Delta\epsilon - (\epsilon_9 - 1) e^{f\gamma} \right] \epsilon_p - (\epsilon_9 + \Delta\epsilon) e^{f\gamma} = 0 \quad . \tag{5}$$

By substitution of $\epsilon_9 = 0.0032$ and $\Delta\epsilon = 0.0036$, Equation (5) becomes

$$\epsilon_p^2 + (0.4948 + 0.4984\, e^{f\gamma})\, \epsilon_p - 0.0068\, e^{f\gamma} = 0. \tag{6}$$

At the time the longitudinal wave reaches the hook, the angle of wrap of the cable around the hook is approximately twice the stabilized kink angle:

$$\gamma = \phi_s + \phi_p \sim 2\phi_9 = 50^\circ = 0.8727 \text{ radian} \quad .$$

Figure 20 shows how the final value of cable strain varies with the coefficient of friction, f.

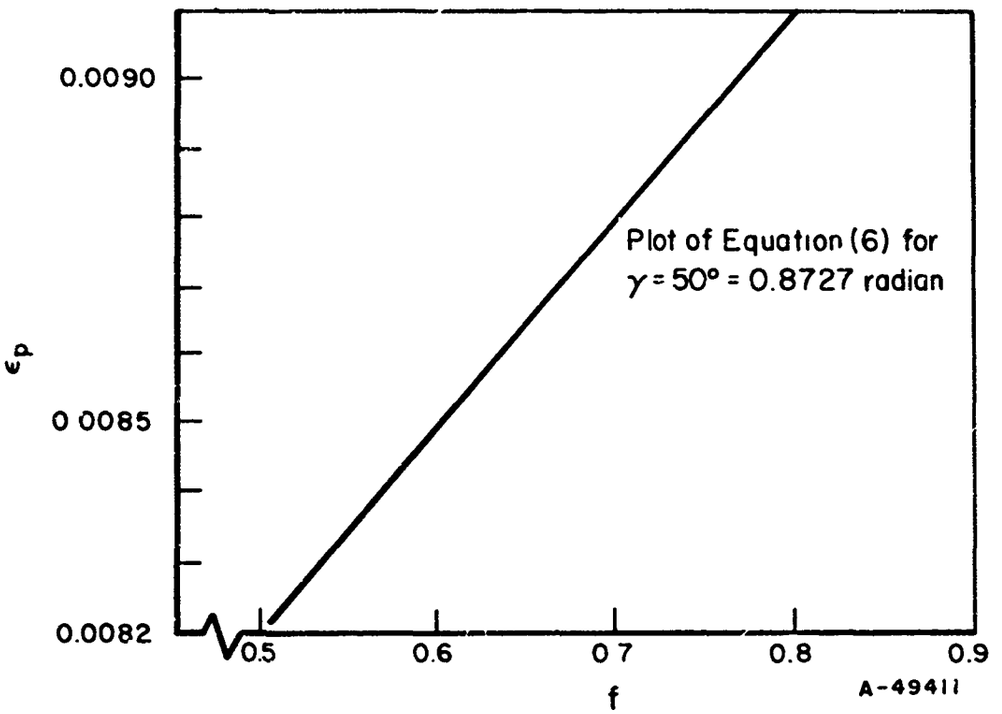

FIGURE 20. VARIATION OF CABLE STRAIN WITH COEFFICIENT OF FRICTION BETWEEN HOOK AND CABLE

Assuming a coefficient of friction of 0.6 results in $\epsilon_p = 0.0085$. This is much lower than the value of 0.0104 obtained assuming perfect wave reflection from the hook. The cable tension corresponding to this strain is

$$T = AE\epsilon = (0.87 \text{ in.}^2)(12.7 \times 10^6 \text{ lb/in.}^2)(0.0085) = 94,000 \text{ lb} \quad .$$

This value of maximum cable tension is probably still too large for two reasons:

(1) All damping has been neglected and waves have been assumed to propagate without attenuation.

(2) An infinite rate of loading for all longitudinal waves has been assumed.

Effect of Longitudinal-Wave Loading Rate

Inspection of the curve for the time history of tension (maximum conditions) reveals that immediately after the peak tension occurs in the cable, two more longitudinal

waves appear, each acting to reduce the tension. The wave producing the peak tension, ϵ_{10}, results from the impact of kink K_1 on the deck sheave. The two succeeding waves, ϵ_{11} and ϵ_{13}, are produced by sheave damper motion immediately following this impact. It is quite possible that the first of these two waves begins to develop before the full magnitude of ϵ_{10} is realized. This would be the case if the time required for buildup of ϵ_{10} exceeds the time interval between the initiation of waves ϵ_{10} and ϵ_{11}. The result of this situation would be a reduction in the magnitude of ϵ_{10} and, thus, a reduction in the magnitude of the peak cable tension.

Figure 21 shows the effects on the peak cable tension of a less than infinite loading rate for the longitudinal waves. Here it is assumed that the loading rates are the same for all waves.

It is, of course, impossible to predict the exact rate of loading for the various longitudinal waves. It can only be said that this rate will be by no means infinite as was assumed for the "ideal" case. It is equally as difficult to predict the exact coefficient of friction between the cable and the hook or the exact amount of wave attenuation. However, the combined effects of these factors will act to reduce the peak tension in the cable. Taking all this into account, the maximum cable tension will probably be no higher than 85,000 pounds for the landing conditions being considered.

THE INFLUENCE OF WIRE-ROPE CONSTRUCTIONAL VARIATIONS ON THE PEAK TENSILE STRESS DEVELOPED DURING AIRCRAFT ARRESTMENT

When considering possible modifications in cable design directed toward an improved cable life, it is desirable to know the effects of changes in the density, ρ, the elastic modulus, E, and the metallic cross section, A, of the cable. These variables affect both the initial tensile stress resulting from hook impact and the peak tensile stress produced by the impact of the first kink on the deck sheave. The following analysis provides approximate expressions for these stresses in terms of ρ, E, and A.

The initial tensile strain, ϵ_1, in the deck pendant produced by the impact of the hook may be found by[28]

$$\epsilon_1 (1 + \epsilon_1) = \left(\frac{V}{c_o}\right)^2 + \left[\sqrt{\epsilon_1 (1 + \epsilon_1)} - (\epsilon_1 - \epsilon_o)\right]^2 + 2\frac{V}{c_o}\left[\sqrt{\epsilon_1 (1 + \epsilon_1)} - (\epsilon_1 - \epsilon_o)\right] \cos \bar{\beta} ,$$

where ϵ_o is the cable strain existing prior to hook impact. Figure 22 shows the resulting strain for impact angles of 84 and 90 degrees and $\epsilon_o = 0$. Ringleb[38] has derived the following approximate expression for ϵ_1 for the case of transverse impact, $\bar{\beta} = 90$ degrees and $\epsilon_o = 0$:

$$\epsilon_1 = \sqrt[3]{1/4 \left(\frac{V}{c_o}\right)^4}, \quad (\bar{\beta} = 90 \text{ degrees}, \ \epsilon_o = 0) .$$

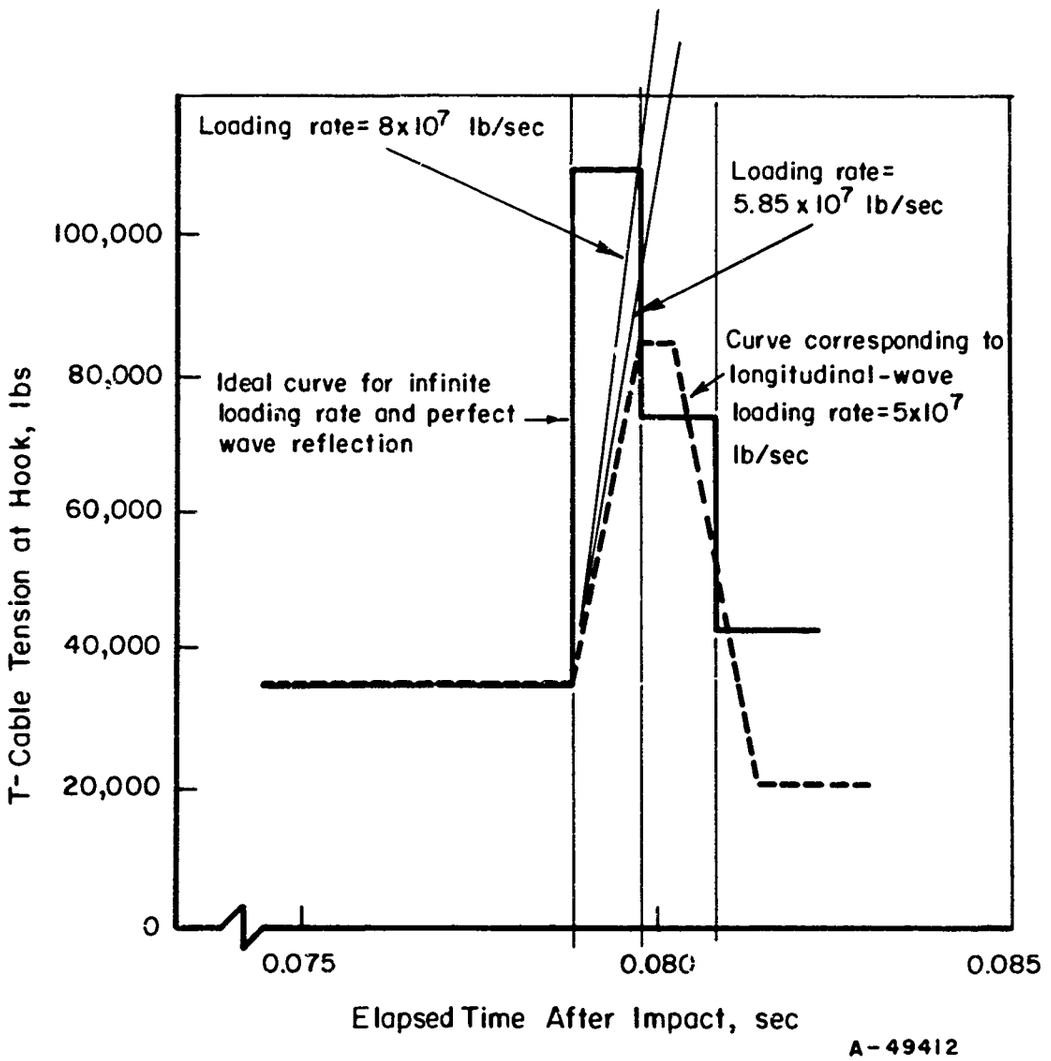

FIGURE 21. EFFECT OF LONGITUDINAL-WAVE LOADING RATE ON PEAK CABLE TENSION

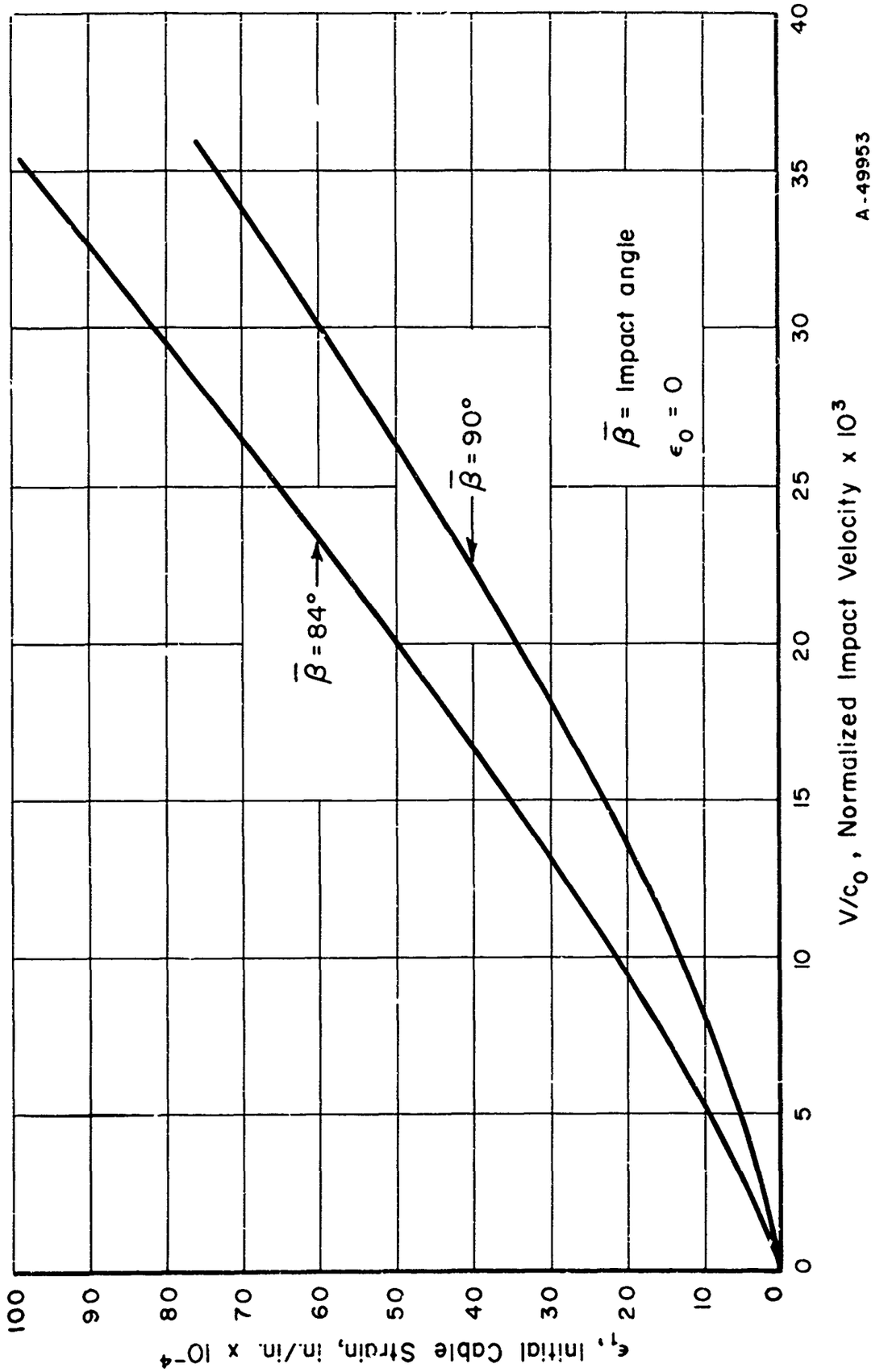

FIGURE 22. VARIATION OF INITIAL CABLE STRAIN WITH NORMALIZED IMPACT VELOCITY

For the "maximum" landing condition of $\bar{\beta}$ = 84 degrees, the authors have found the following expression to be an excellent approximation:

$$\epsilon_1 = 0.054\left(\frac{V}{c_o}\right)^{1.2}, \quad (\bar{\beta} = 84 \text{ degrees}, \ \epsilon_o = 0). \tag{7}$$

For a maximum impact velocity of 150 knots or 253 ft/sec, this becomes

$$\epsilon_1 = 413\left(\frac{1}{c_o}\right)^{1.2} = 413\left(\frac{\rho}{AEg}\right)^{0.6}, \tag{8}$$

where

A = rope metallic cross section, in.^{2}

g = acceleration due to gravity = 32.2 ft/sec^2

ρ = cable density, lb/ft

E = cable elastic modulus, lb/in.^{2}

In terms of cable stress, this is

$$\sigma_1 = 413\left(\frac{\rho}{Ag}\right)^{0.6} E^{0.4}. \tag{9}$$

Thus Equation (9) provides an expression for the initial cable stress in terms of ρ, A, and E for the "maximum" conditions of $\bar{\beta}$ = 84 degrees, and V = 150 knots = 253 ft/sec. This is the upper limit for the initial cable stress produced by the arrestment of present-day aircraft. In Figure 23, σ_1 has been plotted against E for three values of $\frac{\rho}{Ag}$. The value of $\frac{\rho}{Ag}$ = 0.1213 corresponds to the 1-3/8 inch, 6 x 30, flattened-strand deck pendants presently in use.

It is now possible to develop an approximate expression for the upper limit of the peak cable stress, the stress resulting from the impact of the first kink on the deck sheave and the subsequent reflection of a high-magnitude longitudinal wave from the hook. In this analysis, it will be assumed that the coefficient of friction between the rope and the hook is 0.6, as discussed previously. Again, V = 150 knots = 253 ft/sec, and $\bar{\beta}$ = 84 degrees.

The analytical methods used in the first section of this report have been repeated in order to obtain a history of cable strain for cable acoustic velocities of 8,000, 10,000, and 12,000 ft/sec. The possible ranges of the peak strain, ϵ_{15} (using the nomenclature of previous calculations), for these values of c_o are indicated in Figure 24. The initial cable strain due to hook impact is plotted as a solid line in this same figure. By trial it has been found that a good approximation to ϵ_{15} is given by

$$\epsilon_{15} = 80\,\epsilon_1^2 + 0.0050. \tag{10}$$

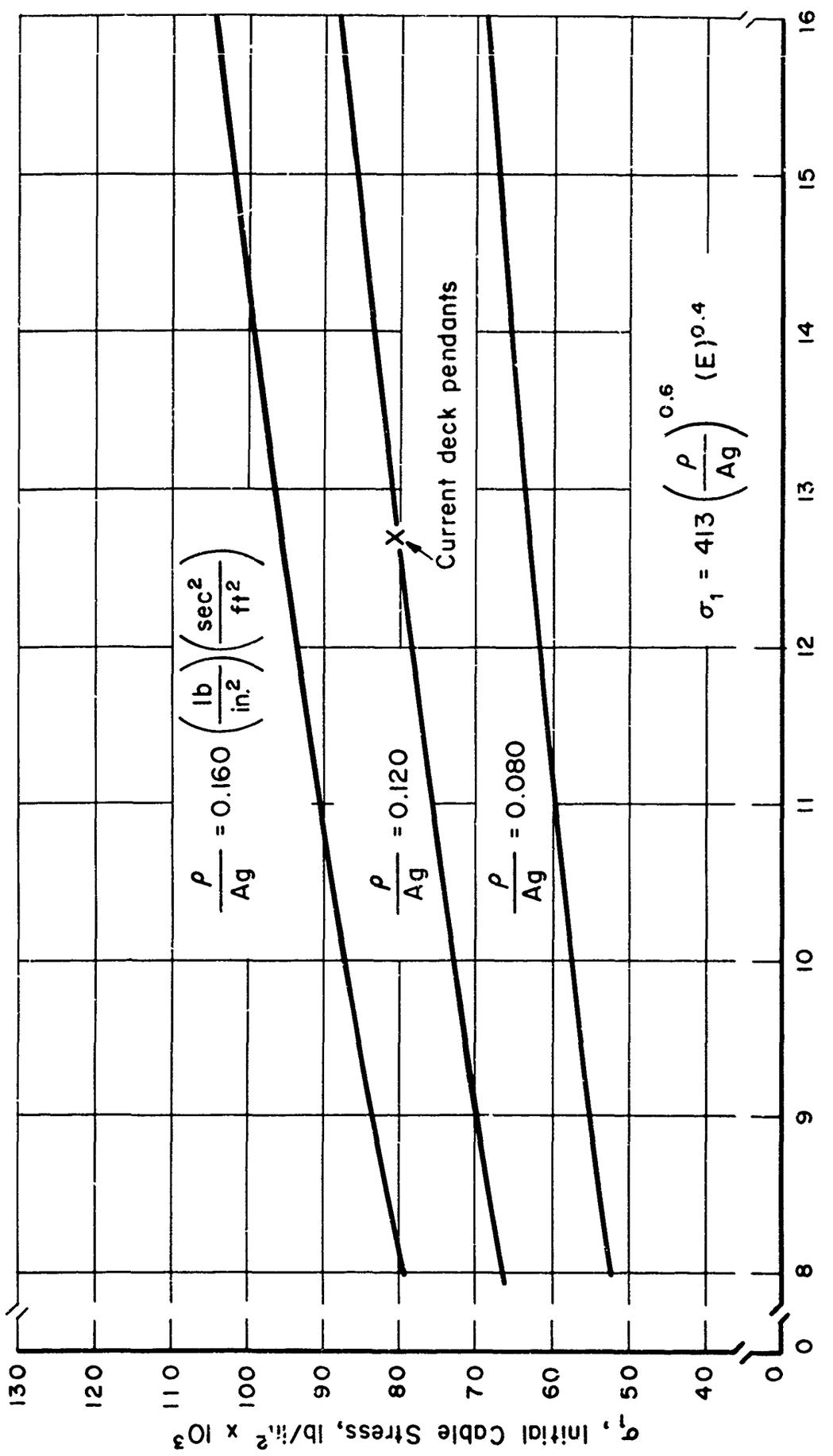

FIGURE 23. EFFECT OF CABLE CONSTRUCTION ON INITIAL TENSILE STRESS PRODUCED BY HOOK IMPACT

V = 150 knots = 253 ft/sec, $\bar{\beta}$ = 84 degrees.

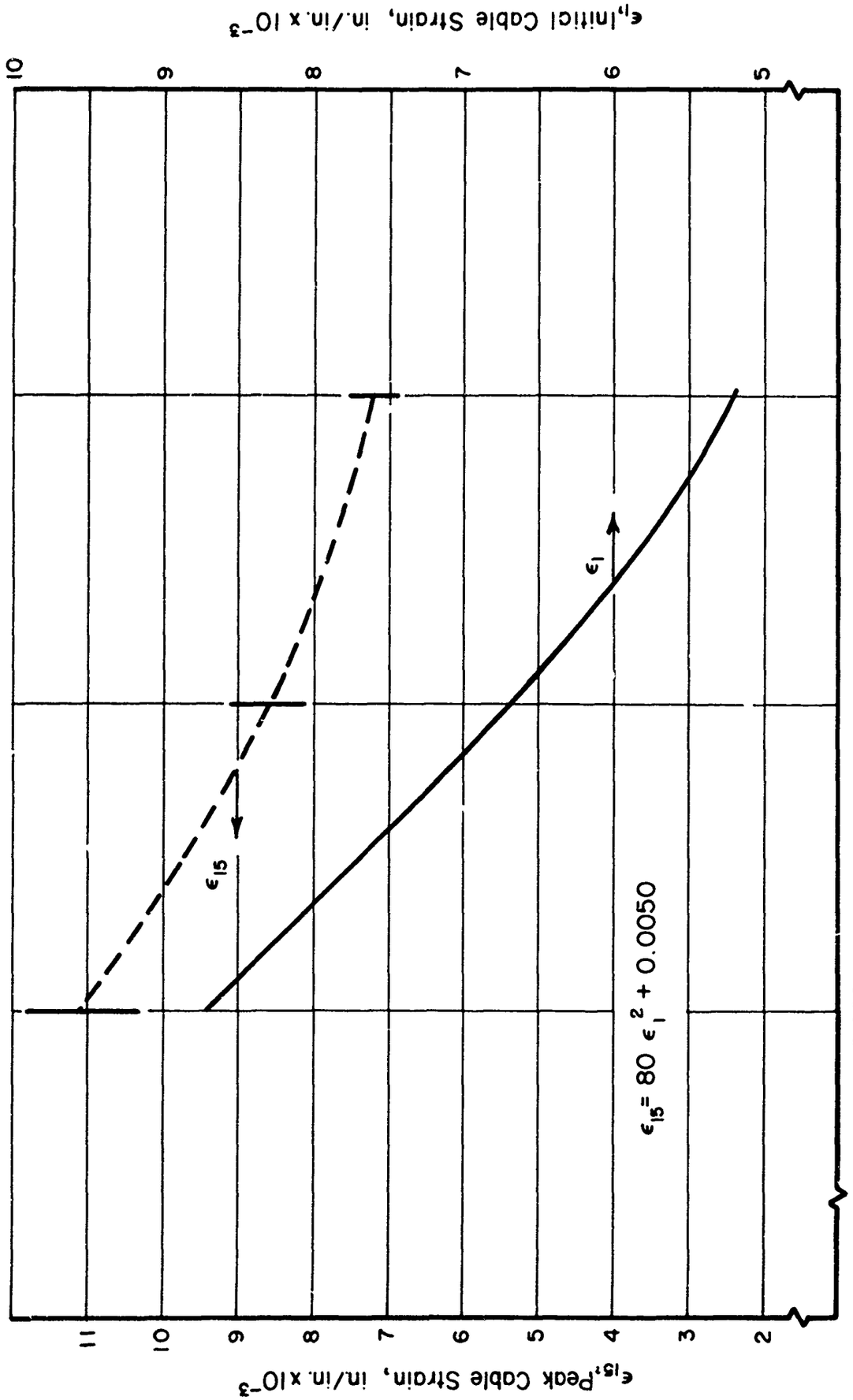

FIGURE 24. VARIATION OF CABLE STRAIN WITH ACOUSTIC VELOCITY

V = 150 knots = 253 ft/sec, $\bar{\beta}$ = 84 degrees.

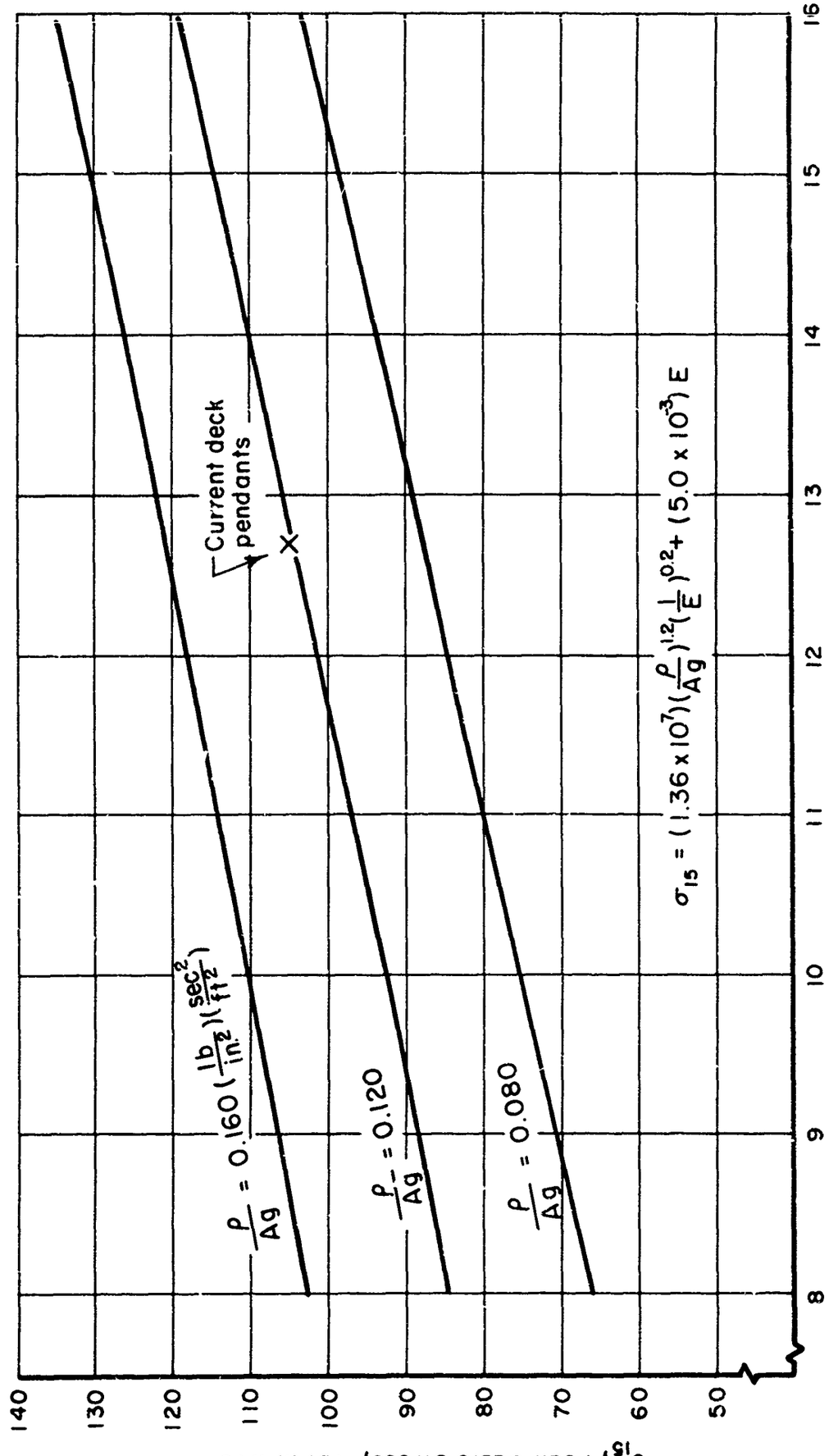

FIGURE 25. EFFECT OF CABLE CONSTRUCTION ON PEAK CABLE STRESS

V = 150 knots = 253 ft/sec, $\overline{\beta}$ = 84 degrees.

This equation is plotted as a dashed line in Figure 24. Combining Equations (8) and (10) gives

$$\epsilon_{15} = 1.36 \times 10^{7} \left(\frac{\rho}{AE_g}\right)^{1.2} + 0.0050 \quad . \tag{11}$$

In terms of cable stress, this is

$$\sigma_{15} = 1.36 \times 10^{7} \left(\frac{\rho}{Ag}\right)^{1.2} \left(\frac{1}{E}\right)^{0.2} + 5.0 \times 10^{-3} E \quad . \tag{12}$$

In Figure 25, Equation (12) has been used to plot the change in σ_{15} with E for three values of $\frac{\rho}{Ag}$. Using Figures 23 and 25 it is now possible to predict the effects of cable constructional variations on the maximum tensile stresses produced during an aircraft arrestment. It is interesting to note that a negligible difference exists between a round-strand and a flattened-strand deck-pendant construction. This fact verifies the theory that it is not the magnitude of the tensile stress that causes cable failure. It is, rather, the combination of abrasion and hook impact. Increased resistance to these latter conditions is the reason for the improved service obtained with flattened-strand Lang-lay rope.

INTERNAL LOADS AND STRESSES FOR FLATTENED STRAND WIRE ROPE

Cable Geometry

The type of cable presently in use for the deck pendant of aircraft arresting gear is 1-3/8 inch, 6 x 30, flattened strand, Lang-lay, Type G, fiber-core wire rope. Both the wires in the strands and the strands in the rope are right lay. Several cross sections of rope strands have been studied to determine the relative positions of the wires. A typical cross section of one strand is shown in Figure 26. The center six core wires of the strand in this particular type of rope are wound about a small hemp core. The resulting strand core is then pulled through a die to give it the final triangular cross section. Two outer layers of wire are then wrapped about the core to produce the final "flattened" strand. Six such strands are wrapped about a hemp core to produce the final wire rope.

Calculation of Tensile Loads on Wires in a Straight Rope

Using the strand cross section shown in Figure 27, it is possible to compute the tension in each individual wire as a function of axial tension on the straight strand. Neglected in this calculation are the effects of internal friction, rope bending, and radial contraction of the strand during axial loading.

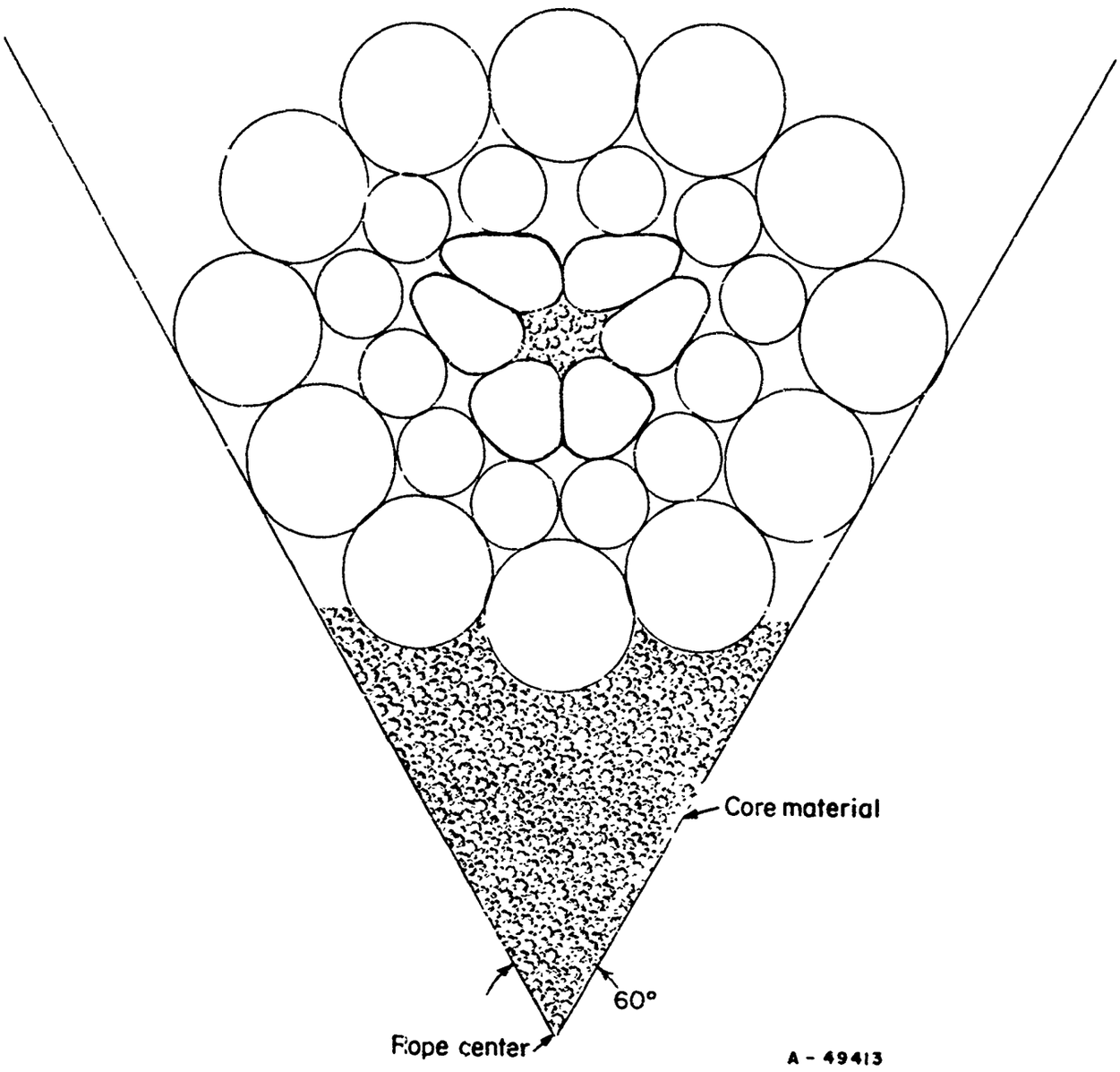

FIGURE 26. CROSS SECTION OF ONE STRAND OF A 6 x 30, FLATTENED STRAND, TYPE G WIRE ROPE

By direct measurement:

Wire Number	Number of Wires	Radius, r_i, in.	Wire Diameter, in.	Wire Area, in.^{2}
1	2	0.105	0.059	0.002734
2	4	0.112	0.059	0.002734
3	2	0.118	0.059	0.002734
4	2	0.131	0.059	0.002734
5	2	0.140	0 059	0.002734
6	1	0.168	0.099	0.007697
7	7	0.186	0.099	0.007697
8	2	0.208	0.099	0.007697
9	2	0.215	0.099	0.007697

d_c = diameter of core wires = 0.065 in.

A_c = area of each core wire = 0.003318 in.^{2}

α_c = lay angle of core wires = 20.0°

α_1 = lay angle of first layer = 4.3°

α_2 = lay angle of second layer = 6.92°

β = lay angle of strands = 18.4°.

The following analysis is based on work done by Hruska. (17)

Consider a strand subjected to axial tension. All wires are made of the same material.

α_c = lay angle of core wires

α_1 = lay angle of wires in first layer

α_2 = lay angle of wires in second layer

ℓ_1 = length of first-layer wires in one lay

ℓ_2 = length of second-layer wires in one lay

c' = length of strand center line = one lay

$\Delta\ell_1$ = elongation of wires in first layer

$\Delta\ell_2$ = elongation of wires in second layer

$\Delta c'$ = elongation of strand center line

S = 2π r where r is the average distance from the center of the strand to the center of the wires in one layer.

Using Figure 28, the following relationships are obtained:

$$(\ell_1 + \Delta\ell_1)^2 = S_1^2 + (c' + \Delta c')^2$$

$$\ell_1^2 + 2\ell_1 \Delta\ell_1 + (\Delta\ell_1)^2 = S_1^2 + c'^2 + 2c'\Delta c' + (\Delta c')^2$$

but

$$(\Delta\ell_1)^2 \sim (\Delta c')^2 \sim 0 \text{ and } \ell_1^2 = S_1^2 + c'^2.$$

Thus

$$\Delta\ell_1 = \Delta c' \; c'/\ell_1 = \Delta c' \cos\alpha_1 \; .$$

Also,

$$\Delta\ell_2 = \Delta c' \; c'/\ell_2 = \Delta c' \cos\alpha_2 \; .$$

Furthermore,

$$\sigma_1 = \epsilon_1 E = \frac{\Delta\ell_1}{\ell_1} E = \frac{c'\Delta c'}{\ell_1^2} E \text{ and } \sigma_2 = \epsilon_2 E = \frac{\Delta\ell_2}{\ell_2} E = \frac{c'\Delta c'}{\ell_2^2} E \; .$$

Thus

$$\sigma_1 \ell_1^2 = \sigma_2 \ell_2^2 \; .$$

But

$$\ell_1 = c'/\cos\alpha_1 \text{ and } \ell_2 = c'/\cos\alpha_2 \; .$$

Thus

$$\sigma_1 = \sigma_2 \frac{\cos^2\alpha_1}{\cos^2\alpha_2} \; .$$

Similarly

$$\sigma_1 = \sigma_c \frac{\cos^2\alpha_1}{\cos^2\alpha_c} \text{ and } \sigma_2 = \sigma_c \frac{\cos^2\alpha_2}{\cos^2\alpha_c} \; . \qquad (13)$$

The strand tension, T_s, may be expressed as

$$T_s = \sigma_c n_c A_c \cos\alpha_c + \sigma_1 n_1 A_1 \cos\alpha_1 + \sigma_2 n_2 A_2 \cos\alpha_2, \qquad (14)$$

where

A = the area of one wire

n = the number of wires in one layer

σ = the stress on the wires in one layer

α = the lay angle of the wires in one layer.

Combining (13) and (14)

$$T_s = \sigma_c \left[n_c A_c \cos\alpha_c + \frac{1}{\cos^2\alpha_c} (n_1 A_1 \cos^3\alpha_1 + n_2 A_2 \cos^3\alpha_2) \right] . \qquad (15)$$

By substitution of measured values, the stress on the core wires is found to be

$$\sigma_c = 6.334 \; T_s \; . \qquad (16)$$

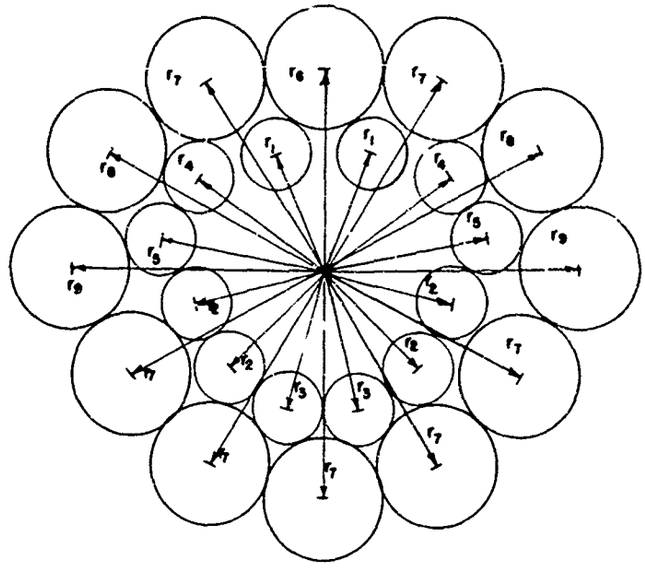

FIGURE 27. DISTANCE OF INDIVIDUAL WIRES FROM STRAND AXIS

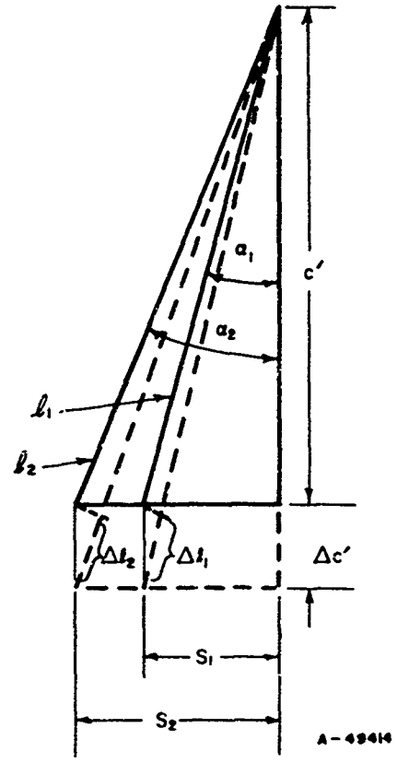

FIGURE 28. DIAGRAM RELATING WIRE ELONGATION TO STRAND ELONGATION

Using Equation (13) and the values for α_1 and α_2:

$$\sigma_1 = 7.133\ T_s \tag{17}$$

$$\sigma_2 = 7.069\ T_s\ . \tag{18}$$

If T is the tension on the rope in pounds, then the tension on each strand will be

$$T_s = \frac{T}{6 \cos \beta} \text{ or } T_s = 0.1756\ T\ . \tag{19}$$

Therefore, in terms of load on the rope,

$$\sigma_c = 1.1125\ T \tag{20}$$

$$\sigma_1 = 1.2529\ T \tag{21}$$

$$\sigma_2 = 1.2416\ T\ . \tag{22}$$

For T_{max} = 85,000 lb, the tensile stresses become

σ_c = 94,560 lb/in.^{2} (stress on strand-core wires)

σ_1 = 106,500 lb/in.^{2} (stress on first-layer wires)

σ_2 = 105,540 lb/in.^{2} (stress on second-layer wires) .

Again, this calculation neglects bending of the rope, radial contraction of the rope under axial loading, and internal rope friction. Each wire of a particular layer of wires is assumed to carry the same load.

As pointed out by Hruska[17], it is of no importance that in a wire rope the individual wires form a double helix. All wires in a cabled strand will elongate in the same manner as in the straight strand. This uniform elongation in the axial direction of the strand was the only assumption made in this analysis.

Calculation of Interstrand Contact Force for a Straight Rope

The radial force per unit length exerted by a helically wrapped strand due to tension on the strand is[31]

$$F_r = \frac{T_s}{\bar{r}} \sin^2 \beta \text{ (lb/in.)}\ ,$$

where

T_s = the load carried by each strand

β = the lay angle of the strands = 18.4°

$\bar{r}$ = the radius of the strand center line measured from the axis of the wire rope = 0.469 in.

Substituting values:

$$F_r = 0.0373\ T\ (lb/in.)\ ,$$

where

T is the tension on the wire rope .

Some portion of this radial force is supported by the hemp core and the remainder is supported by the two adjacent strands (see Figure 29). This interstrand force can

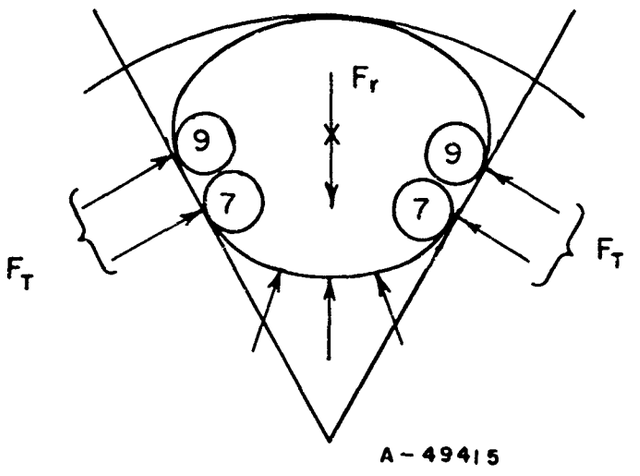

FIGURE 29. FORCES ACTING ON CABLE STRAND

produce high stresses in the contacting wires and lead to wire failure. In the 6 x 30, flattened strand, Lang-lay wire rope, it is found that the most critical condition exists where only two wires support this interstrand force.

In order to calculate the maximum possible interstrand force, it will be assumed that the core supports no part of the radial load. This assumption will allow the results of this work to be compared with those found by Chou[31] for a round strand, regular-lay wire rope. In this case the interstrand force is

$$F_T = \frac{F_r}{2 \sin 30^\circ} = F_r = 0.0373\ T\ (lb/in.)\ .$$

This force is supported by two wires in each region of interstrand contact. There are twelve of these outer wires in each strand, and their average lay angle and distance from the strand axis are 6.92° and 0.193 in., respectively. The length of one lay of these wires is then

$$c' = \frac{(2\pi)\ (0.193\ in.)}{\tan 6.92^\circ} = 9.9914\ in.$$

Therefore, there is $\frac{c'}{12} = 0.8326$ in. between each region of interstrand contact. The force per contact region, P_T', is then

$$P_T' = \left(0.0373\ T \frac{lb}{in.}\right)(0.8326\ in.) = 0.03106\ T\ lb\ .$$

For $T_{max} = 85{,}000$ lb:

$F_T = F_r = 3{,}170$ lb/in. (interstrand contact force)

$P_T' = 2{,}640$ lb (force per region of interstrand contact) .

These values are quite high due to the assumption that the core supports no part of the radial load.

The force P_T' is supported by four points of contact between the wires of the two strands. There is one point of contact between No. 7 wires, one point of contact between No. 9 wires, and two points where the No. 7 wire of one strand contacts the No. 9 wire of the other strand.

Calculation of Interstrand Crossed-Wire Contact Stresses for a Straight Rope

The stresses are computed at the points of interstrand contact by use of the general theory developed by Hertz. This theory is applicable only within the elastic limit of the material. Several authors have previously applied this theory to round strand, regular-lay wire rope.(4, 31, 43)

Radius of Curvature of Wires

Computation of the contact stresses requires knowledge of the radii of curvature of the wires at the points of contact. A method for making this calculation has been presented by Bert and Stein(44). The radius of curvature of a double helix, such as a wire in a rope, is given by

$$R' = \frac{(\bar{Z}' \cdot \bar{Z}')^{3/2}}{|\bar{Z}' \times \bar{Z}''|}\ ,$$

where

$$(\bar{Z}' \cdot \bar{Z}')^{3/2} = [(Z_1')^2 + (Z_2')^2 + (Z_3')^2]^{3/2}$$

$|\bar{Z}' \times \bar{Z}''|$ = the absolute value of

$$\begin{vmatrix} i & j & k \\ Z_1' & Z_2' & Z_3' \\ Z_1'' & Z_2'' & Z_3'' \end{vmatrix}$$

$$\frac{Z_1'}{\bar{r}} = \left(\frac{\tan\alpha}{\sin\beta} + \bar{R}\cos\beta\right)\sin\phi_o$$

$$\frac{Z_2'}{\bar{r}} = 1 + \left(\bar{R} + \frac{\tan\alpha}{\sin\beta}\right)\cos\phi_o$$

$$\frac{Z_3'}{\bar{r}} = \cot\beta - \tan\alpha\cos\phi_o$$

$$\frac{Z_1''}{\bar{r}} = -1 - \left(\frac{\tan^2\alpha}{\bar{R}\sin^2\beta} + \bar{R} + 2\frac{\tan\alpha}{\tan\beta}\right)\cos\phi_o$$

$$\frac{Z_2''}{\bar{r}} = \left(2\frac{\tan\alpha}{\sin\beta} + \frac{\tan^2\alpha}{\bar{R}\sin\beta\tan\beta} + \bar{R}\cos\beta\right)\sin\phi_o$$

$$\frac{Z_3''}{\bar{r}} = -\frac{\tan^2\alpha}{\bar{R}\sin\beta}\sin\phi_o$$

α = lay angle of wires in strand at the point of interstrand contact (positive when right lay)

β = lay angle of strands in rope (positive when right lay)

$\bar{r}$ = radius of strand center line, measured from axis of cable

r = radius of wire center line, measured from strand center line

R = radius of wire

$$\bar{R} = \frac{r + R}{\bar{r}}$$

ϕ_o = angle measured as shown in Figure 30.

For the flattened strand rope under consideration, the following values are obtained:

	Wire No. 7	Wire No. 9
α	6.66°	7.70°
β	18.4°	18.4°
$\bar{r}$	0.469 in.	0.469 in.
r	0.186 in.	0.215 in.
R	0.0495 in.	0.0495 in.
$\bar{R}$	0.50213	0.56397
ϕ_o	117.3°	89.3°

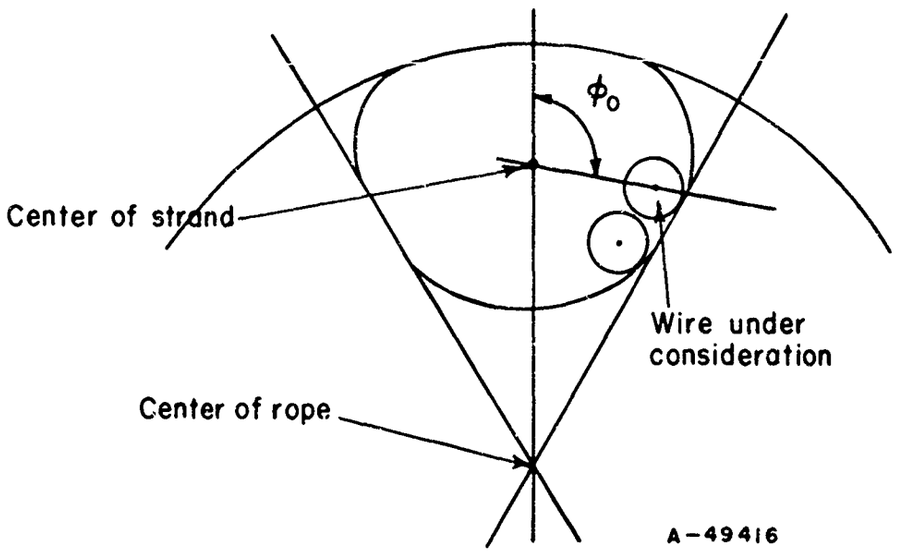

FIGURE 30. MEASUREMENT OF REFERENCE ANGLE USED FOR CALCULATING RADIUS OF CURVATURE

Here the values of α_7 and α_9 are found by using

$$\alpha_i = \arctan\left(\frac{r_i}{r_2'}\right)(\tan \alpha_2') \quad .$$

Substitution of these values into the formulas for radius of curvature gives

$$R_7' = 3.578 \text{ in. and } R_9' = 2.598 \text{ in.}$$

Elastic Contact Stresses

In order to solve for the stresses at the points of interstrand contact, it is necessary to solve the following simplified formulas[41]:

$$A = \frac{1}{2}\left(\frac{1}{R} + \frac{1}{R'}\right) - \frac{1}{2}\left(\frac{1}{R} - \frac{1}{R'}\right)\cos\theta$$

$$B = \frac{1}{2}\left(\frac{1}{R} + \frac{1}{R'}\right) + \frac{1}{2}\left(\frac{1}{R} - \frac{1}{R'}\right)\cos\theta$$

$$\Delta = \frac{2}{A+B}\left(\frac{1-\mu^2}{E}\right) ,$$

where

$$\mu = 0.26 \text{ and } E = 30 \times 10^6 \text{ lb/in.}^2 .$$

In these equations, θ is the crossing angle of two contacting wires. The lay angle of wire No. 7 on the outer surface of the strand may be found by

$$\alpha_7 = \arctan\left(\frac{r_7 + R_7}{r_2'} \tan \alpha_2'\right).$$

Similarly,

$$\alpha_9 = \arctan\left(\frac{r_9 + R_9}{r_2'} \tan \alpha_2'\right).$$

Substitution of measured values gives

$$\alpha_7 = 8.42° \text{ and } \alpha_9 = 9.45°.$$

Thus, the wires in contact between two strands cross at angles of

$$\theta_{(7-7)} = 2\alpha_7 = 16.84°$$

$$\theta_{(9-9)} = 2\alpha_9 = 18.90°$$

$$\theta_{(7-9)} = \alpha_7 + \alpha_9 = 17.87° \ .$$

Then, using Figure 183, page 356 of Reference (41) and the value of B/A, the appropriate values are found for the constants c_b, c_σ, c_τ, and c_G. Then

$$b = c_b \sqrt[3]{P\Delta} \ ,$$

where

P is the contact force.

Finally,

$$\sigma_{max} = -c_\sigma \left(\frac{b}{\Delta}\right) \text{ (maximum compressive stress)}$$

$$\tau_{max} = c_\tau \left(\frac{b}{\Delta}\right) \text{ (maximum shear stress)}$$

$$\tau_{Gmax} = c_G \left(\frac{b}{\Delta}\right) \text{ (maximum octahedral stress)} \ .$$

For the rope in question the following values are obtained.

	Wires No. 7 in Contact	Wires No. 9 in Contact
A	0.7067 in.$^{-1}$	0.919 in.$^{-1}$
B	19.7749 in.$^{-1}$	19.658 in.$^{-1}$
Δ	3.035×10^{-9} in.^{3}/lb	3.019×10^{-9} in.^{3}/lb
σ_{max}	$-1.777 \times 10^5 [P_{T(7-7)}]^{1/3}$ lb/in.^{2}	$-1.904 \times 10^5 [P_{T(9-9)}]^{1/3}$ lb/in.^{2}
τ_{max}	$0.5439 \times 10^5 [P_{T(7-7)}]^{1/3}$ lb/in.^{2}	$0.5889 \times 10^5 [P_{T(9-9)}]^{1/3}$ lb/in.^{2}
τ_{Gmax}	$0.4895 \times 10^5 [P_{T(7-7)}]^{1/3}$ lb/in.^{2}	$0.5300 \times 10^5 [P_{T(9-9)}]^{1/3}$ lb/in.^{2}

As a matter of convenience in solving for the contact stresses, it is not unreasonable to set $\sigma_{max(7-7)} = \sigma_{max(9-9)}$. This gives

$$P_{T(7-7)} = 1.23\, P_{T(9-9)} .$$

Assuming that

$$P_{T(7-7)} + P_{T(9-9)} = \frac{1}{2} P_T' = 0.01553\, T ,$$

the contact forces become

$$P_{T(7-7)} = 0.008565\, T \text{ (lb)}$$

$$P_{T(9-9)} = 0.006965\, T \text{ (lb)} .$$

Finally

$$\sigma_{max(7-7)} = -3.64 \times 10^4\, T^{1/3}$$

$$\tau_{max(7-7)} = 1.11 \times 10^4\, T^{1/3}$$

$$\tau_{Gmax(7-7)} = 1.00 \times 10^4\, T^{1/3}$$

$$\sigma_{max(9-9)} = -3.64 \times 10^4\, T^{1/3}$$

$$\tau_{max(9-9)} = 1.12 \times 10^4\, T^{1/3}$$

$$\tau_{Gmax(9-9)} = 1.01 \times 10^4\, T^{1/3} .$$

Nearly identical values exist for $\sigma_{max(7-9)}$, $\tau_{max(7-9)}$, and $\tau_{Gmax(7-9)}$.

For

$$T_{max} = 85{,}000 \text{ lb},$$

$$\sigma_{max} = -1.60 \times 10^6 \text{ lb/in.}^2 \text{ (maximum compressive stress)}$$

$$\tau_{max} = 4.92 \times 10^5 \text{ lb/in.}^2 \text{ (maximum shear stress)}$$

$$\tau_{Gmax} = 4.42 \times 10^5 \text{ lb/in.}^2 \text{ (maximum octahedral stress)} .$$

The magnitudes of these values indicate that at the points of interstrand contact the wires will be stressed above their elastic limit. Plastic flow will take place, and the wires will retain some permanent deformation. (Again note that the above values result from neglecting strand support by the core.)

Discussion of Contact Stresses

In the preceding analysis, the tensile stresses on the wires and the interstrand contact stress have been evaluated independently. The resulting values of σ_{max} and τ_{max} are acceptable, based on the theory used. However, the value of τ_{Gmax} has been calculated using an approximation which has a small effect on the accuracy of the result.

This maximum octahedral stress has been calculated assuming that the wires are subjected to compressive contact stress only. The tensile stress on the wires has been neglected. This approximation has only a small effect on the value of τ_{Gmax} for the particular magnitudes of stresses being considered here. But, as pointed out by Chou[30], the general effect of adding axial tension to the condition of crossed-wire contact is to reduce the indentation resistance of the wires.

The general conditions that exist at the points of interstrand crossed-wire contact may be described as follows. The load at the point of contact builds up until the yield point of the material is reached. At this time, as the contact force continues to increase, a region of plastic strain begins to develop. This region of plastic strain is in the interior of the wire and completely surrounded by material still in the elastic range. The plastic region continues to increase in size with increasing contact force until it reaches the surface of the wire. At this time the material begins to flow plastically. As the material flows outward, the effective area supporting the contact force increases, thus reducing the existing contact stress. For a given contact force above the "flow limit", the material will continue to flow until a new nonflow equilibrium condition is established. Again the strain will be of the "contained plastic" type. When the contact force is removed, the wire will now retain a permanent deformation.

The reduction in wire cross-sectional area caused by the plastic deformation in the regions of interstrand contact produces a stress concentration which contributes to tensile failure of the wires.

In the preceding analysis, no mention has been made of the parallel wire contact stresses that exist within each strand of the rope. This problem has been discussed in several papers[9, 30-32, 43] with the general conclusion that the parallel-wire contact stresses are not significant as compared with the interstrand crossed-wire contact stresses.

It is very significant that, for a tension of 85,000 lb, the values of the contact stresses for the flattened strand, Lang-lay rope are approximately 25 percent less than those values found by Chou[31] for the round strand, regular-lay rope of the same diameter. Looking at the situation from another point of view, the flattened strand, Lang-lay rope develops approximately the same interstrand contact stress at 85,000-lb tension as the round strand, regular-lay rope develops at 45,000-lb tension. This is an important factor contributing to the improved service obtained with flattened strand rope.

The primary reasons for this improved condition of contact stress are that the Lang-lay rope presently in use has wires of larger diameter in the outer layer of the strands and all lay angles are reduced. As a result of the reduced lay angles, the interstrand contact force, F_T, and the wire crossing angles, θ, are smaller. This reduced load applied to wires of larger diameter produces contact stresses of lower magnitude.

Effects of Bending Rope Around a Hook or Sheave

Increase in Interstrand Contact Stress

When a wire rope under tension, T, is bent around a sheave or hook, the radial force between the rope and the contacting body increases the interstrand contact force.

As pointed out by Chou[31], the force, F_H, exerted on the cable by the body is approximately

$$F_H = \frac{T}{R_H} \text{ (lb/in.)} ,$$

where R_H is the radius of the body. This equation applies if friction between the rope and the body is neglected and the wrap angle does not become too large.

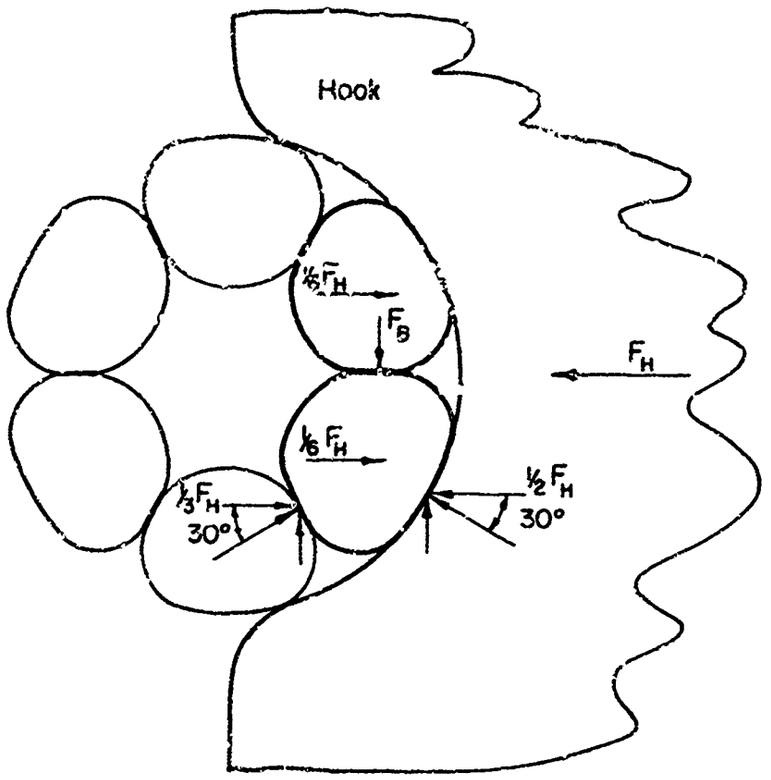

FIGURE 31. POSITION OF CABLE AGAINST HOOK PRODUCING THE MAXIMUM INTERSTRAND CONTACT FORCE

For the case of the rope being bent around an aircraft arresting hook, the most critical condition exists when two strands are in contact with the hook. This is the existing situation when the cable experiences the maximum dynamic tension. As shown in Figure 31, the maximum increase in the interstrand contact force, F_B, due to F_H, may be found by a summation of forces acting in the vertical direction on one strand:

$$\frac{1}{3} F_H \tan 30° + \frac{1}{2} F_H \tan 30° - F_B = 0$$

$$F_B = 0.481 F_H \text{ (lb/in.)} .$$

In this calculation it is assumed that each strand contributes one-sixth of the total load on the hook and the core carries no tensile or compressive load. Therefore, for $R_H = 3.25$ in.,

$$F_B = (0.481) \left(\frac{1}{3.25}\right) T = 0.1481 T \text{ (lb/in.)} .$$

Now the maximum interstrand contact force, F_{TB}, due to both tension and bending is

$$F_{TB} = F_T + F_B = 0.0373\ T + 0.1481\ T = 0.1854\ T\ (lb/in.)\ ,$$

where F_T was determined in previous calculations.

The maximum force per region of interstrand contact is, then,

$$P_{TB}' = (0.8326\ in.)\left(0.1854\ T\ \frac{lb}{in.}\right) = 0.1543\ T\ lb.$$

Using the assumptions of the previous section that $\sigma_{max(7-7)} = \sigma_{max(9-9)}$ and $P_{TB(7-7)} + P_{TB(9-9)} = \frac{1}{2} P_{TB}'$, the contact forces and contact stresses become

$$P_{TB(7-7)} = 0.0426\ T,$$

$$P_{TB(9-9)} = 0.0346\ T,$$

$$\sigma_{max} = -62,100\ T^{1/3}$$

$$\tau_{max} = 19,200\ T^{1/3}$$

$$\tau_{Gmax} = 17,300\ T^{1/3}\ \text{(tensile stress on wire neglected)}\ .$$

For

$$T_{max} = 85,000\ lb,$$

$$\sigma_{max} = -2.73 \times 10^{6}\ lb/in.^2$$

$$\tau_{max} = 8.44 \times 10^{5}\ lb/in.^2$$

$$\tau_{Gmax} = 7.61 \times 10^{5}\ lb/in.^2\ .$$

Again these values are approximately 25 percent lower than those for the round strand, regular-lay rope. It is found that the flattened strand rope develops approximately the same interstrand contact stresses with bending and 85,000-lb tension as the round strand rope develops with the same amount of bending and only 35,000-lb tension.

All previous calculations for wire tension and interstrand contact stress, while being applicable for any magnitude of rope tension, give a good indication of the state of stress in the rope only for small angles of rope bending. For this situation the cable tension remains equally divided among the strands, and bending stress in the wires remains small. In the case of aircraft arresting gear, the maximum cable tension does occur when the angle of cable wrap around the hook is small.

However, as time progresses, the bending stresses in the wires play a role of increasing importance as the cable wrap angle becomes larger. The maximum value of this bending stress may be calculated by $\sigma_b = \frac{MR}{I} = \left(\frac{EI}{R'}\right)\left(\frac{R}{I}\right) = \frac{ER}{R'}$, where R' is the radius to which the neutral axis of the wire is bent. However, in aircraft arresting gear, as the wrap angle increases the cable tension decreases rapidly. Very soon the interstrand contact stresses become less significant, and tension and bending become the important considerations. Of course, all stresses due to tension and bending will be aggravated by any interstrand wire notching that may have taken place. Therefore, interstrand contact stress is an important criterion in wire rope evaluation.

Contact Stresses Between Rope and Hook

In addition to interstrand contact stresses, it is necessary to consider also the contact stresses developed between the hook and the cable. The maximum contact force exists when these two bodies are in contact as shown in Figure 32. If $F_3 = F_4 = F_5 = \frac{1}{6} F_H$, and $F_1 + 2F_2 = F_H$, the maximum contact force becomes $F_1 = \frac{2}{3} F_H$.

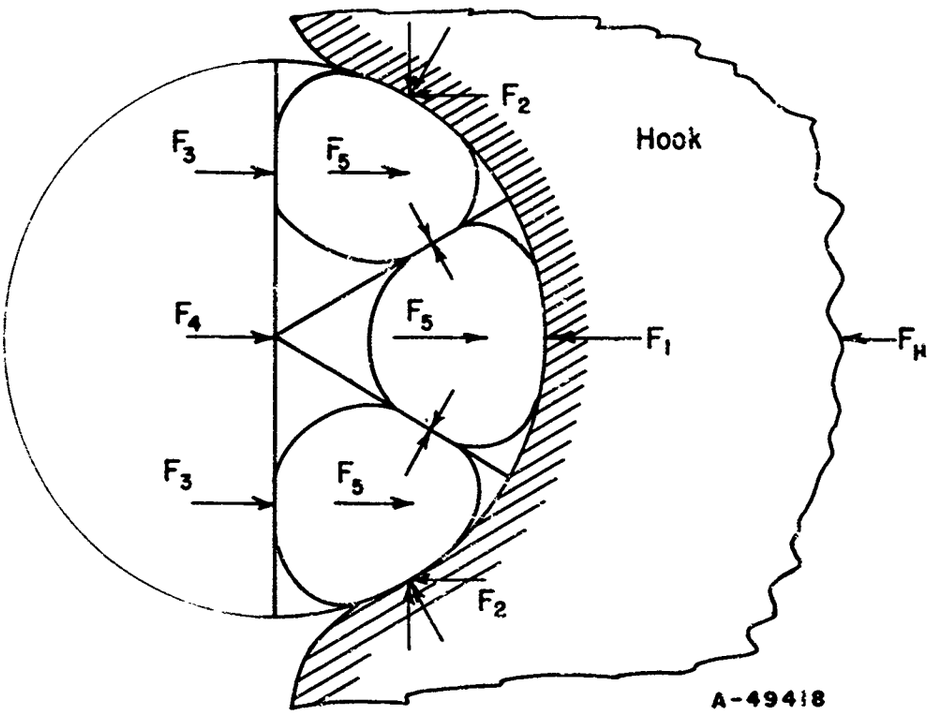

FIGURE 32. POSITION OF CABLE AGAINST HOOK PRODUCING THE MAXIMUM CONTACT FORCE BETWEEN THE HOOK AND ONE STRAND

The distance between strands, measured axially along the rope equals one-sixth of the strand lay length = $\left(\frac{1}{6}\right)$ (9.9914) = 1.665 in. Therefore, the contact force on each strand is (1.665 in.) $\left(F_1 \frac{\text{lb}}{\text{in.}}\right) = (1.665)\left(\frac{2}{3}\right) F_H = (1.665)\left(\frac{2}{3}\right)\left(\frac{T}{3.25}\right) = 0.3416$ T lb.

This load is carried by a minimum of three wires, so the load on each wire is 0.1139 T lb. The average contact length of each wire is approximately 2.2 in. resulting in a contact force of 0.0518 T lb/in.

In order to calculate the resulting contact stress between the hook and a No. 6 wire, the appropriate radii of curvature in the region of contact must be determined. The hook geometry is shown in Figure 33.

Wire No. 6 is in line contact with the hook channel at angle of 33.8° as shown in Figure 34.

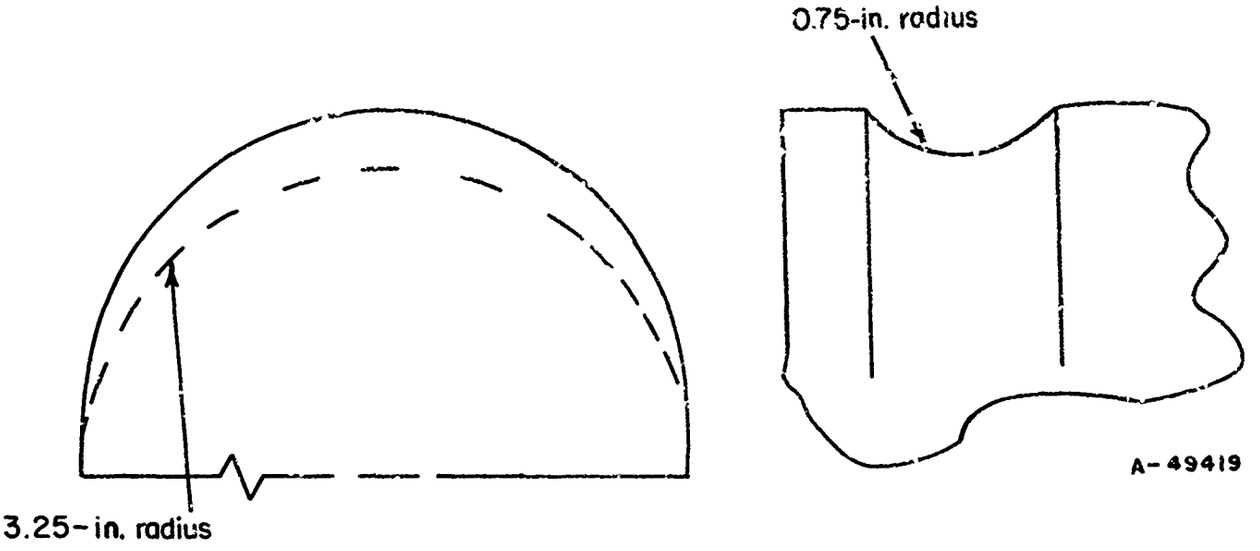

FIGURE 33. HOOK GEOMETRY

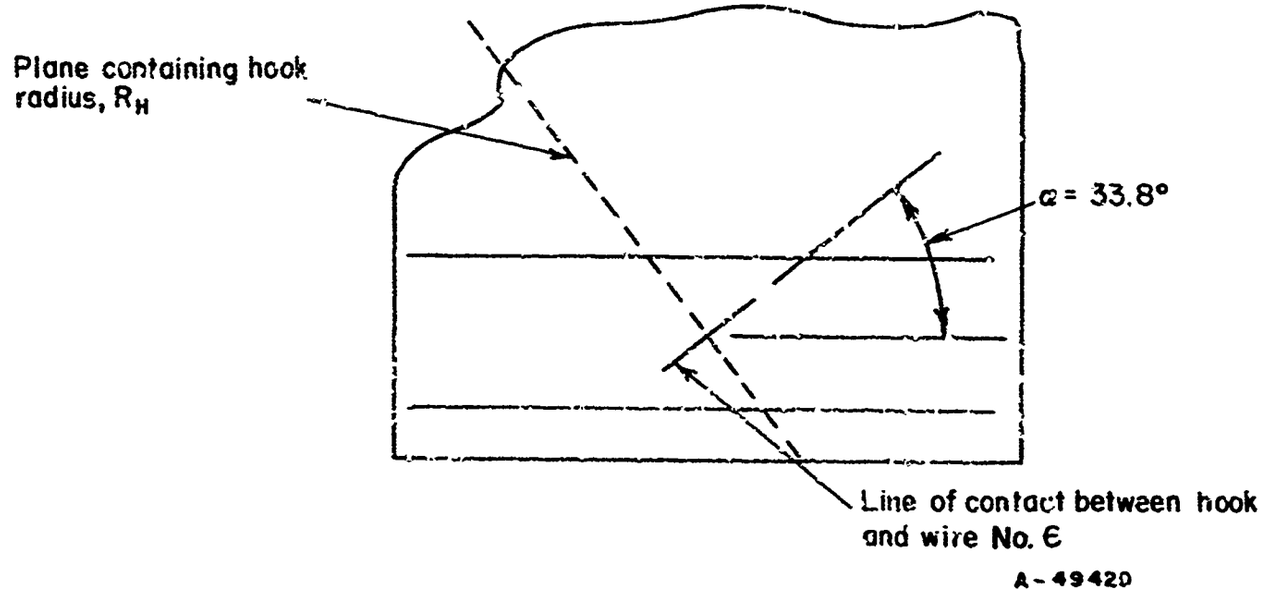

FIGURE 34. LINE OF CONTACT BETWEEN HOOK AND WIRE NO. 6

The radius of curvature of the hook, R_H, at the midpoint of the channel may be calculated using the general equations of Bert and Stein[44] and the following data:

$$\bar{r} = 4.00 \text{ in.} \qquad \alpha = -(90° - 33.8°) = -56.2°$$

$$r = 0.75 \text{ in.} \qquad \beta = 90°$$

$$\bar{R} = \frac{0.75}{4.00} = 0.1875 \qquad \phi_o = 180°$$

Here, the hook channel is treated in the same way as a cable strand with a lay angle of 90°. Substitution of the above values into the formulas for radius of curvature gives $R_H = 2.724$ in. This value was checked experimentally on a full-scale model of an arresting hook.

The necessary parameters for the Hertz contact stress calculations are found to be

$$A = 0$$

$$B = \frac{1}{2}\left(\frac{1}{R_6} + \frac{1}{R_H}\right) = \frac{1}{2}\left(\frac{1}{0.0495} + \frac{1}{-2.724}\right) = 10.2845$$

$$\Delta = \frac{1}{B}\left(\frac{1 - \mu_6^2}{E_6} + \frac{1 - \mu_H^2}{E_H}\right) = 6.044 \times 10^{-9} \ ,$$

in which $\mu_6 = \mu_H = 0.26$ and $E_6 = E_H = 30 \times 10^6$ lb/in.^{2} have been used.

$$b = \sqrt{\frac{2F\Delta}{\pi}} = \left[\frac{(2)(6.044)(10^{-9})(0.0518)\,T}{\pi}\right]^{1/2}$$

$$= 1.412 \times 10^{-5}\sqrt{T}$$

$$\frac{b}{\Delta} = \frac{1.412 \times 10^{-5}\sqrt{T}}{6.044 \times 10^{-9}} = 2336\sqrt{T}$$

$$\sigma_{max} \simeq -\frac{b}{\Delta} = -2336\sqrt{T} \text{ (lb/in.}^2\text{)}$$

$$\tau_{max} = 0.3\frac{b}{\Delta} = 701\sqrt{T} \text{ (lb/in.}^2\text{)}$$

$$\tau_{Gmax} = 0.27\frac{b}{\Delta} = 631\sqrt{T} \text{ (lb/in.}^2\text{)}$$

(tensile stress on wire neglected) .

For a cable tension of 85,000 lb,

$$\sigma_{max} = -6.811 \times 10^5 \text{ lb/in.}^2$$

$$\tau_{max} = 2.044 \times 10^5 \text{ lb/in.}^2$$

$$\tau_{Gmax} = 1.840 \times 10^5 \text{ lb/in.}^2$$

These values of contact stresses for the flattened strand, Lang-lay rope are approximately 30 percent less than the values obtained by Chou[31] for the round strand, regular-lay rope. It is found that a flattened strand rope under 85,000-lb tension develops the same contact stresses against the hook as a round strand rope develops at only 40,000-lb tension. This improved condition of contact stress is due to the increased number of wires touching the hook and the increase in length of wire contact.

It should be pointed out at this time that the preceding analysis of contact stresses between the cable and the hook assumes a condition of static tension on the cable. This approach is not unrealistic for times exceeding a few thousandths of a second after hook impact. However, the transient impact phenomenon that takes place at the instant of impact is an entirely different situation. This is investigated in a following section.

Comparison of Flattened Strand, Lang-Lay and Round Strand, Regular-Lay Ropes

The results of the previous calculations indicate the effects of certain wire rope constructional variations. It has been found that the interstrand contact stresses are much lower for the flattened strand, Lang-lay rope than for the round strand, regular-lay construction. This is true for either pure tension or a combination of tension and bending. Also, the contact stresses between the rope and hook are much lower for the flattened strand rope. The following table summarizes the results for a cable tension of 85,000 lb. The stresses for the round strand, regular-lay rope were obtained from work by Chou.[31]

Rope Construction:	Round Strand, Regular Lay			Flattened Strand, Lang Lay		
Contact Stress, lb/in.^{2} x 10^5	σ_{max}	τ_{max}	τ_{Gmax}	σ_{max}	τ_{max}	τ_{Gmax}*
Interstrand Stress for Tension Only	-19.8	6.6	5.9	-16.0	4.9	4.4
Interstrand Stress for Tension and Bending Around Hook	-35.2	11.6	10.1	-27.3	8.4	7.6
Stress Between Rope and Hook	-9.9	3.0	2.7	-6.8	2.0	1.8

*Note: These values for τ_{Gmax} neglect the stress component due to axial tension on the wires.

MODE OF FAILURE OF DECK PENDANT

Before it is possible to make appropriate recommendations for an improved wire-rope design, it is necessary to identify and understand the various factors which limit the life of existing ropes. The magnitudes of the contact stresses between two strands and between the rope and the hook were discussed previously. The effects of these stresses were indicated. However, due to the transverse impact loads imposed on deck pendants, there are other unexpected sources of cable deterioration that require careful consideration.

Upon examination of a 1-3/8-inch, round-strand, regular-lay deck pendant that had been discarded after moderate use during carrier landings, the following conditions were found to exist:

(1) Wire failure was not due to tension alone.

(2) Abrasion caused severe loss of wire material in regions where the cable scraped along the deck or moved across the hook due either to off-center or oblique engagements. This greatly reduced wire strength and probably promoted cracks in the wires where other investigators have found a layer of martensite formed by the heat of friction.

(3) Interstrand, crossed-wire contact stress caused some wire deformation and reduction in cross section. This was most severe in the section of the rope that experienced hook impact. Such wire deformation produces stress concentrations and reduces the load-carrying capacity of the wire.

(4) Intrastrand, parallel-wire contact stress in the sections of the rope that did not experience direct hook impact was not sufficient to cause significant wire deformation or loss of strength.

(5) Intrastrand, parallel-wire contact stress in the region of hook-cable impact was sufficient to cause axial shear failure of the wires.

(6) Almost without exception, wire failure was due to either initial impact shear (Condition 5 above) or a combination of abrasion and impact shear. No wire failures were found due to interstrand wire notching.

Of these observations, the last requires additional examination. This situation of wire failure due to shear is unlike that found in other wire-rope applications. Figure 35 shows the cross section of one strand of a 6 x 25, round-strand deck pendant at the instant of contact with the arresting hook. The initial impact force is transmitted from the outer wire to one "inner" wire and one "filler" wire. These two wires in turn transmit the force to the remainder of the strand wires. As shown in Figure 36, the relatively small-diameter filler wire must support a very large force at the instant of hook-cable impact. Experience has shown that this force is sufficient to cause the filler wire to fail in shear for some distance along the axis of the wire. Typical filler-wire failures are shown in Figure 37. Failures up to 0.9 inch long have been observed. In many cases, the filler wires have been completely severed although there were no wire failures visible on the surface of the rope.

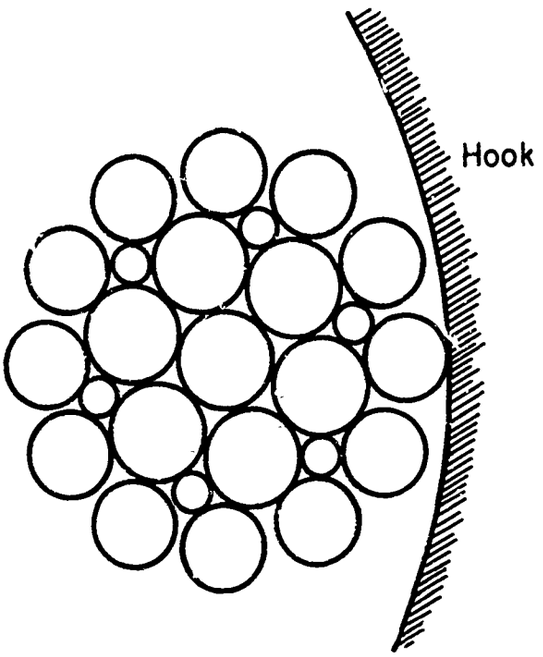

FIGURE 35. HOOK AND ROUND STRAND AT INSTANT OF IMPACT

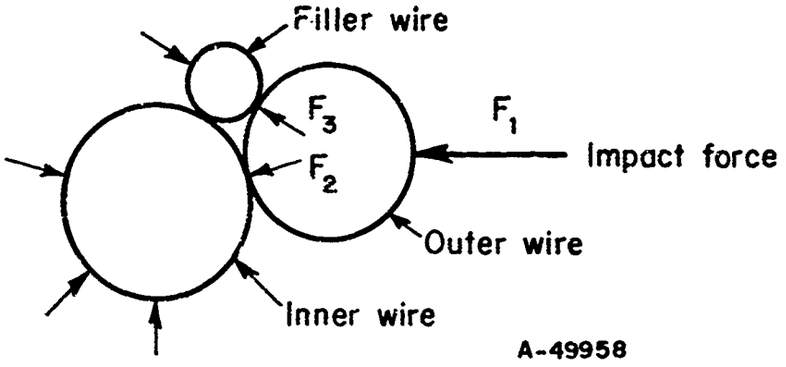

FIGURE 36. DISTRIBUTION OF IMPACT FORCE THROUGH CABLE STRAND

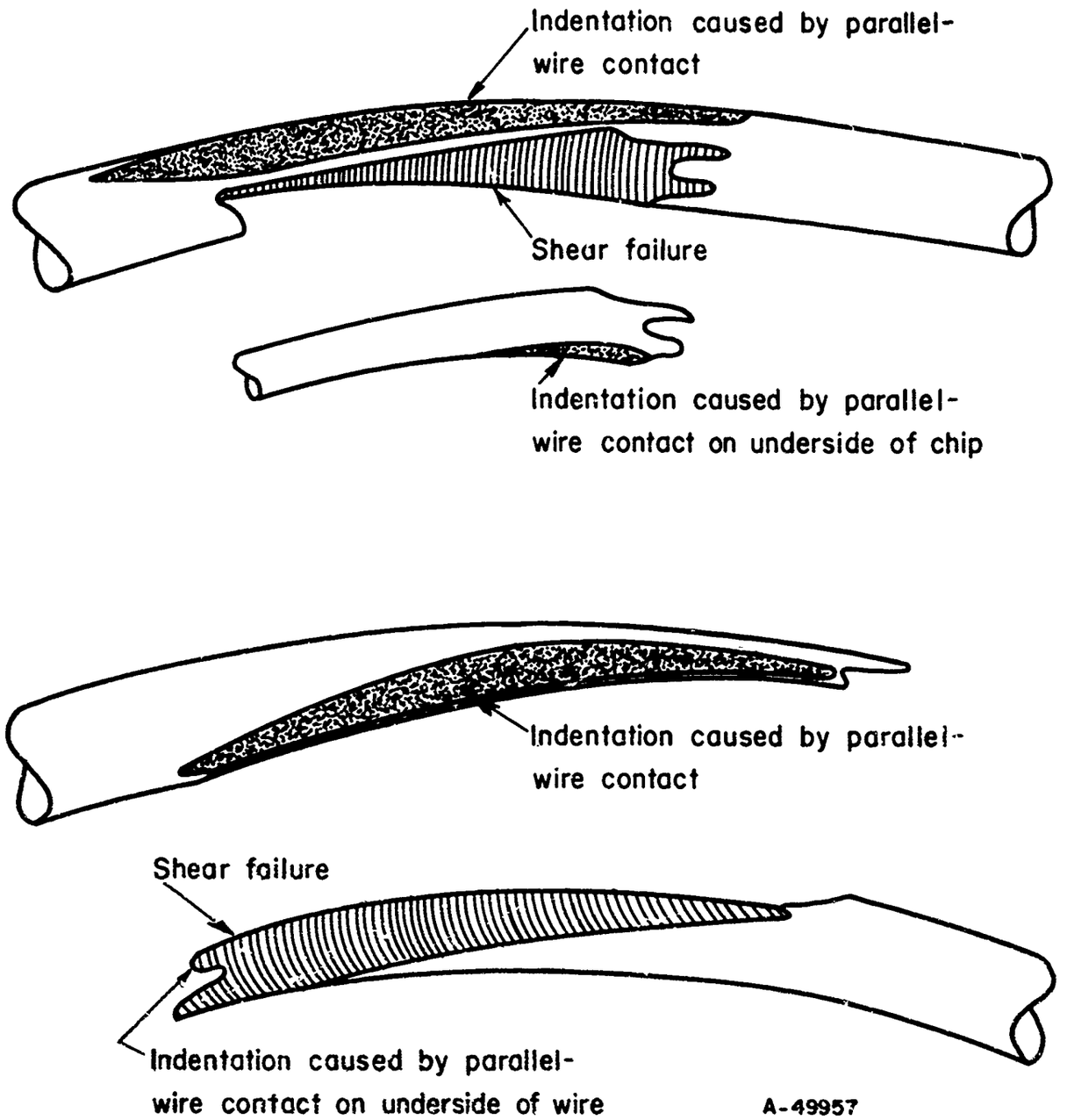

FIGURE 37. TYPICAL FILLER-WIRE FAILURES

The failure of filler wires is not critical from the standpoint of loss in over-all cable tensile strength. However, these failures result in a loss of support for the outer wires of the strand. When this happens, the outer wires are placed in a condition that leads to their eventual failure in shear. After a sufficient loss of material through abrasion, an outer wire cross section is reduced to a point that allows the subsequent impact force to cause a shear failure very similar to those observed in the filler wires. This condition is shown in Figure 38. In this case, the loss of over-all cable tensile strength produced by a number of these failures is sufficient to warrant replacement of the peak pendant. Thus, it is seen that a combination of abrasion and hock impact is responsible for the limited service life of round-strand, regular-lay deck pendants.

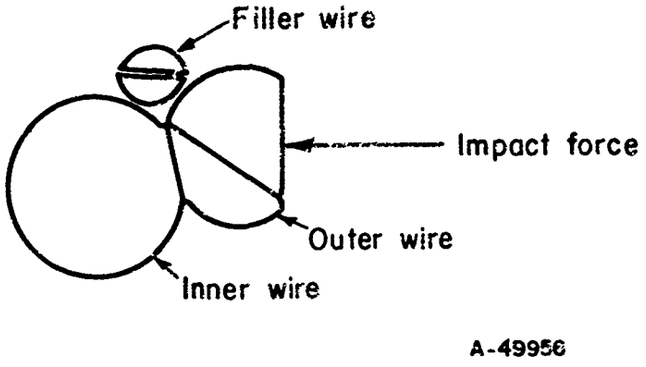

FIGURE 38. SHEAR FAILURE OF BOTH THE FILLER WIRE AND THE OUTER WIRE

The failure of filler wires could be caused in one of the two following ways:

(1) The high compressive force acting on a filler wire could produce a shear failure along a plane at 45 degrees to the direction of the force, as shown in Figure 39.

(2) Plastic deformation of the filler wire due to repeated impact loading could result in the wire's being placed in a condition favoring direct shear failure by a subsequent impact force, as shown in Figure 40.

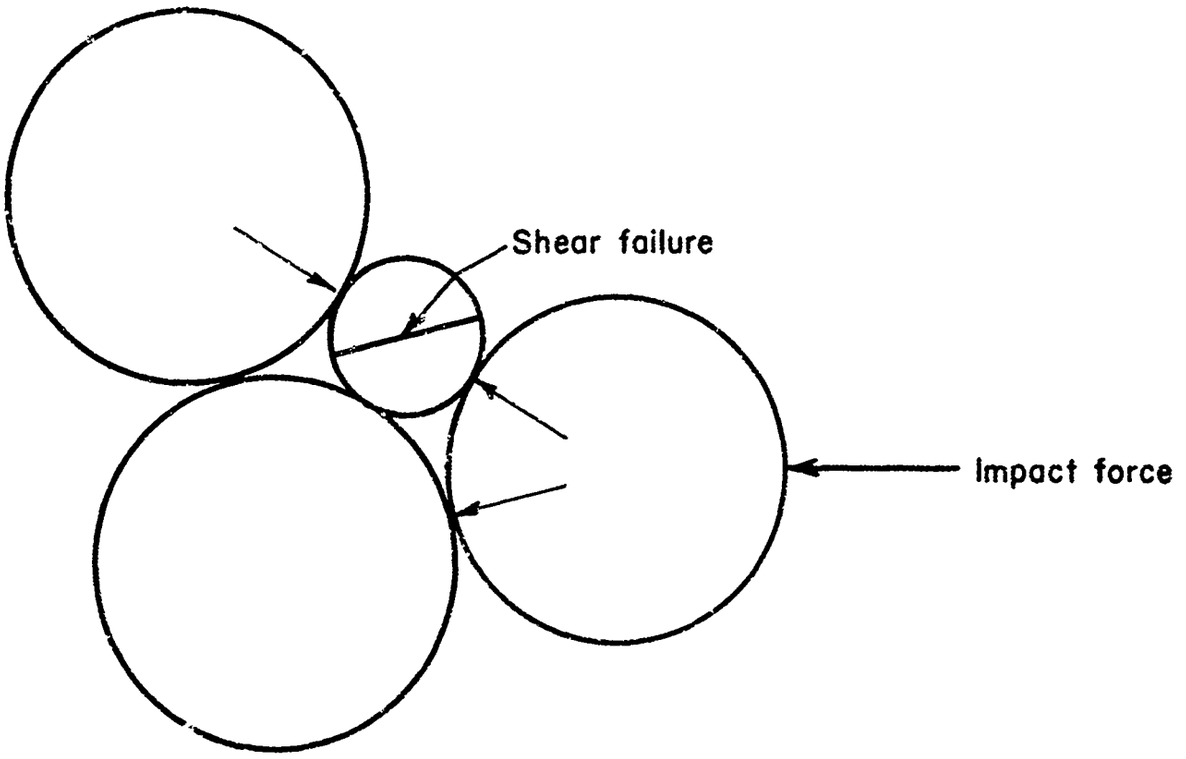

FIGURE 39. FILLER WIRE UNDER COMPRESSIVE FORCE

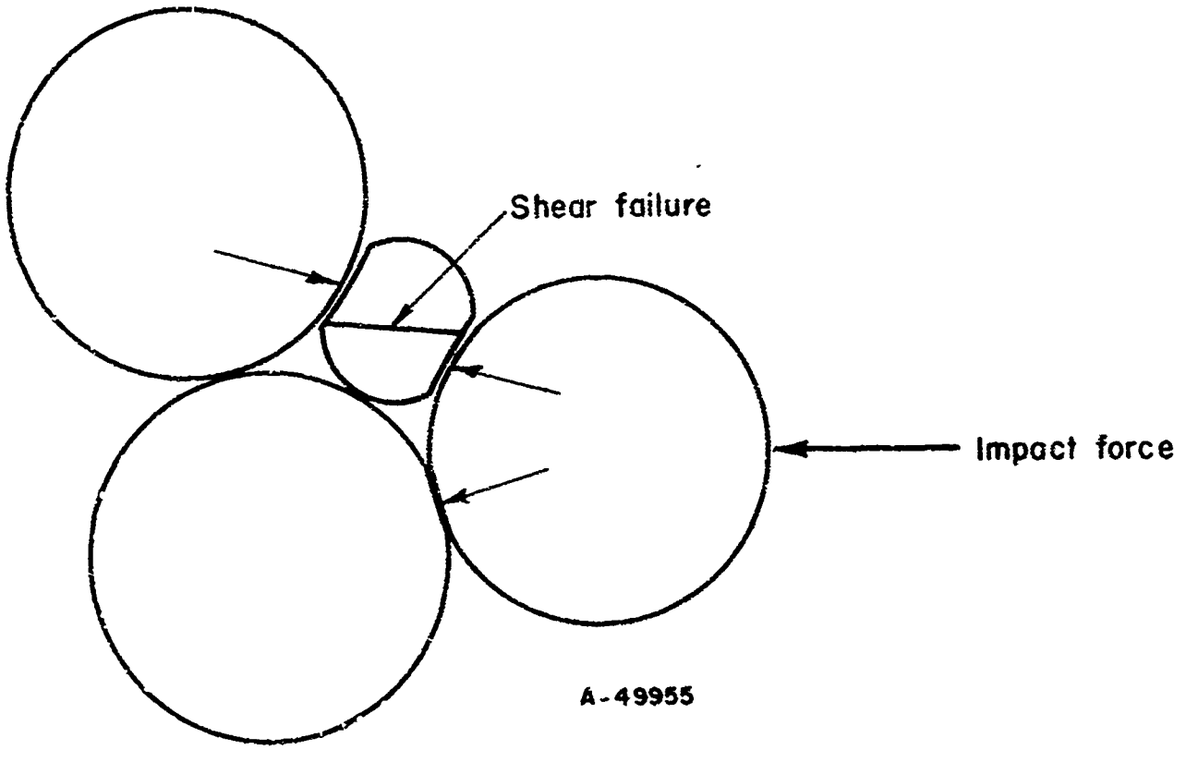

FIGURE 40. FILLER WIRE UNDER SHEARING FORCE

The compressive force required to cause the first type of shear failure is

$$F_3 = (d)(\sigma_{yp}) = (d)(2\tau_{yp}) = (0.040)(2)(10^5) = 8,000 \text{ lb/in.} \quad ,$$

where

d = diameter of filler wire = 0.040 in.

σ_{yp} = yield-point stress in compression = 200,000 lb/in.^{2}

τ_{yp} = yield-point stress in shear - 100,000 lb/in.^{2}

The shearing force required to cause the second type of shear failure is

$$F_3 = (d)(\tau_{yp}) = (0.040)(10^5) = 4,000 \text{ lb/in.}$$

Since the actual failure is probably caused by a combination of these two conditions, it is reasonable to assume a value of F_3 = 6,000 lb/in. As shown in Figure 41, the average force applied to the strand to cause failure is then

$$F_1 = 2.65\ F_3 = (2.65)(6,000) = 15,900 \text{ lb/in.}$$

For the case of hook impact on a flattened-strand rope, as shown in Figure 42, a similar condition exists. Here, one of the second-layer wires supports slightly less than one-half of the total impact force just as the filler wire did in the round-strand rope. However, in this case, the second-layer wire is larger in diameter than a filler wire, and it supports a more evenly distributed load. As a result, the shear failure of internal wires in flattened-strand rope is not a serious problem as it is in round-strand rope. Also, since improved internal support is maintained for the outer wires, the flattened strand is more resistant to failure of the outer wires due to hook impact.

For the flattened-strand construction, the compressive force required to cause a shear failure of one of the second-layer wires is

$$F = (d)(\sigma_{yp}) = (0.059)(2 \times 10^5) = 11,800 \text{ lb/in.}$$

Similarly, the shearing force required to cause a shear failure is

$$F = (d)(\tau_{yp}) = (0.059)(10^5) = 5,900 \text{ lb/in.}$$

These values are 47.5 per cent higher than the respective forces required to produce a shear failure in a filler wire of a round-strand rope.

The preceding discussion points out the importance of strand geometry on the service life of a deck pendant. The sizes and positions of the wires in the strands determine to a great extent the impact resistance of the rope. This situation should be examined thoroughly for any new wire-rope design.

Since the flattened strand, Lang-lay construction provides improved impact resistance for deck pendants, the deterioration of this type of cable is caused mainly by abrasion. Examination of a deck pendant that had experienced six arrests of a 50,000-pound dead load, impacting at 20 feet off center with velocities of 98, 113, 110, 117, 129, and 138 knots, revealed some evidence of damage due to direct impact. However, it appeared that the several broken wires had failed mainly due to abrasion.

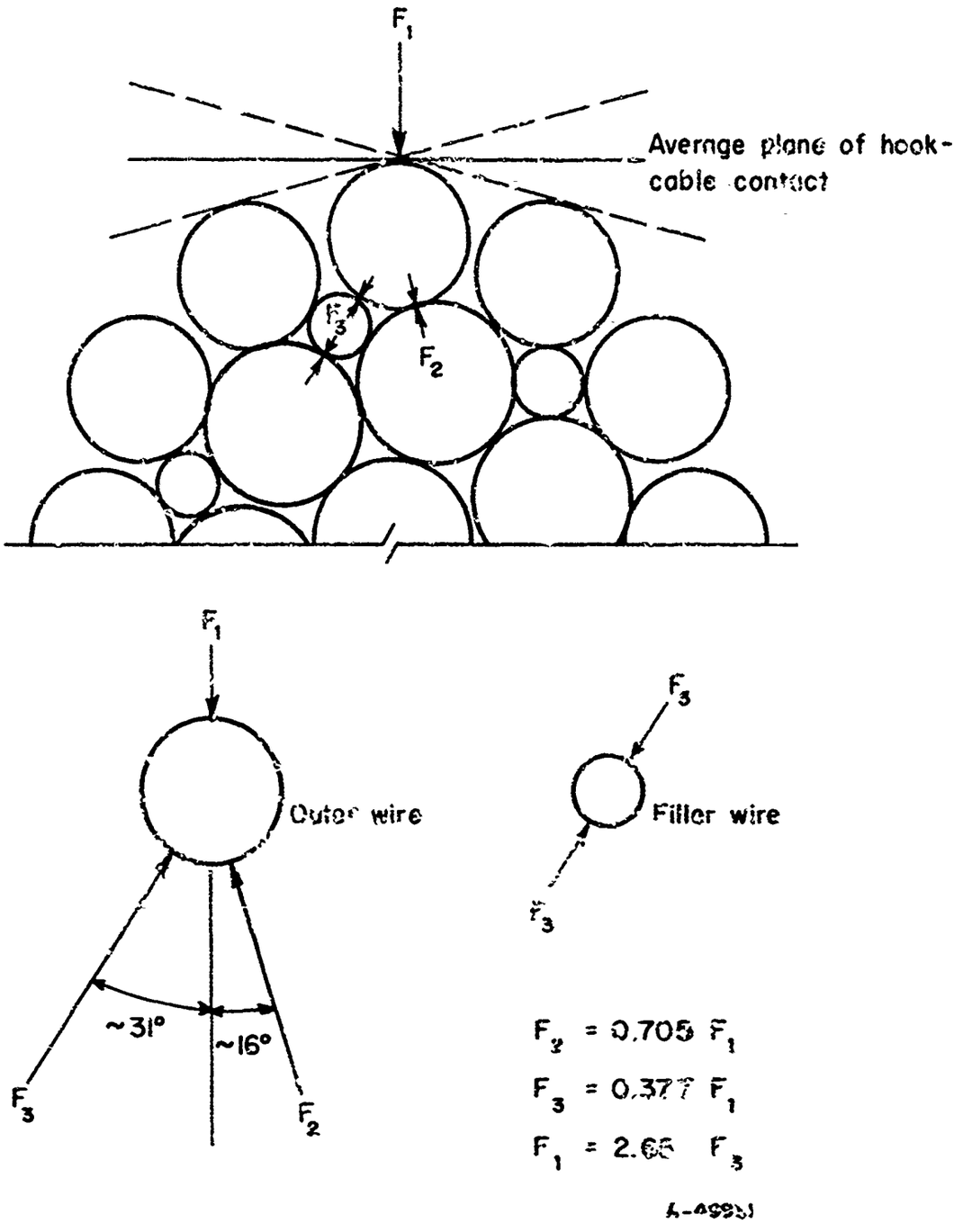

FIGURE 41. INTERWIRE CONTACT FORCES DUE TO HOOK-CABLE IMPACT

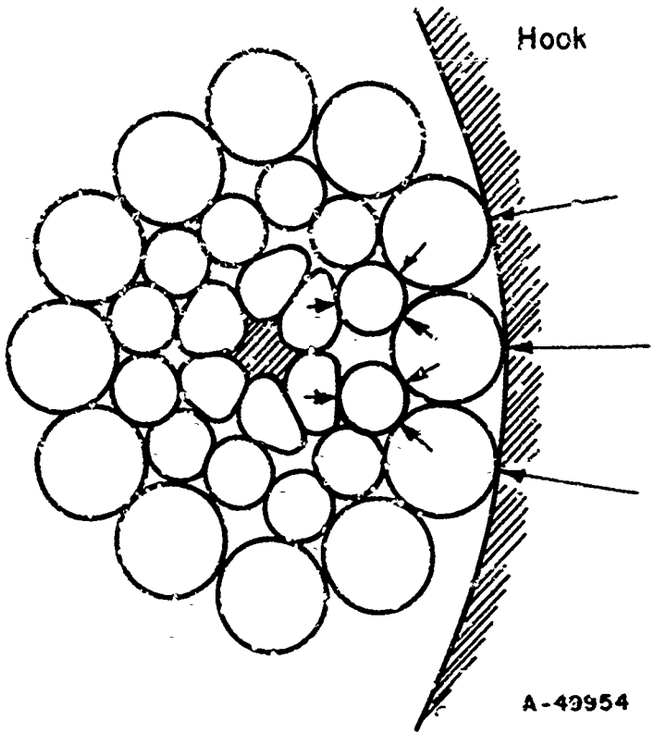

FIGURE 42. HOOK AND FLATTENED STRAND AT INSTANT OF IMPACT

CONTACT FORCE PRODUCED BY IMPACT OF HOOK ON DECK PENDANT

Previously in this report, the problem of the contact force between the hook and the cable was solved assuming a static condition. No attempt was made to investigate the transient-impact phenomenon that exists at the instant of hook-cable contact. This transient-impact problem is extremely difficult owing to the wire geometry and the inhomogeneity of the cable cross section. Any solution that assumes the cable to be a long circular cylinder with some average cross-sectional elastic modulus can hardly be expected to yield a reliable result. However, the fact remains that the instantaneous hook-cable contact force is one of the two main factors contributing to wire failure in the deck pendant. (The abrasive deterioration of the rope is the other important factor.) For this reason, it is of value to find an approximate magnitude for this contact force.

Consider the hook and a round-strand deck pendant as they first come into contact during an aircraft arrestment. The maximum contact force develops when the hook first impacts on a single wire of one strand of the rope (see Figure 35). Knowing the hook and cable geometry, it is possible to obtain a relationship for this contact force in terms of the mass of the wire being hit.

The Hertz force-deformation law for contact between two elastic bodies is[16]

$$F = K_2 \alpha_c^{3/2} \quad ,$$

where

F = the contact force between the two bodies

α_c = the approach or relative compression of the two bodies

$$K_2 = \frac{4}{3} \frac{q_k}{(\delta_1 + \delta_2)\sqrt{A + B}} ,$$

and

$$\delta_i = \frac{1 - \mu_i^2}{E_i \pi}$$

μ_i = Poisson's ratio for Body "i"

E_i = the elastic modulus of Body "i"

$$A = \frac{1}{4}\left(\frac{1}{R_1} + \frac{1}{R_1'} + \frac{1}{R_2} + \frac{1}{R_2'}\right) - \frac{1}{4}\left[\left(\frac{1}{R_1} - \frac{1}{R_1'}\right)^2 + \left(\frac{1}{R_2} - \frac{1}{R_2'}\right)^2 + 2\left(\frac{1}{R_1} - \frac{1}{R_1'}\right)\left(\frac{1}{R_2} - \frac{1}{R_2'}\right)\cos 2\theta\right]^{1/2}$$

$$B = \frac{1}{4}\left(\frac{1}{R_1} + \frac{1}{R_1'} + \frac{1}{R_2} + \frac{1}{R_2'}\right) + \frac{1}{4}\left[\left(\frac{1}{R_1} - \frac{1}{R_1'}\right)^2 + \left(\frac{1}{R_2} - \frac{1}{R_2'}\right)^2 + 2\left(\frac{1}{R_1} - \frac{1}{R_1'}\right)\left(\frac{1}{R_2} - \frac{1}{R_2'}\right)\cos 2\theta\right]^{1/2}$$

q_k = a constant with a value found in Table 5, page 87, Reference 16

R_i and R_i' = the principal radii of curvature of Body "i" at the point of contact, considered positive when the corresponding centers of curvature fall inside the body

θ = the angle formed by the two normal planes containing the two curvatures $1/R_1$ and $1/R_2$, respectively.

If the hook is Body 1, then

R_1 = -0.75 inch and R_1' = 3.25 inches (see Figure 33).

For a 6 x 25, filler wire, round-strand wire rope of 1-3/8-inch diameter, the radius of the outermost wire and its radius of curvature are R_2 = 0.044 inch and R_2' = 3.276 inches, respectively. Here the radius of curvature, R_2', has been found using the equations of Stein and Bert[44] as presented previously. In these equations the following data have been used:

α = lay angle of outer strand wires = -17°5'[31]

β = lay angle of strands = +18°30'[31]

R = radius of the outer wire = 0.044 in.[31]

r = radius of wire center line, measured from strand centerline = 0.182 in.

$\bar{r}$ = radius of strand center line, measured from rope center line = 0.460 in.

$\bar{R} = \frac{r + R}{\bar{r}} = 0.491$

ϕ_o = reference angle for the outermost wire of the rope = 0 degree (see Figure 30).

The angle θ for contact between these two bodies is approximately zero. Thus,

$$A = 0.3065 \text{ in.}^{-1}, \quad B = 10.6970 \text{ in.}^{-1}, \quad \text{and } q_k = 0.7162 \quad .$$

If $\mu_1 = \mu_2 = 0.26$ and $E_1 = E_2 = 30 \times 10^6$ lb/in.^{2}, then $\delta_1 = \delta_2 = 9.893 \times 10^{-9}$ in.^{2}/lb and, finally, $K_2 = 1.455 \times 10^7$ lb/in.$^{3/2}$. This gives the following Hertz force-deformation relationship:

$$F = (1.455 \times 10^7)\, \alpha^{3/2} \quad .$$

For the case of impact of two elastic bodies, if the vibrations produced by the collision can be neglected, the maximum compression is[16]

$$\alpha_m = \left(\frac{5V^2}{4K_1K_2}\right)^{2/5} \quad ,$$

where

V = initial relative velocity, ft/sec

$$K_1 = \frac{m_1 + m_2}{m_1 m_2}$$

m_i = mass of Body "i", lb.

Since the mass of the hook, m_1, includes the mass of the aircraft,

$$m_1 \gg m_2 \text{ and } K_1 \sim \frac{1}{m_2} \quad .$$

Thus

$$F = K_2\left(\frac{5V^2 m_2}{4K_2}\right)^{3/5} \quad .$$

For an average impact velocity of 110 knots or 186 ft/sec,

$$F = (2.45 \times 10^5) m_2^{\,3/5} \quad .$$

This equation provides a relationship between the impact force and the mass of the wire being hit.

From this equation it is found that a contact force of 5000 pounds is developed if the mass of the outer strand wire, m_2, is taken to be only 1.52×10^{-3} pound. (This is the mass of a wire 0.87 inch long.) It is not unreasonable to assume that the mass initially acted upon by the hook is of such a magnitude. This impact force is sufficient to cause a filler-wire shear failure 0.32 inch long.

While this analysis is not sufficiently accurate to predict the exact value of the impact force, it indicates that the magnitude of the force is in the range of 5000 pounds as opposed to 500 or 50,000 pounds. This would be adequate to cause the types of wire shear failures that have been observed. It may be assumed that a similar impact force exists when the hook strikes a flattened-strand rope.

CRITERIA FOR ARRESTING GEAR CABLE EVALUATION

The previous analyses indicate how it is possible to reduce the magnitude of internal stresses in a wire rope by varying the geometry of the individual strands. Several authors[3, 4, 31, 33, 40, 43] have suggested that a large number of variable parameters contribute to the over-all strength and service life of wire ropes. They have shown how changing one of these parameters may reduce certain undesirable characteristics while aggravating others. Due to the large number of these parameters and their conflicting effects, it is necessary to establish reliable criteria for the evaluation of wire ropes. The following discussion points out the various items which should be considered in wire rope evaluation and indicates how they are affected by variations in the rope construction.

Tensile Stresses and Bending Stresses on Wires

The first consideration in evaluating a wire rope design is, of course, the magnitude of the tensile stresses developed in the wires. These stresses must remain within reasonable limits when the rope is subjected to its maximum service tension and bending.

For a rope under axial tension, the tensile stresses in the wires may be calculated if the wire cross-sectional areas, wire lay angles, and strand lay angle are known. It is found that for a given metallic cross section, the tensile stresses may be reduced by a decrease in the lay angles.

For a rope subjected to both tension and bending, the tensile stresses on the wires depend also on the radius of the bend and the magnitude of internal rope friction. During bending, the rope experiences relative motion between the strands and between the strands and the core. If no internal friction were present, the strands would move so as to more evenly distribute their tensile loads. However, the internal friction retards this motion and results in unequal load distribution and increased tensile stresses on some wires. For this reason it is desirable for a wire rope to have ample internal lubrication.

It has been found that the core in a wire rope becomes notched by the wires pressing against it. In regular-lay rope, these notches are at an angle of approximately 35 degrees with the axis of the rope. In Lang-lay rope, this angle is reduced to nearly zero. As a result, the strands of the Lang-lay rope may move more easily along the core during bending, thereby providing more evenly distributed strand loads and lower tensile stresses on the wires.

The relative motion between the rope components increases with decreasing bend radius. This fact should be kept in mind when sizing sheaves or drums for a particular rope. In general, the bending radius should be kept as large as possible. Tables are available for determining the minimum bending radii for all types of rope.

Another consideration for the condition of bending is the "flexibility" of the rope. This "flexibility" is actually an indication of the bending stresses produced in the wires. The stiffer a rope is, the higher will be the bending stresses in wires for a given bend radius. For this reason, when relatively small-radius bends are necessary, it is desirable to construct the rope of strands consisting of many wires of small diameter rather than a few wires of large diameter.

Interstrand Contact Stresses

When a wire rope is subjected to loading, the individual strands are pressed against each other and the rope diameter decreases. This interstrand loading produces high stresses at the points of wire contact. If these stresses are large enough to produce local yielding, a notch forms in the wires and the resulting stress concentration reduces the tensile strength of the wire.

As pointed out in this report, it is possible to calculate these interstrand contact stresses using the Hertz theory and the rope geometry. In order to maintain maximum rope strength, it is desirable to reduce these stresses as much as possible.

For a rope under axial tension, it is possible to eliminate the interstrand contact stresses by providing a core that will support the strands sufficiently to keep them from touching each other. However, when a rope is subjected to bending or transverse impact, a simple core will not prevent contact between strands. It then becomes necessary to use other means to reduce the stresses produced by the existing contact force.

One method is to use a shaped core that will eliminate interwire contact by providing a thin layer or core material between the strands. It is also possible to use shaped wires (noncircular cross section) for the outer layers of the strands, thus providing area contact rather than point contact between touching wires. This second method, however, may tend to reduce rope flexibility.

If it is desirable to use a simple round core and round wires, the interstrand contact stresses may be reduced in four ways:

(1) By reducing the lay angle of the strands, the contact force, and thus the contact stress, between the strands is reduced.

(2) By reducing the lay angle of the wires in the strands, the crossing angle of two contacting wires is made smaller and the contact stress is lessened.

(3) By using larger wires in the outer layers of the strands, the effect of contact stresses will be reduced.

(4) By using alternate lay rope – the strands alternating between regular lay and Lang lay – two wires in contact between strands will be parallel, thus further reducing the contact stress.

Stresses Resulting From Hook Impact

The impact of the arresting hook on the cable tends to distort the rope cross section and increase the interstrand contact forces. This aggravates the crossed-wire contact stress. In addition, there also exists the contact stress between the rope and the hook. The latter is affected very little by the lay angles or the characteristics of the rope core, but it may be reduced considerably by use of shaped wires, Lang lay, shaped strands, or a combination of these. The Lang lay and the shaped strands (e.g., flattened strands) both provide an increase in length of wire contact with the hook. The shaped wires provide area contact rather than line contact.

In addition to the compressive stresses produced in the region of hook impact, there is also a longitudinal tensile wave established, which travels along the cable away from the point of hook impact. For the case of perpendicular impact on a cable initially at zero strain, the value of this tensile stress is given approximately by Ringleb[38] as

$$\sigma = \left(\frac{E\rho^2 V^4}{4g^2 A^2}\right)^{1/3} ,$$

where A is the cable metallic cross section. For a given cable metallic cross section and impact velocity, this tensile stress may be reduced by decreasing the value of $(E\rho^2)$. ρ may be reduced by decreasing the lay angles or using a lighter core material. However, the value of E depends on both the wire material used and the rope geometry. Here it is probable that a reduction in the lay angles will tend to raise E. This is one example of the conflicting results that may occur due to rope-design modifications.

Stresses Produced by the Reflection of Kinks and Longitudinal Waves

One of the most significant conclusions that can be drawn from the results given in the first part of this report is that the maximum tensile stress exerted on the cable is due to the impact kink K_1 on the deck sheave. When this kink hits the deck sheave, a longitudinal wave is initiated. It is the reflection of this tensile wave from the hook that produces the peak cable stress. It has been shown previously that the magnitude of this stress may be reduced by lowering the cable elastic modulus and/or the ratio of the cable density to the metallic cross-sectional area.

Abrasion Resistance

The abrasion resistance of wire rope is an important factor determining the useful life of a deck pendant. High abrasion is experienced during aircraft arrestment when the cable slides across the face of the hook as a result of an off-center or oblique landing. The cable is again subjected to abrasion as it is drawn back over the rough deck into position for the following engagement. A numerical analysis of this problem was found to be extremely difficult because of the number of variables involved and the lack of knowledge of their interrelationships. The derivation of an accurate numerical

abrasion criterion would be a major research project in itself. However, a number of qualitative relations were identified that can be used in directing rope design for improved abrasion resistance.

In general, for a cable of given diameter, it is desirable to present to the abrading surface as large a cable surface area as possible. This means that the wires should have a flattened shape exposed to the outer surface of the rope, and that the strands should have a flattened shape to provide a large number of wires for contact with the hook and deck. Also, low lay angles should be used in order that each wire on the surface of the rope will have the longest possible line of contact with the hook or deck and the tendency of the wires to spring away from the strand as they wear will be reduced. All of these factors tend to reduce the unit pressure during abrasion, the result being a decrease in the total depth of wear on the wires. Obviously, if the outer wires are large in diameter, more metal can be lost before a complete wire breakage occurs. It may also be possible to make the outer wires in a rope from a material that is more resistant to abrasion than that now used.

Corrosion Resistance

Since aircraft arresting gear cable is exposed to sea water, it is necessary for it to have good corrosion resistance. Any amount of corrosion that occurs causes stress concentrations that promote tensile failure of the wires. Several authors, including Sasaki, et al.[40], have discussed this problem and indicate the desirable characteristics of a corrosion-preventative lubricant. They also suggest possible characteristics that should be avoided. It is pointed out that corrosion can be eliminated by electrodepositing a protective coating of zinc or aluminum on the wires prior to the final drawing operation. This, however, reduces the strength of the wires by approximately 10 percent.

RECOMMENDATIONS FOR AN IMPROVED WIRE-ROPE DESIGN

As a result of the previous investigations it is possible to make a number of recommendations for an improved wire-rope design. Recommendations that apply generally to any deck-pendant design are:

(1) The wires exposed to the surface of the rope should:

- (a) Be large in cross section so that wire breakage due to abrasion will be retarded
- (b) Be made of highly abrasion-resistant material (if necessary, some reduction in the tensile strength could be tolerated)
- (c) Have shaped cross sections to provide large areas for hook-cable and parallel wire contact.

(2) The wires not exposed to the surface of the rope should:

- (a) Be small in cross section so that bending stress will be low and the rope will be flexible
- (b) Be made of material with high tensile strength.

(3) The rope geometry should:

(a) Curtail the tendency of the wires to fail in shear due to transverse impact by the hook
(b) Provide good rope stability and prevent excessive "bird-caging".

(4) The ratio of rope density to metallic cross section should be as low as possible.

(5) The rope elastic modulus should be as low as possible.

(6) Rope fatigue life and corrosion resistance need not be primary in the criteria for evaluating a deck-pendant design, but they should be considered in any purchase-cable evaluation.

Additional recommendations applicable to "conventional" wire rope designs – the rope being composed of a number of strands wrapped around a central rope core – are:

(1) The rope should be made up of a sufficient number of strands to maintain adequate stability and flexibility.

(2) The strands should have shaped cross sections to increase the length of hook-cable and interstrand wire contact.

(3) Lang lay should be used.

(4) The wire lay angles should be as low as possible without producing an excessive amount of "bird-caging".

(5) The wires on the surface of the strands should have shaped cross sections to provide large areas for crossed-wire interstrand contact.

New Cable Designs

On the basis of these recommendations it is possible to propose new designs for arresting-gear cable. The analytical methods presented in this report may then be used to evaluate these new designs and to predict their performance. Such an evaluation will provide a comparison of the new designs with the arresting cable presently in use by indicating approximate values for:

(1) Peak cable stress during arrestment

(2) Peak tensile loads and stresses on individual wires

(3) Cable tensile strength

(4) Peak hook-cable contact force and contact stress

(5) Peak interstrand contact force and contact stress

(6) Peak parallel-wire contact force and contact stress within the cable.

In some cases, further analysis and comparison of the different designs allow a prediction of:

(1) Elastic modulus

(2) Flexibility

(3) Abrasion resistance

(4) Impact resistance.

Figures 43, 44, and 45 show three new designs for wire ropes for use as deck pendants. It must be pointed out that these are preliminary designs chosen to demonstrate the points suggested in the recommendations for an improved wire-rope design. The actual practicality of these designs can be determined only through full-scale testing.

The strand designs shown in Figures 43 and 44 are intended for use in six-strand, Lang-lay ropes. These ropes would be very similar to the standard 6 x 30 flattened-strand rope presently used for deck pendants (see Figure 26). For similar lay angles and outer diameters, the three ropes composed of these three different types of strands should have nearly the same flexibility, stability, density, tensile strength, and elastic modulus. The major difference is the use of noncircular wire in the new designs.

For the designs shown in Figures 43 and 44, the noncircular shape of the outer wires should result in lower hook-cable, crossed-wire, and parallel-wire contact stresses. This would increase the impact resistance of the rope and decrease the inter-strand wire notching. Furthermore, the shape of the outer wires would provide a larger metallic area to resist abrasion for a given depth of rope wear. This would reduce the unit pressure during abrasion and thereby reduce the rate of metal removal. As a result, the rope abrasion resistance would also be improved.

The rope cross section shown in Figure 45 is a departure from the more conventional deck-pendant designs. This rope would consist of a single strand made up of a large number of very small-diameter wires. All wire layers consisting only of wires with round cross sections would be laid in one direction, and all layers containing the "half-lock" wires would be laid in the other direction. This would contribute to rope stability and reduce the tendency of the rope to rotate under a tensile load. The stability, flexibility, and elastic modulus of such a rope depends on the wire size, the number of wire layers, and the lay angle of each layer. It is difficult to predict, without experimental work, whether such a rope would be suitable as a deck pendant, since the flexibility and stability of this design are questionable. However, the impact resistance and abrasion resistance of such a rope should be greatly improved over that of the currently used deck pendants. Future experimental investigations will prove or disprove the usefulness of such rope for deck-pendant applications.

Purchase Cable Design

The above discussion has been primarily directed toward the deck-pendant problem because the bulk of the work on this program has had that direction. However, the problems for the purchase cable are, with some obvious exceptions, quite similar, and the same solutions should be applicable.

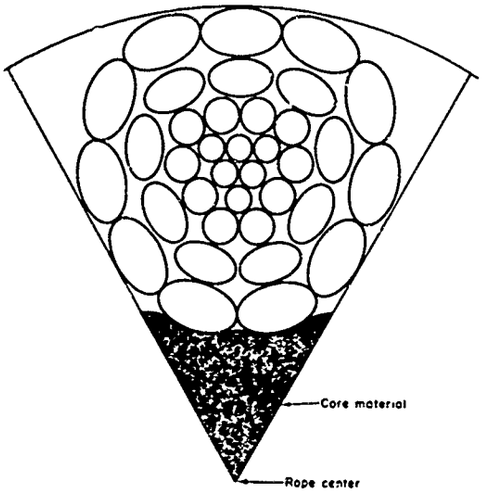

FIGURE 43. ALTERNATE CABLE DESIGN NUMBER ONE

Single strand of six-strand rope.

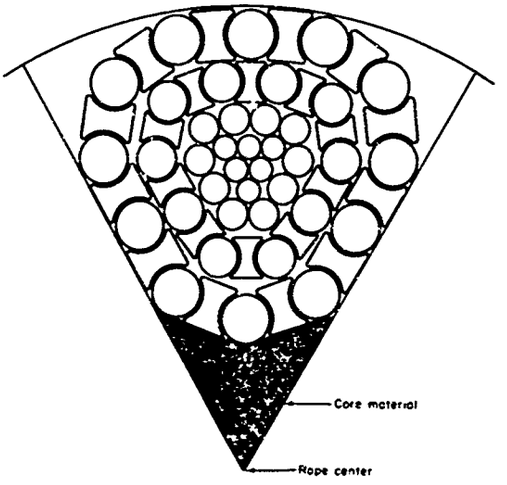

FIGURE 44. ALTERNATE CABLE DESIGN NUMBER TWO

Single strand of six-strand rope.

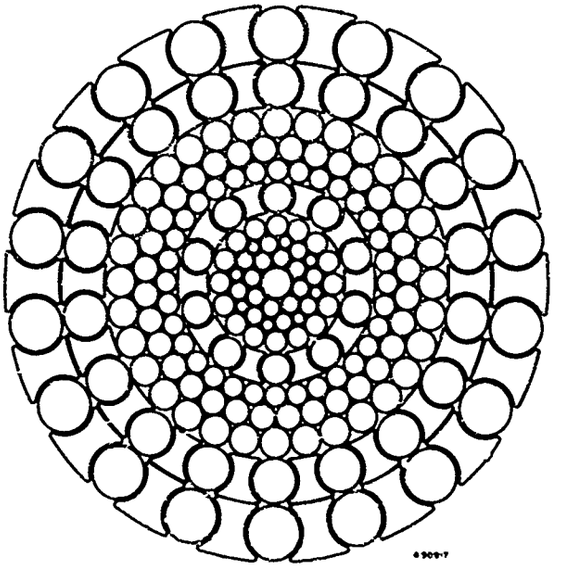

FIGURE 45. ALTERNATE CABLE DESIGN NUMBER THREE

Single strand consisting of a large number of very small diameter wires.

The exceptions are:

(1) The purchase cable is not subjected to hook impact as is the deck pendant.

(2) The life of the purchase cable is relatively long so that fatigue and corrosion are important problems. This is not the case for the deck pendant which has a short life of approximately 70 load cycles. Even if the life of a deck pendant were significantly extended, this should be true.

The designs of Figures 43 and 44 are recommended for experimental evaluation for use in purchase cables. The design of Figure 45, although it has several advantages over the present cable, may be too stiff for this application. It is also recommended that an electrodeposited zinc coating be tried, both on these designs and on the standard purchase cable. The small loss in static strength of the cable due to such a coating is not expected to seriously affect cable performance, and the increase in corrosion resistance and fatigue strength should be highly desirable.

EVALUATION OF A NEW WIRE-ROPE DESIGN

Consider the strand design shown in Figure 44. Assume that this design is used in a six-strand, Lang-lay wire rope. Due to the similarity between this rope and the 6 x 30, flattened-strand rope shown in Figure 26, the ratios of rope density to metallic cross-sectional area will be nearly the same for the same wire and core materials. Furthermore, if the wire and strand lay angles are approximately the same for both types of rope, the elastic moduli should also be nearly identical. For these reasons, the peak tensile stress developed in these two types of cable during aircraft arrestment will not differ by a significant amount (see Figure 25).

With similar lay angles and outside diameters, these two types of cable will also have nearly the same tensile stresses on the wires for a given load. This stress is approximately $\sigma_w = 1.25\ T$, where T is the tensile load on the cable. The actual values may be found using Equations (13), (15), and (19). Also, the over-all tensile strengths of the two cables will be similar.

One significant difference between these two designs is in the magnitude of the interstrand contact stress. Although the interstrand force is no different, the large interstrand contact area provided by the new design greatly reduces the resulting contact stress for this rope.

As for the 6 x 30, flattened-strand rope, the new design will have an interstrand contact force of approximately $F_T = 0.0373\ T$ lb/in. (assuming similar strand lay angles and negligible core support). Likewise, the force supported at each region of interstrand contact will be approximately $P'_T = 0.031\ T$ pounds. For a cable tension of 85,000 pounds this load is $P'_T = 2,640$ pounds.

This load is supported almost entirely by the two "half-lock" type wires of each strand. Thus, just as for the 6 x 30 rope, there are four points of crossed-wire contact with wire crossing angles of approximately $\theta = 18$ degrees. This is shown in Figure 46.

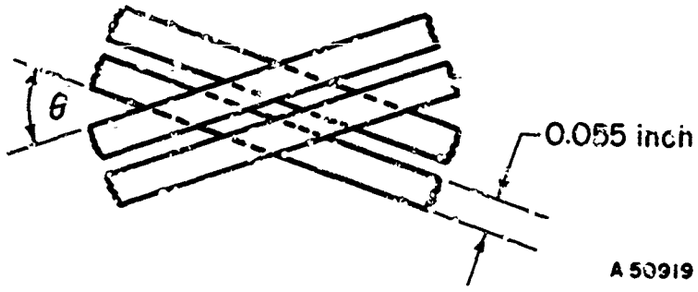

FIGURE 46. REGION OF INTERSTRAND CROSSED-WIRE CONTACT

For a surface width of 0.055 inch for the "half-lock" wires, as would be the case for a 1-3/8-inch cable using the strand design shown in Figure 44, the total contact area available to support the load P_T' is

$$(4)\frac{(0.055)^2}{\sin\theta} \sim 0.04 \text{ in.}^2$$

The resulting contact stress, neglecting stress concentration, is

$$\sigma = \frac{2640}{0.04} = 66,000 \text{ lb/in.}^2 \quad .$$

This is much lower than the theoretical contact stress of $1,600,000$ lb/in.^{2} found for the 6 x 30 flattened-strand rope. It is felt that with this new design, the problem of interstrand wire notching is virtually eliminated.

A similar reduction in contact stress can also be expected for the area of contact between the wires and the hook.

Thus, it is found that the use of shaped wires greatly improves the interstrand and hook-cable contact stress situation. Furthermore, as discussed previously, the smoother surface of the new rope provides a much larger effective area to resist abrasion. This reduces the unit pressure during abrasion and thereby reduces the rate of metal removal.

It appears, upon initial evaluation, that a Lang-lay deck pendant made up of strands of the design shown in Figure 44 would be significantly superior to the flattened-strand rope presently in use. The degree of this superiority can be determined only through experimental evaluation.

BIBLIOGRAPHY

(1) Ayre, R. S., and Abrams, J. I., "An Analytical and Scale Model Investigation of Aircraft Arresting Gear; Experimental and Phase-Plane Analytical Methods", Tech. Report No. 1, Bureau of Aeronautics Contract NOas53-891-c, Johns-Hopkins University, July 1954.

(2) Ayre, R. S., and Abrams, J. I., "Dynamic Analysis and Response of Aircraft Arresting Systems", Proc. ASCE, Journal of the Engineering Mech. Div., April 1958.

(3) Baisley, B. H., "Study of Designs for an Optimum Wire Rope for Aircraft Arresting Systems", U. S. Naval Air Material Center, Report NAEL-ENG-7014, February 1964.

(4) Bert, C. W., and Stein, R. A., "Stress Analysis of Wire Rope in Tension and Torsion", Wire and Wire Products, May, June 1962.

(5) Carrier, G. F., "A Note on the Vibrating String", Quar. Appl. Math. Vol. VII, p. 97-101, 1949.

(6) Carrier, G. F., "On the Non-Linear Vibration Problem of the Elastic String", Quar. Appl. Math. Vol. III, p. 157-165, 1945.

(7) Cole, J. D., Dougherty, C. B., and Huth, J. H., "Constant-Strain Waves in Strings", Vol. 75, Trans. ASME, 1953.

(8) Cosgrove, H. N., Ralston, R. H., and Westberg, J. V., "Dynamic Analysis of Aircraft Effects on Carrier Arresting Gear", U. S. Navy, Bureau of Aeronautics, Contract NOw 61-0404t, Douglas Aircraft Co. Rept. ES-40497-4 April 1963.

(9) Cress, H. A., "A Theoretical Investigation of Contact Stresses in a 6 x 7 Wire Rope", Master's Thesis, The Ohio State University, 1955.

(10) Cristescu, N., "On Waves of Loading and Unloading Produced by Motion of an Elastic or Plastic Flexible Fiber", Priklad. Mat. Mekh., 18, 1954. (In Russian).

(11) Cristescu, N., "Wave Propagation in Flexible Fibers (Influence of Speed of Deformation)", Priklad. Mat. Mekh., 21, 1957. (In Russian).

(12) Davidsson, W., "Investigation and Calculation of the Remaining Tensile Strength in Wire Ropes with Broken Wires", Ingeniörsvetenskapsakademiens, Handlingar NR 214, 1955.

(13) Den Hartog, J. P., "Mechanical Vibrations", Second Edition, McGraw-Hill (New York), 1940.

(14) de Saint Venant, B., "Choc Longitudinal de Deux Barres Élastiques", Comptes Rendue de l'Academie des Sciences, Paris, Vol. 66 (1868).

(15) Drucker, D. S., and Tachau, H., "A New Design Criterion for Wire Rope", Journal of Applied Mechanics, Vol. 12, Trans. ASME, 1945.

(16) Goldsmith, W., "Impact: The Theory and Physical Behaviour of Colliding Solids", Arnold (London), 1960.

(17) Hruska, F., "Calculation of Stresses in Wire Ropes", Wire and Wire Products, September 1951.

(18) Hruska, F., "Radial Forces in Wire Ropes", Wire and Wire Products, May 1952.

(19) Hruska, F., "Tangential Forces in Wire Ropes". Wire and Wire Products, May 1953.

(20) Kaufman, W. J., "Recovery Equipment Study and Proposed Mark 8 Arresting Gear Program", U. S. Naval Air Material Center, Report No. M-6070, 1956.

(21) Kawashima, S., "On the Vibration and the Impact of Elastic Cables", Memoirs of the Faculty of Engineering, Kyushu University, Vol. XII, p. 59-138, 235-243, 1950.

(22) Knecht, F. E., "Nylon Deck Pendant Evaluation and Effect on Arresting Cable Vibratory Loads", U. S. Naval Air Material Center, Report No. [illegible], 1955.

(23) Layland, C. L., Rao, A. R. S., and Ramsdale, H. A., "Experimental Investigation of Torsion in Stranded Mining Wire Ropes", K. G. F. Mining and Metallurgical Society, Vol. 3, 1952.

(24) Leissa, A. W., "A Theoretical Analysis of a 6 x 7 Wire Rope Subjected to a Pure Tensile Load", Master's Thesis, The Ohio State University, 1954.

(25) Love, A. E. H., "A Treatise on the Mathematical Theory of Elasticity", Cambridge University Press, London, 1927.

(26) Marble, F. E., "The Motion of a Finite Elastic Cable", Report of North American Instruments, Inc., Altadena, California, 1954.

(27) Moisil, G. C., "Shock Waves in a Cable", Proc. 9th International Congress of Appl. Mech., Brussels, 1956.

(28) Neidhardt, G. L., Eslinger, N. F., and Sasaki, F., "An Analytical Approach to the Alleviation of Dynamic Tensions in Aircraft Arresting Gear Cables", WADC Tech. Report 58-217, May 1958.

(29) Owada, S., "Effect of Process of Laying upon Elastic Behavior of Wire Ropes or Cables", Proc. 5th Japan National Congress for Appl. Mech., 1955.

(30) Pei Chi Chou, "Plastic Contact Stress in Circular Cylinders", U. S. Naval Air Material Center, Report NAEF-ENG-6740, January 1961.

(31) Pei Chi Chou, "Theoretical Analysis of Deck Pendant During Arresting Hook Impact and Runout", U. S. Naval Air Material Center, Report NAEF-ENG-6584, October 1959.

(32) Pei Chi Chou, "Theoretical Analysis of Deck Pendant During Arresting Hook Impact and Runout", U. S. Naval Air Material Center, Report NAEF-ENG-6682, June 1960.

(33) Pei Chi Chou, "Theoretical Analysis of the Sliding Abrasion Between Hook Point and Deck Pendant", U. S. Naval Air Material Center, Report NAEL-ENG-6815, February 1962.

(34) Pong, L. C., "Longitudinal Motion of Arresting Gear Cables under Transverse Impact", U. S. Naval Air Missile Test Center, Point Mugu, California, Memo. Report No. 55-54, 1954.

(35) Rayleigh, J. W. S., "Theory of Sound, Volume I", First American Edition, Dover Publications (New York), 1945.

(36) Reabova, E. V., "Normal Impact with Varying Velocity upon a Flexible Fiber", Moskva Universitet, Vestnik, 10, 1953. (In Russian).

(37) Ringleb, F. O., "Cable Dynamics", U. S. Naval Air Material Center, Report NAEF-ENG-6169, December 1956.

(38) Ringleb, F. O., "Dynamics of a Moving Cable", U. S. Naval Air Material Center, Report No. M-4812, 1948.

(39) Ringleb, F. O., "Motion and Stress of an Elastic Cable Due to Impact", ASME Paper No. 57-APM-10.

(40) Sasaki, F. T., Eslinger, N. F., and Neidhardt, G. L., "Model Tests and Studies of the Problems of Dynamic Tensions in Aircraft Arresting Gear Cables", WADC Tech. Report 59-495.

(41) Seeley, F. B., and Smith, J. O., "Advanced Mechanics of Materials", Second Edition, John Wiley & Sons, Inc., New York, 1952.

(42) Smith, R. L., and Brown, R. M., "A Determination of the Dynamic Modulus of Elasticity of a 1" and 1-3/8" Arresting Gear Cable", Propulsion Research Corp., Santa Monica, Calif., Report No. R-239, 1956.

(43) Starkey, W. L., and Cress, H. A., "An Analysis of Critical Stresses and Mode of Failure of a Wire Rope", Journal of Engineering for Industry, November 1959.

(44) Stein, R. A., and Bert, C. W., "Radius of Curvature of a Double Helix", Journal of Engineering for Industry, August, 1962, p. 394-395.

(45) Stevens, G. W. H., "Experiments on Waves in Wires with Fixed End", R. A. E. Report DI 57.

(46) Tuman, C., "High Velocity Engagement of Arresting Wires", Report of U. S. Naval Air Missile Test Center, Point Mugu, California, 1954.

(47) Wen-Hsiung Li, "Elastic Flexible Cable in Plane Motion under Tension", Journal of Applied Mechanics, December 1959.

PTG:HAC/slp